

**Acclimation of photosynthesis to  
irradiance in *Arabidopsis thaliana***

**Shaun Bailey**

July 1999

PhD Thesis

Robert Hill Institute  
Department of Molecular Biology and Biotechnology  
University of Sheffield  
Sheffield, U.K.

**PAGE  
NUMBERING  
AS  
ORIGINAL**

## **Acknowledgements**

I would like to thank my supervisor Peter Horton for all his invaluable help and guidance. I would also like to thank my co-supervisor Robin Walters for guidance and discussion. Thanks also to Stefan Jansson for the use of antibody and for welcoming into his lab in Umea. Thanks to Sasha Ruban and Erik Murchie and Jeanette Webster for useful discussion and assistance with various techniques. Thanks also to Pam Scholes, Jenni Rogers and Freya Shepard for technical support. Thanks to all in C24, past and present, and those non-lab members for helping to make my time in Sheffield a memorable experience.

This project was funded by a NERC studentship and I would like to NERC for their financial support.

## Abstract

The work contained within this thesis describes the acclimation of photosynthesis in *A.thaliana* to growth over a broad range of irradiance. Using Pmax and Chl *a/b* as an index, the ability of *A.thaliana* to modulate the composition of the photosynthetic apparatus across a range of irradiance has been demonstrated. A non-linear response to growth irradiance was seen for both parameters, the shape of which was similar. In addition the overall magnitude of the response was large compared to other plant species. These changes took place with no alteration in overall chlorophyll content per unit leaf area.

A detailed analysis of the changes in chloroplast composition followed. This revealed a good correlation between changes in Chl *a/b* and bulk LHCII as well as Pmax and Rubisco content. However measurement of the reaction centre content along with immunoblot analysis of all ten Chl *a/b* binding light harvesting polypeptides established that changes in other thylakoid components were also responsible for changes in Chl *a/b*. Significant changes in reaction centre content were seen at both the low and high extremes of growth irradiance with PSI content doubling at  $35 \mu\text{mol m}^{-2} \text{s}^{-1}$  and PSII content rising significantly at  $600 \mu\text{mol m}^{-2} \text{s}^{-1}$ . The extent of the changes in reaction content is well beyond those previously reported for other plant species. Other previously unreported changes in thylakoid composition are also observed for *A.thaliana*. For example there was a doubling in the minor LHCII complexes, Lhca5 and 6, at very low growth irradiance. In addition a complex pattern of change was observed for all 4 LHCI polypeptides.

The functional consequence of photosynthetic acclimation was also investigated using room temperature chlorophyll fluorescence. Measurements of the maximum rate of

electron transport (ETR) for plants grown at all irradiance revealed a higher rate for plants grown at  $400 \mu\text{mol m}^{-2} \text{s}^{-1}$  than would have been predicted from the maximum photosynthetic rate ( $P_{\text{max}}$ ). This discrepancy suggested an alternative fate for electrons (other than  $\text{CO}_2$  fixation) for plants grown at this irradiance. Since this electron sink must involve molecular oxygen it is suggested that enhanced Mehler reaction accounts for the increased ETR.

Relaxation kinetics of chlorophyll *a* fluorescence quenching was used to resolve  $q_N$  into two components,  $q_E$  and  $q_I$ . The maximum capacity for  $q_E$  clearly increased with increasing growth irradiance and correlated well with Chl *a/b* and the xanthophyll cycle pool size establishing that the capacity for short term photosynthetic regulation is itself subject to acclimation. Finally the dynamic nature of photosynthetic acclimation was demonstrated following transfers between high and low irradiance.

## Table of contents

<b>Chapter 1 –General Introduction</b>	<b>1</b>
<b>1.1 The chloroplast</b>	<b>2</b>
<b>1.2 Photosynthesis: the basic reactions</b>	<b>3</b>
<b>1.2.1 The Light Reactions</b>	<b>4</b>
<b>1.2.2 The Z scheme</b>	<b>4</b>
<b>1.2.3 The Chemiosmotic Hypothesis</b>	<b>5</b>
<b>1.2.4 Cyclic Electron Transport</b>	<b>7</b>
<b>1.2.5 The Dark Reactions</b>	<b>8</b>
<b>1.3 Thylakoid Membrane Components</b>	<b>10</b>
<b>1.3.1 Photosystem II</b>	<b>10</b>
<b>1.3.1.1 Photosystem II function</b>	<b>11</b>
<b>1.3.1.2 Structural Aspects of Photosystem II</b>	<b>11</b>
<b>1.3.1.2.1 Reaction Centre Core</b>	<b>11</b>
<b>1.3.1.2.2 Oxygen Evolving Complex</b>	<b>13</b>
<b>1.3.1.2.3 Photosystem II Distal Antenna</b>	<b>14</b>
<b>1.3.1.2.4 Photosystem II Subunit Organisation</b>	<b>18</b>
<b>1.3.2 Cytochrome <math>b_6f</math> complex</b>	<b>19</b>
<b>1.3.3 Photosystem I</b>	<b>22</b>
<b>1.3.3.1 Photosystem II function</b>	<b>22</b>
<b>1.3.3.2 Structural Aspects of Photosystem I</b>	<b>23</b>
<b>1.3.3.2.1 Reaction Centre Core</b>	<b>23</b>
<b>1.3.3.2.2 Light Harvesting</b>	<b>24</b>
<b>1.3.3.2.3 Photosystem I Subunit Organisation</b>	<b>24</b>
<b>1.3.4 ATP Synthase</b>	<b>26</b>
<b>1.3.5 Organisation of the Thylakoid Membrane and its Components</b>	<b>27</b>
<b>1.4 Photosynthetic Acclimation to Irradiance</b>	<b>31</b>
<b>1.4.1 Photosynthetic Acclimation to Constant Growth Irradiance</b>	<b>32</b>
<b>1.4.2 Photosynthetic Acclimation to Changes in Growth Irradiance</b>	<b>34</b>

<b>1.43 The Regulatory Mechanism of Photosynthetic</b>	
<b>Acclimation to Irradiance</b>	<b>35</b>
1.4.3.1 Molecular Feedback	36
1.4.3.2 'Excitation Pressure'	37
1.4.3.3 Redox Regulation of Photosynthetic Acclimation	40
1.4.3.4 Regulatory Proteolysis of LHCII	40
<b>1.5 Short Term Regulation of Photosynthesis</b>	<b>41</b>
1.5.1 High Energy quenching: qE	42
1.5.2 Slowly Relaxing Non-photochemical quenching: qI	46
1.5.3 State Transition	47
<b>1.6 Aims</b>	<b>48</b>

## ***Chapter 2 –Materials and Methods***

<b>2.1 Plant Growth</b>	<b>50</b>
<b>2.2 Chlorophyll Determination</b>	<b>50</b>
<b>2.3 Oxygen Evolution</b>	<b>51</b>
<b>2.4 Photosystem II Content</b>	<b>51</b>
<b>2.5 Thylakoid Preparation</b>	<b>52</b>
<b>2.6 Photosystem I Content</b>	<b>52</b>
<b>2.7 Gel Electrophoresis</b>	<b>53</b>
2.7.1 SDS PAGE	53
2.7.2 Western Blotting	54
<b>2.8 Rubisco Content</b>	<b>54</b>
<b>2.9 Room Temperature Chlorophyll Fluorescence</b>	<b>55</b>
2.9.1 <i>in situ</i> Measurements	57
2.9.2 Measurements of State Transition	58
<b>2.10 Low Temperature Chlorophyll Fluorescence</b>	<b>59</b>
<b>2.11 HPLC Analysis of Carentoid Composition</b>	<b>59</b>

**Chapter 3 – Acclimation to growth irradiance: changes in chlorophyll content,  $P_{max}$ , in situ chlorophyll fluorescence.**

3.1 Introduction	61
3.2 Results	62
3.2.1 Plant Growth and Morphology	62
3.2.2 Chlorophyll Content	63
3.2.3 Photosynthetic Capacity	67
3.2.4 Room Temperature Chlorophyll Fluorescence ( <i>in situ</i> )	71
3.3 Discussion	71

**Chapter 4 –Acclimation to growth irradiance: changes in the composition of the photosynthetic apparatus.**

4.1 Introduction	75
4.2 Results	76
4.2.1 Rubisco Content	76
4.2.2 Photosystem II Content	77
4.2.3 Photosystem I Content	80
4.2.4 Light Harvesting Polypeptide Composition	83
4.2.4.1 Immunoblotting	83
4.2.4.2 Photosystem II Light Harvesting Polypeptide Composition	83
4.2.4.3 Photosystem I Light Harvesting Polypeptide Composition	91
4.2.4.4 Antenna Polypeptide Composition Models	91
4.2.5 77K Fluorescence	91
4.3 Discussion	101

**Chapter 5 –Acclimation to growth irradiance: chlorophyll fluorescence and carotenoid content.**

5.1 Introduction	107
5.2 Photochemical quenching	108
5.3 Non-photochemical quenching	112
5.3.1 Total qN	112
5.3.2 qE	114
5.3.3 qI	116

5.4 $\phi$ PSII	116
5.5 Fv/Fm	118
5.6 Carotenoid Content	121
5.7 State Transition	125
5.8 Discussion	129
<b>Chapter 6-Acclimation to a change in irradiance.</b>	
6.1 Introduction	135
6.2 Transfer from Low to High Irradiance	136
6.2.1 Plant Morphology	136
6.2.2 Chlorophyll Content	137
6.2.3 Pmax	139
6.2.4 Room Temperature Chlorophyll Fluorescence	139
6.2.4.1 qP	140
6.2.4.2 qN	142
6.2.4.3 qE	142
6.2.4.4 qI	145
6.2.4.5 $\phi$ PSII	145
6.3 Transfer from High to Low Irradiance	148
6.3.1 Plant Morphology	148
6.3.2 Chlorophyll Content	149
6.3.3 Pmax	151
6.3.4 Room Temperature Chlorophyll Fluorescence	151
6.3.4.1 qP	152
6.3.4.2 qN	152
6.3.4.3 qE	154
6.3.4.4 qI	154
6.3.4.5 $\phi$ PSII	154
6.4 Discussion	159

**Chapter 7-Discussion**

**164**

**Chapter 8-References**

**173**

## Abbreviations.

ADP	adenosine diphosphate (triphosphate)
An	antheraxanthin
APS	ammonium persulphate
$\beta$ -car	$\beta$ -carotene
Cab	chlorophyll <i>a/b</i> -binding
Chla/b	chlorophyll <i>a/b</i> ratio
DCMU	3-(3',4'-dichlorophenyl)-1,1-dimethyl urea
DES	de-epoxidation state
DHAP	dihydroxyacetone phosphate
DTT	dithiothreitol
E4P	erythrose-4-phosphate
EDTA	ethylenediamine-tetraacetic acid
ELIP	early light-induced protein
F6P	fructose 6-phosphate
FBP	fructose bis phosphate
F <sub>m</sub>	maximal fluorescence when the reaction centres are closed
F <sub>o</sub>	fluorescence when the reaction centres are open
F <sub>v</sub>	variable fluorescence
GAP	glyceraldehyde 3-phosphate
HEPES	N-(2-hydroxyethyl) piperazine-N'-(2-ethanesulphonic acid)
HPLC	high performance liquid chromatography
L	lutein
LHCI (II)	light harvesting complex of photosystem I (II)
NADP <sup>+</sup>	oxidised nicotinamide adenine dinucleotide phosphate

NADPH	reduced nicotinamide adenine dinucleotide phosphate
Neo	neoxanthin
OEC	oxygen evolving complex
PAGE	polyacrylamide gel electrophoresis
3PGA	3-phospho-glycerate
PSI(II)	photosystem I (II)
$\phi$ PSII	efficiency of photochemistry
Pmax	maximum rate of photosynthesis
qE	“high-energy state” quenching
qN	non-photochemical quenching
qNf	fast component of non-photochemical quenching
qNm	medium component of non-photochemical quenching
qNs	slow component of non-photochemical quenching
qI	photoinhibition
qP	photochemical quenching
qT	state transitions
Rubisco	ribulose biphosphate carboxylase-oxygenase
RUBP	ribulose 1,5 biphosphate
Ru5P	ribulose 5 phosphate
S7P	sedoheptulose 7-phosphate
SDS	sodium dodecyl sulphate
SBP	sedoheptulose 1,7-biphosphate
TEMED	N,N,N',N'-tetra methylethylenediamine
Tris	Tris(hydroxymethyl)methylamine
Viola	violaxanthin
XC	Xanthophyll cycle pool

Xu5P xylulose 5-phosphate

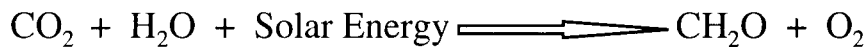
Zea zeaxanthin

## **Chapter One**

### **Introduction**

# 1 General Introduction

Photosynthesis has a well-documented role as the entry point of solar energy into the biosphere and therefore the sustainer of all life on earth. Oxygenic photosynthesis, as carried out by higher plants, utilises sunlight to synthesise energy rich organic compounds from lower energy inorganic materials. The overall process can be represented by the equation:



In addition to providing energy to drive the photosynthetic process light provides a rich and essential source of information for the plant. Perception of the signals provided by the light environment allow for orientation in both space and time leading to a host of responses including stem extension, leaf expansion, chloroplast development, flowering and circadian entrainment. With respect to photosynthesis the ability to sense changes in the light environment and in particular the level of irradiance is vital. At lower irradiance, where light limits the rate at which photosynthesis can proceed, the photosynthetic machinery is optimised to make efficient use of the available light. With increasing irradiance light absorption rises linearly and exceeds the levels at which it can be utilised for photosynthesis, which eventually becomes saturated. At this point the combination of powerful oxidants, required for H<sub>2</sub>O oxidation, and the presence of O<sub>2</sub> can lead to the formation of highly reactive species such as singlet O<sub>2</sub>. These reactive oxygen species are capable of causing great damage to the photosynthetic machinery threatening the viability of the whole organism. Plants have therefore evolved two strategies to sense and respond to changes in irradiance. In the short term the reorganisation of existing photosynthetic components provides photoprotection, mainly by safely dissipating the excess absorbed energy as heat (Horton *et al.* 1996).

On the other hand sustained changes in the levels of irradiance, i.e. hours, days and weeks, are accommodated by the selective synthesis and degradation of the photosynthetic apparatus (Anderson *et al.* 1995). This long-term response to growth irradiance, termed photosynthetic acclimation, forms the basis of this thesis and one of the aims of this chapter is to give a detailed description of our current understanding of the subject. In addition a complete description of the fundamental process and the molecular components of oxygenic photosynthesis in higher plants is provided. Short-term responses to changes in irradiance are also considered.

## 1.1 The chloroplast

In higher plants photosynthesis takes place exclusively in the chloroplast, a subcellular organelle that is generally located in the mesophyll tissue of leaves. Remarkably the chloroplast is believed to be a descendant of the photosynthetic prokaryotes, probably the Cyanobacteria (Dalwiche and Palmer 1997). Each chloroplast contains its own DNA and RNA and for most plant species DNA replication takes place almost entirely independent of the cell nucleus. Despite this a number of chloroplast proteins are encoded for by nuclear genes and translated on cytoplasmic ribosomes before import into the organelle. As illustrated in figure 1.1 the chloroplast, which resides in the cytosol, is surrounded by a double outer membrane often termed the envelope. This double membrane encompasses a cytosol like matrix known as the stroma. Embedded within the stroma are the lamellae, or thylakoids as they are otherwise known, which enclose a space that is separate from the stroma called the lumen. The thylakoid membrane houses a number of supramolecular complexes which are collectively responsible for the light reactions of photosynthesis, while the dark reactions take place

within the stroma. A more complete description of the division of photosynthesis into light and dark reactions can be found in section 1.2. The highly ordered thylakoid membrane system can be further subdivided into two distinct regions; the appressed grana lamellae and the stroma exposed, non appressed, stroma lamellae. This division of thylakoid membranes into grana and stroma lamellae is associated with the spatial segregation of a number of photosynthetic components (section 1.3.5).

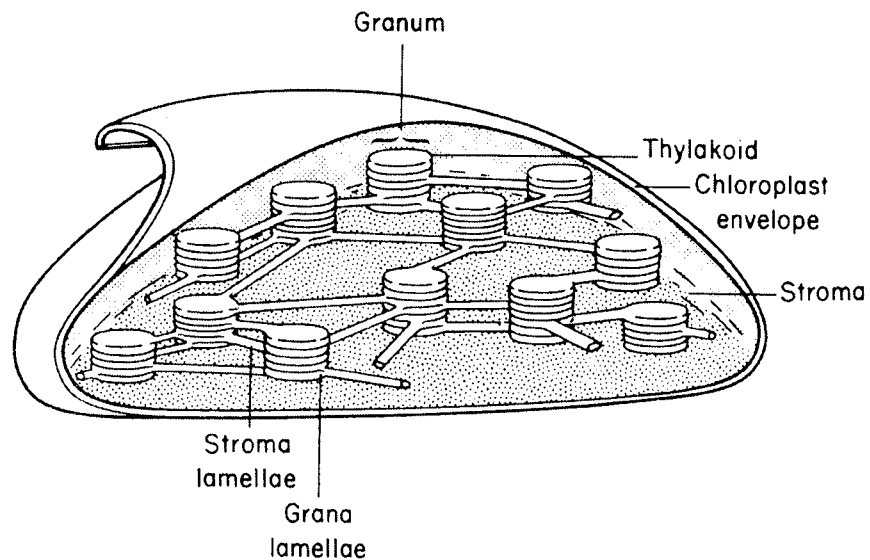


**Figure 1.1** diagram showing chloroplast ultrastructure (from Hall and Rao 1994)

## 1.2 Photosynthesis: the basic reactions

It has long been accepted that oxygenic photosynthesis can be conveniently viewed as a two step mechanism involving a set of reactions that are photochemically driven and therefore light dependant and a series of enzymatic reactions which may proceed regardless of whether or not light is provided. These reactions are respectively referred to as the light and dark reactions of photosynthesis.

### 1.2.1 The Light Reactions

The light reactions take place within the thylakoid membrane and are carried out by four major protein complexes: Photosystem II (PSII), the cytochrome *b<sub>6</sub>f* complex, photosystem I (PSI) and the ATP synthase. They use light energy to drive the endergonic transfer of electrons from H<sub>2</sub>O to NADPH. In addition the flow of electrons is coupled to ATP production by the generation of a proton gradient across the thylakoid membrane. ATP and NADPH generated by the light reactions are then consumed during the light independent fixation of CO<sub>2</sub>. The generation of energy and reducing power by the photosynthetic light reactions can be simply described using two long standing models: the Z scheme and the Chemiosmotic Hypothesis.

### 1.2.2 The Z Scheme

The Z scheme describes the linear flow of electrons from H<sub>2</sub>O to NADPH in oxygenic photosynthesis. Proposed by Hill (1960) it links two photochemical reactions in series by a number of electron carriers, each of which is plotted vertically against its midpoint redox potential (figure 1.2). Furthermore the midpoint potentials are plotted with the more reducing electron carriers above the more oxidising ones so that the thermodynamically favourable reactions run downhill. The diagram is then completed by the use of arrows to connect those components that are known to react with each other. Specific details regarding the flow of electrons through and between individual complexes can be found in section 1.3.

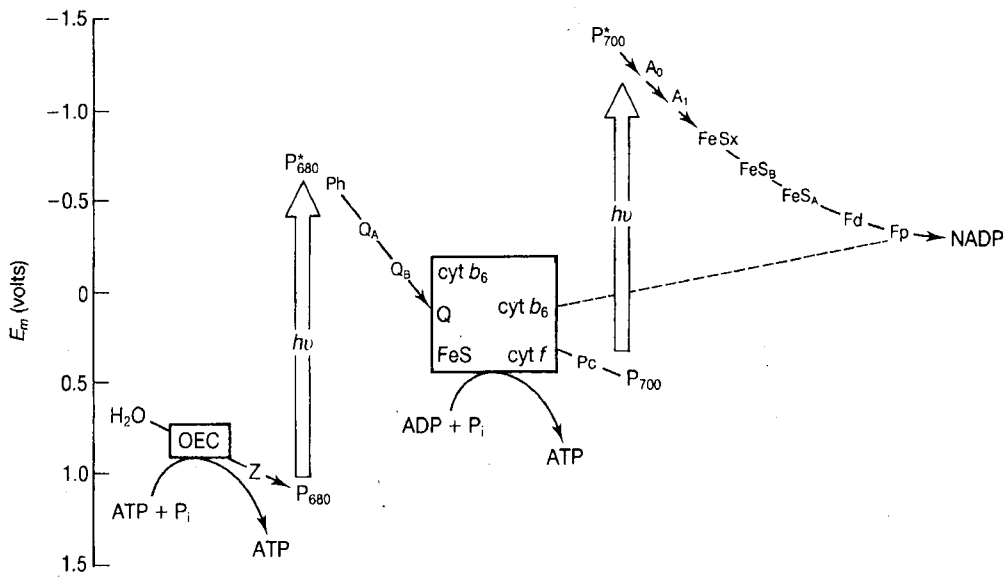


**Figure 1.2** The z scheme for oxygenic photosynthesis. OEC represents the oxygen evolving complex, P680 represents the special chlorophyll pair of photosystem II, the central complex binding cytochrome b6 (cyt b6) and cytochrome f (cyt f) is the cytochrome b6f complex, p700 represents the primary donor of photosystem I and PC represents the mobile electron carrier plastocyanin. (Blankenship and Prince 1985)

### 1.2.3 The Chemiosmotic Hypothesis

The chemiosmotic hypothesis was proposed by Mitchell (reviewed in Mitchell 1966) to account for the coupling of photosynthetic (and mitochondrial) electron transport to the storage of energy in the form of ATP. The hypothesis suggests that in addition to their role as electron donors and acceptors some thylakoid redox components may also accept a proton along. Electron donors, and electron and proton acceptors, are then arranged vectorially in the thylakoid membrane. During photosynthetic electron transport protons are taken up from the stroma and since the next component in the transport chain accepts only the electron the proton is deposited in the thylakoid lumen (figure 1.3).

The thylakoid membrane is almost completely impermeable to the passive transport of protons therefore the translocation of protons into the lumen results in the generation of an electrochemical potential known as the proton motive force (pmf). Finally the energy of the pmf is released during proton flow through a membrane bound coupling factor and utilised for the synthesis of ATP. The thylakoid membrane bound coupling factor, ATP synthase, is covered in detail in section 1.3.4. The reduction and oxidation of plastoquinone by PSII and the cytochrome *b<sub>6</sub>f* complex represents the site at which protons are actively transported across the thylakoid membrane during photosynthetic electron transport. However the removal of protons from the stroma upon the reduction of NADP<sup>+</sup> and the addition of protons to the lumen upon oxidation of H<sub>2</sub>O both contribute to the generation of the pmf .

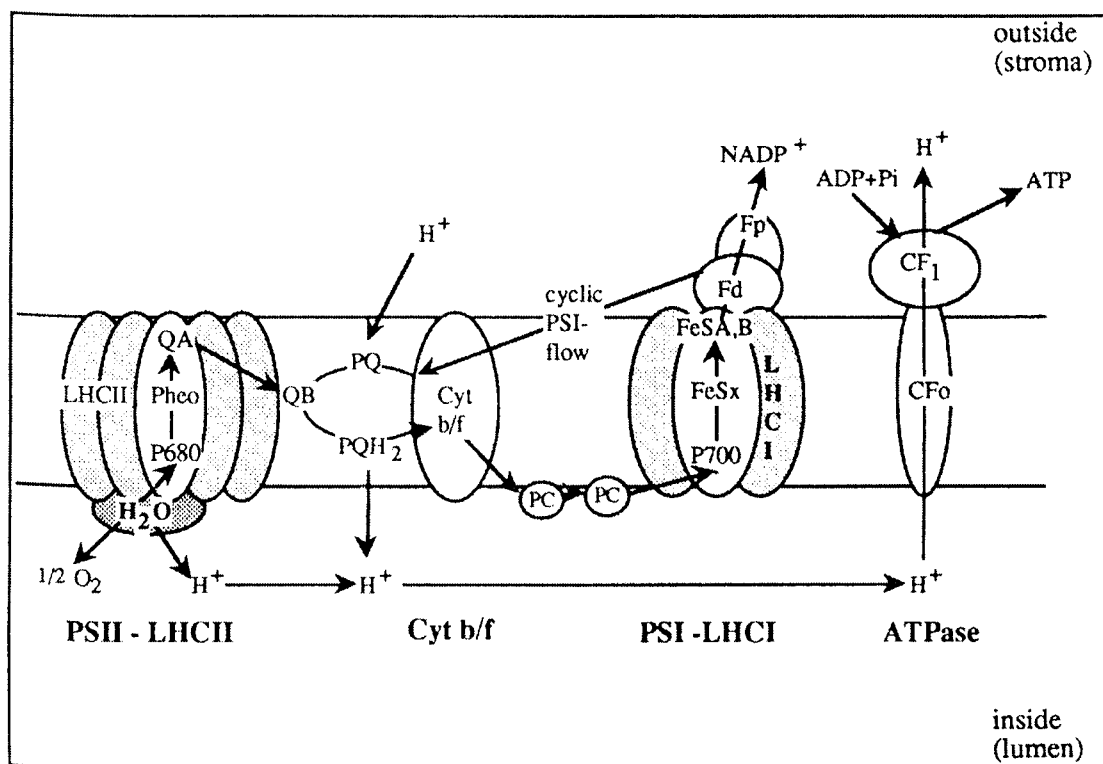


**Figure 1.3** Proton translocation across the thylakoid membrane during electron transport.

## 1.2.4 Cyclic Electron Transport

In addition to linear electron flow from H<sub>2</sub>O to NADP electrons may have alternative fates. One of these alternatives is cyclic electron transport around PSI. As indicated in figure 1.3, cyclic electron flow involves the passage of electrons from reduced ferridoxin back into the electron transport chain downstream of PSI. Since there is no reduction of NADP during this process the only net product is ATP. Although there has been some debate regarding the occurrence of cyclic electron transport in vivo new measuring techniques have served to provide evidence that strengthens the argument for its existence. These include photoacoustic spectroscopy (Malkin and Canaani 1994) and P700 redox state measurements (Harbinson *et al* 1989). The occurrence of cyclic electron transport is therefore now widely accepted however the process has attracted a number of other contentions. It was initially assumed that ferridoxin is the physiological cofactor responsible for mediating cyclic flow and that the cytochrome *b<sub>6</sub>f* complex represents the entry point for electrons back into the electron transport chain. However the initial evidence for this step (Bohme and Cramer 1972) is no longer accepted and it now seems equally likely that electrons are fed back into the plastoquinone pool, possibly via an unidentified enzyme known as ferridoxin-plastoquinone reductase (Cleland and Bendall 1992). The physiological function of cyclic electron transport is also unresolved. One suggestion is that cyclic flow simply serves to increase the ATP/NADPH ratio in order to drive the dark reactions of the Calvin Cycle (section 1.2.5) or to provide ATP for other cellular processes (reviewed in Bendall and Manasse 1994). Alternatively there is evidence that cyclic electron transport significantly contributes to the acidification of the thylakoid lumen thereby playing a role in PSII energy dissipation (reviewed in Heber and Walker 1992).

## 1.2.5 The Dark Reactions

The generation of 'assimilatory power' in the form of ATP and NADPH by the photosynthetic light reactions serves to drive the reduction of CO<sub>2</sub> to the level of carbohydrate during the light independent, or dark reactions of photosynthesis. The mechanism of CO<sub>2</sub> fixation, known as the Calvin cycle, or reductive pentose phosphate cycle, takes place in the stroma and can essentially be broken down into three phases (figure 1.4). Step one is carboxylation during which CO<sub>2</sub> reacts with the 5 carbon sugar, ribulose 1,5-bisphosphate, to form 2 molecules of phosphoglyceric acid (PGA). This reaction is catalysed by the multisubunit enzyme Rubisco. The next phase of the Calvin cycle is the reduction of the low energy organic acid PGA to form an energy rich triose phosphate, phosphoglyceraldehyde. The conversion of PGA to the 3-carbon sugar requires two steps and the input of energy and reducing power in the form of ATP and NADPH. At this stage CO<sub>2</sub> has been reduced to the level of carbohydrate and the triose phosphate may be used for the synthesis of starch in the chloroplast or exported for sucrose synthesis in the cytosol. However, in order to continue, the Calvin cycle must regenerate the acceptor for the carboxylation step, ribulose 1, 5-bisphosphate. The third and final step of the Calvin cycle therefore requires that five out of every six molecules of triose phosphate formed must enter a series of reactions to regenerate 3 molecules of ribulose 1, 5-bisphosphate.

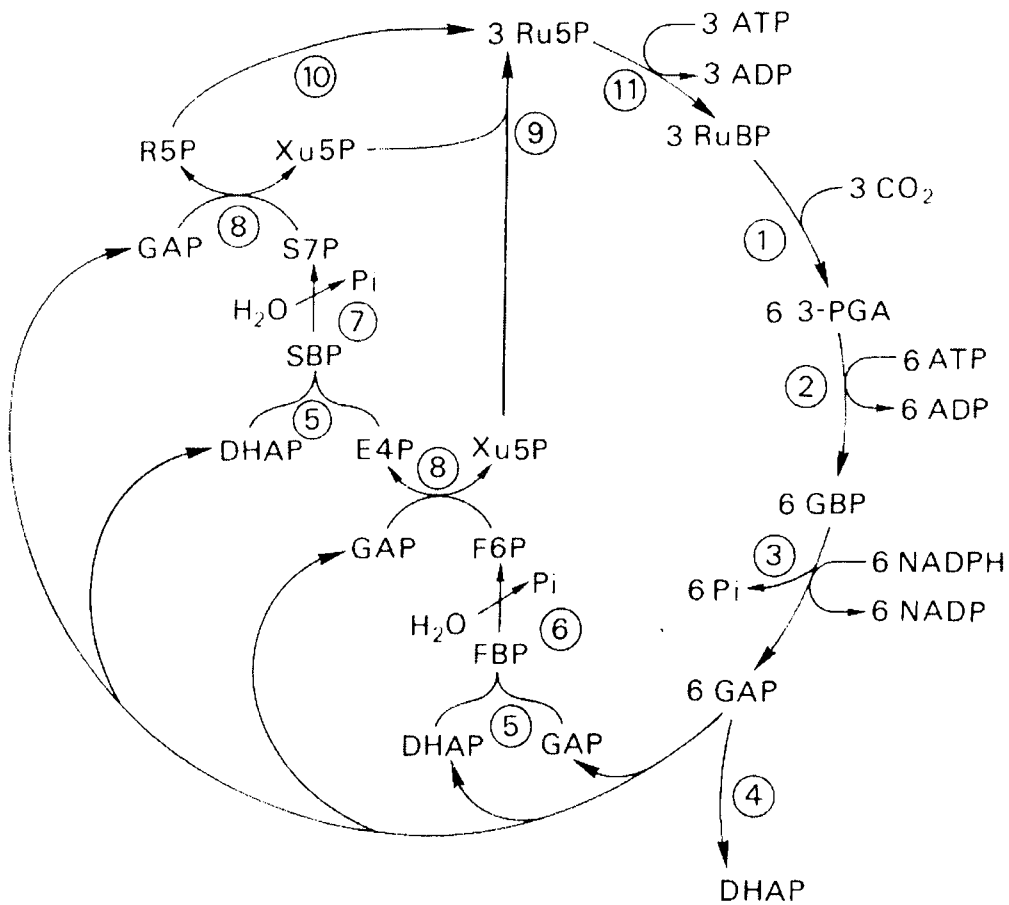


**Figure 1.4** The Calvin Cycle. Enzymes responsible for each step are numbered as follows: 1. Rubisco, 2. 3-phosphoglycerate kinase, 3. glyceraldehyde-3-phosphate dehydrogenase, 4. triose phosphate isomerase, 5. aldolase, 6. fructose-1,6-bisphosphate phosphatase, 7. sedoheptulose-1,7-bisphosphate phosphatase, 8. transketolase, 9. ribulose-5-phosphate epimerase, 10. ribose-5-phosphate isomerase (Leegood 1990). For abbreviations of metabolites see list of abbreviations.

## 1.3 Thylakoid Membrane Components

### 1.3.1 Photosystem II

Photosystem II (PSII) catalyses the light dependant transfer of electrons from H<sub>2</sub>O to the membrane soluble redox mediator, plastoquinone. In doing so light energy is captured as it is converted to chemical energy following a photochemical event which sees the rapid separation of charge across the thylakoid membrane. Structurally PSII is complex, comprising well over 20 polypeptide subunits. These subunits are associated with three functionally distinct regions of the photosystem: the reaction centre core including a tightly bound proximal antenna, the oxygen evolving complex and the chlorophyll *a/b* binding distal antenna.

#### 1.3.1.1 Photosystem II function: charge separation and electron transfer.

The first step in PSII charge separation is the conversion of the primary electron donor, P680, from a weak to a strong reductant, P680\*. P680, which is believed to be comprised of two chlorophyll molecules (Durrant *et al* 1995), becomes unstable when excited to P680\* and readily gives up an electron to a nearby molecule of pheophytin. This primary charge separation results in the formation of the radical pair P680<sup>+</sup>Pheo<sup>-</sup>. In order to stabilise the charge separation Pheo\* rapidly transfers an electron to the first stable electron acceptor, Q<sub>A</sub>, giving rise to P680<sup>+</sup> Pheo Q<sub>A</sub><sup>-</sup>. This reaction takes place in 250-500 picoseconds. Since the reverse reaction is now several orders of magnitude slower, charge separation is effectively complete and energy capture is ensured. P680\* is rereduced by a nearby tyrosine residue on the D1 polypeptide, named Z or Yz (Hoganson *et al* 1995), which in turn receives electrons derived from water via the

manganese cluster of the oxygen evolving complex (section 1.3.1.2.2). Electron transport on the reducing side of PSII continues as  $Q_A^-$  passes its electron on to  $Q_B$ , a plastoquinone molecule which associates with PSII at the  $Q_B$  binding site. This transfer of electrons is facilitated by a non heme iron situated between  $Q_A$  and  $Q_B$  (Diner *et al* 1991). The plastoquinone molecule remains bound while a second photochemical event serves to reduce it to a fully reduced plastoquinol with the uptake of two protons from the stroma. Plastoquinol is then released from the  $Q_B$  binding site to the plastoquinone pool. This process of coupling the single electron events of the primary reactants of PSII with the two step reduction of plastoquinone at the  $Q_B$  binding site is often referred to as a two electron gate (Velthuys 1981).

### **1.3.1.2 Structural Aspects of Photosystem II**

#### **1.3.1.2.1 Reaction Centre Core**

The core complex of the PSII reaction centre is composed of four chlorophyll *a* binding polypeptides and two distinct heme binding proteins. In addition to chlorophyll *a* and heme the core also binds small amounts of the carotenoids  $\beta$ -carotene and lutein as well as the cofactors involved in electron transfer. The chlorophyll *a* binding proteins fall into two categories: those associated with binding the PSII electron transfer components and those associated with light harvesting. The two polypeptides responsible for binding PSII electron transfer components are the products of the *psbA* and *psbD* genes, named D1 and D2 respectively. D1 and D2 form a heterodimeric structure which collectively binds P680 along with at least two other molecules of chlorophyll *a* (Namba and Satoh 1987) and a non heme iron. In addition the D1/D2 heterodimer binds

pheophytin,  $Q_A$  and  $Q_B$  with all but  $Q_A$  being assigned to the D1 polypeptide which also incorporates  $Y_Z$ . The chlorophyll *a* binding polypeptides of the reaction centre core that are involved in light harvesting are the *psbB* gene product, CP47, and the *psbC* gene product, CP43. These two polypeptides, which collectively bind around 50 chlorophyll *a* molecules (Bassi *et al* 1992), absorb at wavelengths that are close to that of the PSII primary donor but longer than those of the distal antenna. This observation suggests that CP43 and CP47 may function to couple energy transfer between the distal antenna and P680 (van Grondelle 1985). The structural importance of CP43 and CP47 is highlighted by the use of site directed mutagenesis in cyanobacteria with the loss of either one or both polypeptides impairing the assembly of the reaction centre core (Vermaas *et al* 1988). However it is possible to isolate a PSII reaction centre that comprises all components of the core, except for CP43 and CP47, that still undergoes charge separation (Danielus *et al* 1987). In addition to their association with the reaction centre core CP43 and CP47 may play a role in the assembly of functional, oxygen evolving, PSII reaction centres through their interaction with the 33KDa polypeptide of the oxygen evolving complex (Enami *et al* 1997, Bricker and Frankel 1998).

The PSII reaction centre core contains at least one heme, cyt b559. Two polypeptide subunits of 4 and 9 kDa each provide histidine residues for the co-ordination of the heme, which may be present in two copies per reaction centre core (Tae *et al* 1988). A physiological function for cyt b559 has not yet been assigned although a number of suggestions have been put forward including a possible role in photoprotection (Thompson and Brudvig 1988), proton pumping (Arnon and Tang 1988) and PSII cyclic electron flow (Falkowski *et al* 1986). A number of low molecular weight intrinsic proteins are also associated with the reaction centre core although their function is currently unclear.

### 1.3.1.2.2 Oxygen Evolving Complex

The unique feature of the PSII reaction centre is its ability to produce molecular oxygen from water upon illumination. The periodicity of oxygen evolution from dark adapted PSII following single turnover flashes reveals the accumulation of four reducing equivalents prior to the release of O<sub>2</sub>. This observation shows that a water splitting complex cycles through four different oxidation states as electrons are transferred through PSII (Kok *et al* 1970). These four oxidation states, named S-states, represent the accumulation of four oxidising equivalents of sufficient potential to release O<sub>2</sub> from H<sub>2</sub>O. It is now known that the water splitting complex in Kok's S-state model has a cluster of four manganese atoms at the catalytic site (Renger 1993) which are stabilised by three extrinsic proteins located at the luminal surface of the thylakoid membrane (Vermaas *et al* 1993). So far little is known about the specific role of the three extrinsic polypeptides, which have apparent molecular weights of 33, 23 and 16 kDa. It is clear however that the interaction of these polypeptides with the intrinsic proteins of the reaction centre core and the manganese cluster is essential for the formation of a fully functional oxygen evolving complex. It is possible that the 33 kDa polypeptide, which is known to interact with CP47, may play a role in the stabilisation of the manganese cluster (Bricker and Frankel 1998). In addition it has been proposed that all three extrinsic polypeptides form a compartment for the creation of high local concentrations of Ca<sup>2+</sup> and Cl<sup>-</sup> at the water splitting site.

### 1.3.1.2.3 PSII Distal Antenna

The distal antenna of photosystem II is comprised of six closely related chlorophyll *a/b* binding proteins. The high degree of homology between the genes encoding these proteins has given them the status of a protein/gene superfamily whose members also include the chlorophyll *a/b* binding proteins of the photosystem I light harvesting antenna (Jansson 1994). A consensus nomenclature for the members of this superfamily has been agreed (Jansson *et al* 1992) and this will be used throughout this thesis. However a number of other methods for naming the chlorophyll *a/b* binding proteins can still be found in the literature (table 1) and these may be referred to where appropriate.

The component proteins of the distal antenna can be subdivided into two categories: the major LHCII complex and the minor LHCII complexes, often referred to as CP29, CP26 and CP24. The most abundant component of the distal antenna is the major or bulk LHCII. This chlorophyll-protein complex accounts for up to one third of the total thylakoid protein and binds up to half the total chlorophyll (Bassi *et al* 1996). It was originally characterised by its migration on polyacrylamide gels of detergent solubilised thylakoid membranes (Thornber 1975). Bulk LHCII can also be distinguished by its detachment and migration away from PSII toward PSI, to which it is believed to transfer energy, following reversible phosphorylation (section 1.5.3, reviewed in Allen 1995). It is now known that this fraction of LHCII is composed of the gene products of *Lhcb1* and *Lhcb2* which are present in almost all preparations regardless of the method. Some preparations also contain the gene product of *Lhcb3* although it is still unclear to what extent this polypeptide associates with *Lhcb1* and *Lhcb2* (Knoetzel and Simpson 1996). The oligomeric form of LHCII *in vivo* is believed to be that of the trimer with all possible mixed trimers of *Lhcb1/Lhcb2* being present. These mixed trimers have been assigned a peripheral location in most PSII models where they are believed to be the component responsible for variable PSII antenna size (Spangfort and Andersson 1989,

Jansson 1994). The structure of LHCII from higher plants has been resolved at 3.4Å resolution using two-dimensional electron crystallography (Kuhlbrandt 1994). From the structure each LHCII monomer is seen to be composed of three transmembrane spanning  $\alpha$ -helical domains connected by stroma and lumen exposed hydrophilic loops (figure 1.5). N and C-terminal peptides are also exposed in the stroma and lumen respectively. Trans-membrane helices A and B, which show two-fold symmetry, are tilted 320° relative to the membrane plane forming an X-shaped structure which is held together by charged pairs of amino acid residues from both helices. The C helix is smaller than helices A and B and is tilted only 90° relative to the membrane plane. A small amphipathic helix at the C terminus was also revealed, while the presence of a stroma exposed helix at the N-terminus is only suggested from secondary structure predictions. The structure also revealed 12 chlorophyll molecules per LHCII monomer, which have been assigned as 7 chlorophyll *a* and 5 chlorophyll *b* on the basis of biochemical data suggesting a Chl *a/b* ratio of 1.4 for highly purified LHCII (Bassi *et al* 1993). At 3.4Å resolution it is not possible to determine the small structural differences between chlorophyll *a* and *b*. Energetic considerations were therefore used to assign all 7 chlorophyll *a* as those that lie closest to two carotenoid molecules which were resolved on either side of helices A and B. These carotenoid molecules, which form a 'cross brace' at the centre of the monomer, have been tentatively identified as luteins since violaxanthin and neoxanthin are the only other pigments known to associate with LHCII and these are present in substoichiometric amounts

	Gene product/pigment protein complex		
Gene	Green <i>et al</i> 1991	Thornber <i>et al</i> 1991	Bassi <i>et al</i> 1991
<i>Lhca1</i>	Type I LHC1	LHC 1b	LHC1-730
<i>Lhca2</i>	Type II LHC1		LHC1-680
<i>Lhca3</i>	Type III LHC1	LHC 1a	LHC1-680
<i>Lhca4</i>	Type IV LHC1	LHC 1b	LHC1-730
<i>Lhcb1</i>	Type I LHCII	LHCIIb 28 kDa	LHCII
<i>Lhcb2</i>	Type II LHCII	LHCIIb 27 kDa	LHCII
<i>Lhcb3</i>	Type III LHCII	LHCIIb 25kDa	LHCIIa
<i>Lhcb4</i>	Type II CP29	LHCIIa	CP29
<i>Lhcb5</i>	Type I CP29	LHCIIc	CP26
<i>Lhcb6</i>	CP24	LHCII d	CP24

**Table 1.** Nomenclature for the chlorophyll *a/b* binding proteins (adapted from Jansson *et al* 1992)

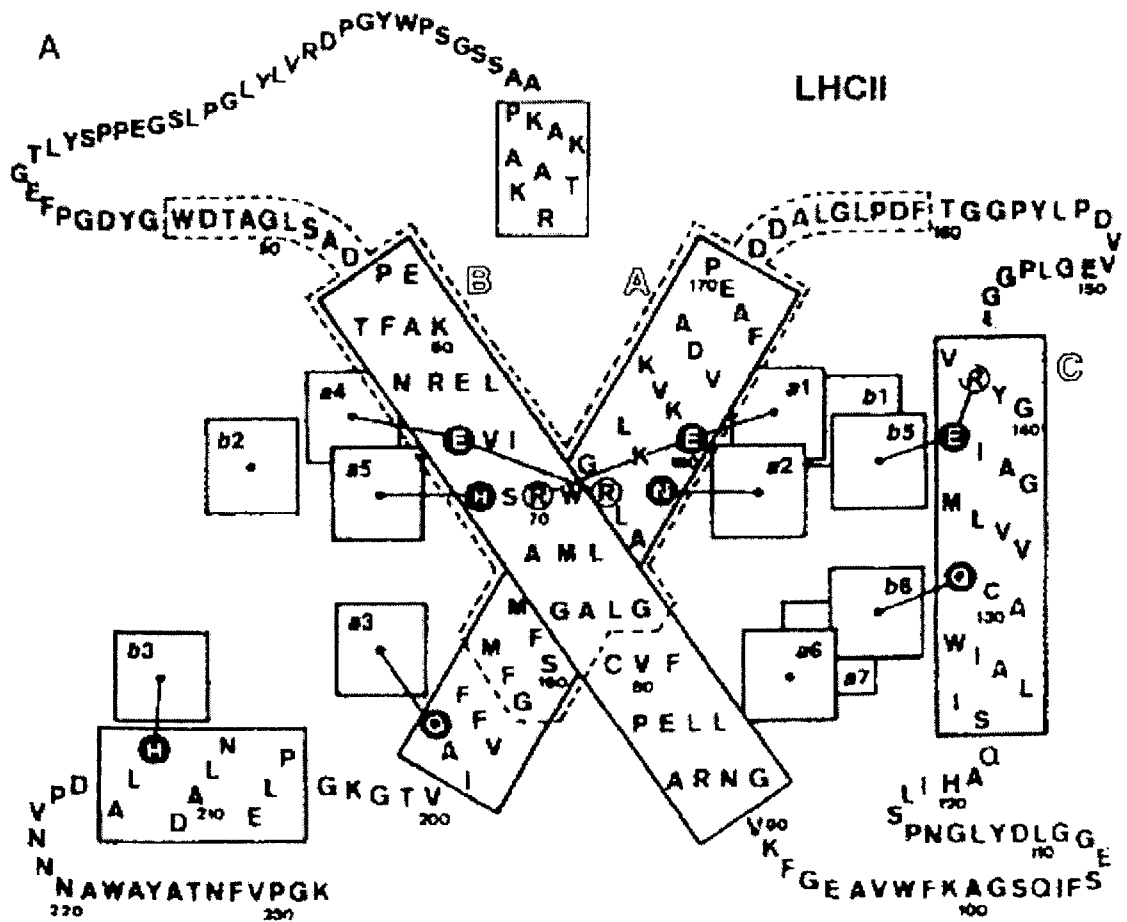


**Figure 1.5** Plan of LHCII structure showing polypeptide arrangement in the membrane and chlorophyll side chain ligands (from Bassi *et al* 1996).

Given the high degree of homology between the chlorophyll *a/b* binding polypeptides, particularly in the membrane spanning regions, it is possible to use the LHCII structure to infer models for the minor components of the PSII distal antenna. The main structural features described for LHCII therefore apply to Lhcb4, 5 and 6. However these minor components do differ from LHCII in that they are probably present as monomers in much lower stoichiometric amounts relative to PSII, these stoichiometries are believed to be fixed relative to PSII and to each other (Jansson 1994), they are less peripherally situated (Bassi *et al* 1990), they have higher Chlorophyll *a/b* ratios and they

bind greater amounts of violaxanthin while Lhcb6 binds no neoxanthin (Bassi *et al* 1996). A recent study suggested that while the minor components Lhcb4 and Lhcb5 show significant homology with bulk LHCII polypeptides they are more closely related to each other with both proteins binding six chlorophyll a and two chlorophyll b molecules (Pascal *et al* 1999). The major differences in these two polypeptides appeared to occur in the carotenoid binding.

#### 1.3.1.2.4 PSII Subunit Organisation

Several models have been proposed to account for the organisation of the subunit components of PSII, based largely on the results of a number of independent biochemical studies (Peter and Thornber 1991, Jansson 1994). More recent models have made use of single particle imaging and 2-dimensional electron crystallography to provide projection maps of PSII complexes at 15-40 Å (Hankamer *et al* 1997). However the precise location of individual components within these models still relies heavily on the existing biochemical and cross linking data used to compose previous models. Figure 1.6 shows two possible models based on both projection mapping and biochemical data. Both models are based on the view that PSII particles exist as dimers in the grana. They differ only in the organisation of the PSII core components. The inability to definitively assign core components within the projection map arises mainly from the lack of cross linking data to confidently locate the proximal antenna subunit CP43. The location of LHCII could however be confidently assigned at the outer most tips of the complex by super imposing a high resolution electron density map of the Lhcb1/Lhcb2 trimer upon the projection map. Trimeric LHCII has also since been shown to bind to PSII in three different positions (Boekema *et al* 1999) with at least one

position placing LHCII and Lhcb4 in close proximity as previously indicated by nearest neighbour cross linking studies (Miao *et al* 1998). In addition a heptameric LHCII supercomplex has been revealed in detergent solubilised thylakoid membranes (Dekker *et al*, in press).

Furthermore the minor distal antenna components, Lhcb4 and 5, could be fitted between LHCII and the reaction centre core using cross linking data and electron density maps of monomers based on Kuhlbrandts' high resolution structure. Lhcb3 and Lhcb6 could not be fitted to the maps because of their absence from isolated PSII-LHCII supercomplexes although Lhcb6 has been fitted to a more recent map of PSII (Boekema *et al* 1999).

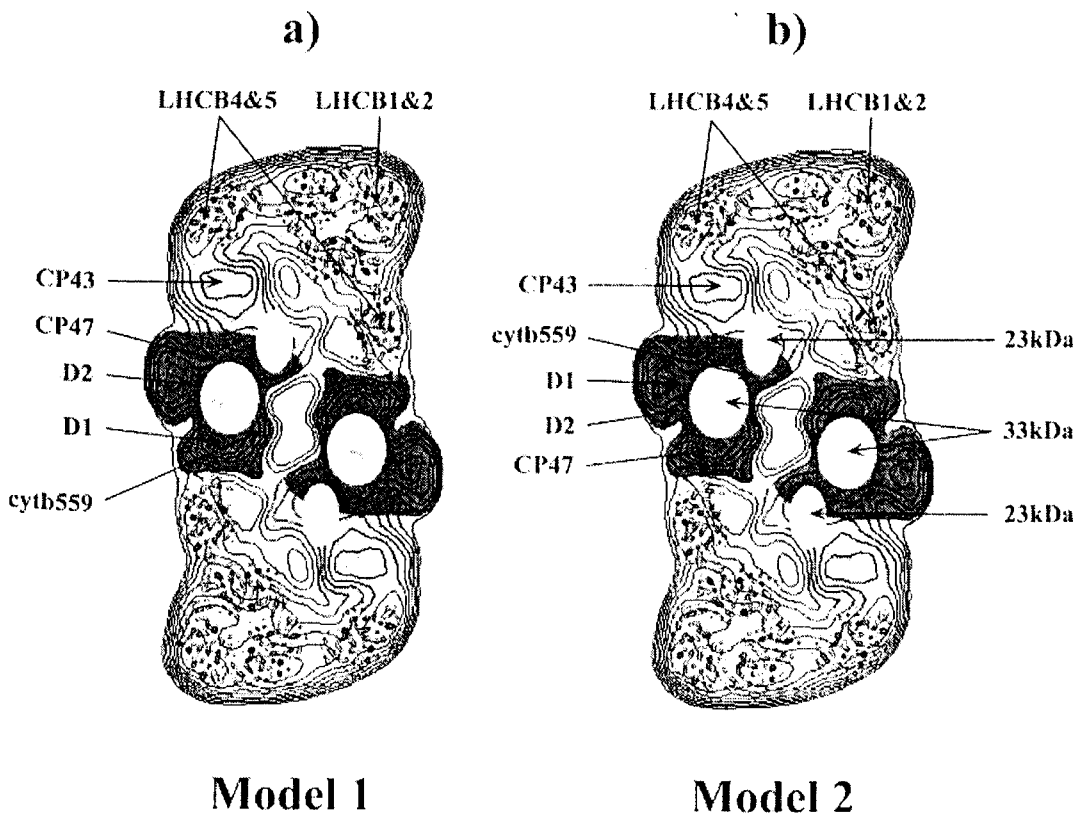


**Figure 1.6** Models showing subunit organisation of PSII (Hankamer *et al* 1997).

### 1.3.1 Cytochrome $b_6f$ complex

The Cytochrome  $b_6f$  complex functions as an oxidoreductase coupling the two electron oxidation of plastoquinone to the one electron reduction of plastocyanin. In addition to its role as an electron mediator the cytochrome  $b_6f$  complex plays a part in the translocation of protons across the thylakoid membrane, since the oxidation of plastoquinol results in the release of protons into the thylakoid lumen while the reduction of plastoquinone by PSII involves the uptake of protons from the stroma. The complex contains four protein bound redox centres: two b-type hemes, one c-type cytochrome and a  $\text{Fe}_2\text{S}_2$ -centre. The two b-type hemes are bound by a single chloroplast encoded polypeptide to form cytochrome  $b_6$  while the c-type cytochrome is associated with a chloroplast encoded polypeptide to form cytochrome  $f$ . In contrast the  $\text{Fe}_2\text{S}_2$ -centre is bound by a nuclear encoded polypeptide named the Rieske iron-sulphur protein. A third chloroplast encoded polypeptide known as subunit IV and three low molecular weight polypeptides are also present. The complex is widely believed to form a dimer in vivo, the functional significance of which is assumed to be related to the translocation of protons (Huang *et al* 1994).

The precise details of electron flow through the cytochrome  $b_6f$  complex are still not fully understood. One long standing model for electron transfer and proton translocation, known as the Q cycle, remains popular because it explains the frequently observed phenomenon that two protons are translocated for every electron transfer. (Mitchell 1976, Rich 1988). This increased  $\text{H}^+/\text{e}^-$  ratio may also account, in part, for the higher levels of ATP often assumed to be required for  $\text{CO}_2$  fixation (Bendall and Menasse 1995). The mechanism of the Q cycle requires that a molecule of plastoquinol binds to the cytochrome  $b_6f$  complex near the lumenal surface of the thylakoid membrane while a molecule of plastoquinone binds near the stromal surface (figure

1.7). The plastoquinol then gives up an electron to the Rieske iron sulphur centre which subsequently reduces plastocyanin via cytochrome *f*. Reduced plastocyanin is released from its binding site on cytochrome *f* to be replaced by a molecule of oxidised plastocyanin. The semiquinone intermediate formed by the oxidation of plastoquinol is not stabilised at the plastoquinol binding site giving the molecule sufficient reducing power to give up its electron to one of the b-type hemes of cytochrome *b<sub>6</sub>*. This heme is known as the low potential *b<sub>6</sub>* because its measured midpoint redox potential is over 100 mV lower than that of the second b-type heme of cytochrome *b<sub>6</sub>* which is therefore known as the high potential *b<sub>6</sub>*. The high potential *b<sub>6</sub>*, which is located close to the plastoquinone binding site, oxidises the low potential *b<sub>6</sub>* before reducing the bound molecule of plastoquinone. The semiquinone formed from this reaction is stabilised by the complex and it remains bound while a second plastoquinol molecule replaces the plastoquinone at the luminal side binding site to initiate a second turnover of the complex through the same series of reactions described above. This time the high potential *b<sub>6</sub>* reduces the stabilised semiquinone to form a plastoquinol molecule which is released back into the plastoquinone pool. Following two turnovers of the cytochrome *b<sub>6</sub>f* complex the Q-cycle achieves the translocation of four protons across the thylakoid membrane for every plastoquinol oxidised, since two plastoquinols are oxidised and one plastoquinone is reduced.

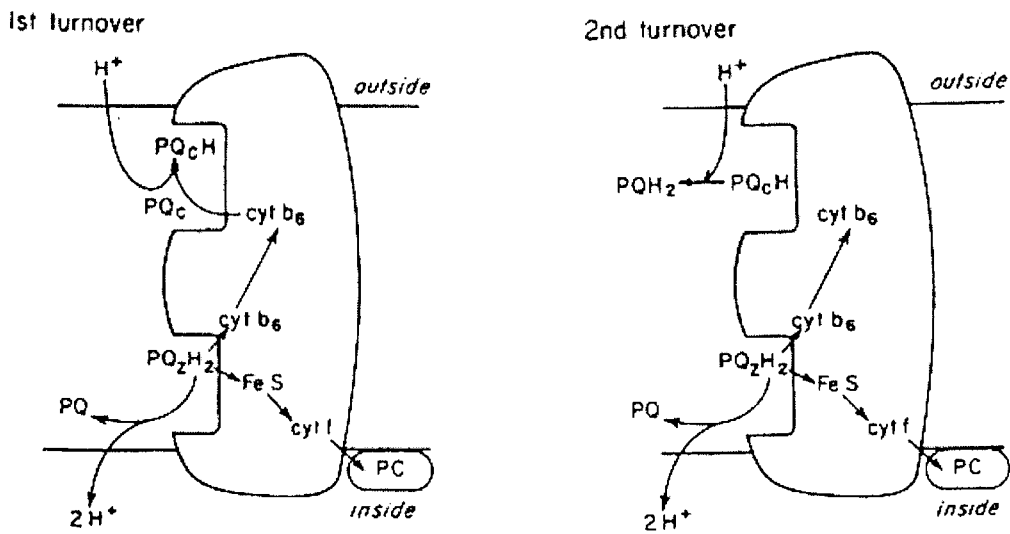


**Figure 1.7** Q-cycle model for the oxidation of plastoquinol by the cytochrome b<sub>6</sub>f complex (Ort and Whitmarsh 1996).

### 1.3.3 Photosystem I

The Photosystem I (PSI) reaction centre catalyses the light dependant transfer of electrons from reduced plastocyanin to the iron sulphur protein ferridoxin, which subsequently reduces NADP via ferridoxin-NADP reductase (FNR) during linear electron flow. As with PSII, light energy is converted to chemical energy by PSI following a photochemical event which sees the separation of charge stabilised by the rapid spatial displacement of electrons across the thylakoid membrane. The photosystem I complex is comprised of around 18 polypeptides which are associated with either the core sub-complex, responsible for charge separation, or light harvesting.

#### 1.3.3.1 Photosystem I function; charge separation and electron transfer

Charge separation within Photosystem I begins with the absorption of a photon by the primary electron donor P700, believed to be a *chlorophyll a* dimer (Moenne-Loccoz *et al* 1990, Krause *et al* 1990). Excited P700 then reduces the primary acceptor, a *chlorophyll a* monomer known as A<sub>0</sub>. The timescale for primary charge separation is believed to be in the pico to sub-picosecond range (Hastings *et al* 1994). Charge separation is then further stabilised by rapid electron transfer across the thylakoid membrane. The first intermediate acceptor in the transfer of electrons away from A<sub>0</sub> is the phyloquinone, A<sub>1</sub>, which reoxidises A<sub>0</sub> in the 20-30 picosecond timescale. Three iron-sulphur centres then mediate the transfer of electrons from A<sub>1</sub> to the soluble electron carrier ferridoxin. Although it is known that the iron sulphur centre F<sub>x</sub> reoxidises A<sub>1</sub>, the order of electron flow through the iron sulphur centres F<sub>A</sub> and F<sub>B</sub> to ferridoxin remains contentious (Malkin 1996). During linear flow from H<sub>2</sub>O to NADP, ferridoxin oxidation and NADP reduction is mediated by the thylakoid associated stromal enzyme FNR. The re-reduction of P700 by the lumen soluble electron carrier plastocyanin takes place in the microsecond timescale to set up another turnover of the reaction centre upon photon absorption.

### 1.3.3.2 Structural Aspects of Photosystem I

#### 1.3.3.2.1 Reaction Centre Core

The photosystem I reaction centre core is responsible for photochemical charge separation and electron transfer. PSI core complexes capable of the photooxidation of plastocyanin and the photoreduction of ferridoxin have been isolated and shown to contain 10-14 polypeptide subunits, approximately 100 *chlorophyll a* molecules, a number of  $\beta$ -carotenes, two phyloquinones (vitamin K<sub>1</sub>) and three Fe<sub>4</sub>S<sub>4</sub> iron sulphur

clusters (Nechushtai *et al* 1996). The polypeptide subunits of the PSI core, some of which are nuclear encoded and some chloroplast encoded, are all believed to be present as one copy per P700 (Scheller *et al* 1989). Two high molecular weight subunits, PsaA and PsaB, bind almost all of the chlorophyll *a* molecules associated with the reaction centre core including the P700 chlorophyll *a* dimer. In addition these homologous polypeptides bind the electron transfer components  $F_x$  and  $A_1$  as well as 12-16 molecules of  $\beta$ -carotene. The remaining electron transfer components  $F_A$  and  $F_B$  are accommodated by PsaC. All other subunits of the PSI core have accessory functions which include docking of the mobile electron carriers and interaction with light harvesting polypeptides (reviewed in Chitnis *et al* 1995).

#### **1.3.3.2.2 Light Harvesting**

The light harvesting antenna of photosystem I is comprised of four polypeptide subunits, Lhca1, 2, 3 and 4, collectively referred to as LHCI. All four polypeptides bind both *Chlorophyll a* and *b* and are members of the nuclear encoded gene family that includes the PSII distal antenna subunits (section 1.3.1.2.3). In addition to chlorophyll, Lhca polypeptides bind the carotenoids lutein, violaxanthin and  $\beta$ -carotene (Bassi *et al* 1996). Two LHCI sub-complexes have been defined according to their low temperature fluorescence emission. Lhca1 and Lhca4 form the subcomplex LHCI-730 while Lhca2 and Lhca3 form LHCI-680, which are suggested to give characteristic 77K fluorescence emission peaks at 730 and 680 nm respectively (Ikeuchi 1991).

#### **1.3.3.2.3 Photosystem I subunit organisation**

A number of lines of experimental evidence have been used to infer the overall subunit organisation of the PSI reaction centre. These experiments have been conducted with a number of photosynthetic organisms including plants, algae and cyanobacteria. Despite some differences between the plant and cyanobacterial reaction centre, including the presence of the *Chlorophyll a/b* binding light harvesting polypeptides and three additional core subunits for the plants, there remains a high degree of structural and functional homology (Goldbeck 1992), permitting data to be applied universally. Information relating to the global shape and size of PSI has been provided by negatively stained electron microscopy, a technique that also made possible the prediction that 8 LHCI subunits must associate with each PSI reaction centre complex (Boekema *et al* 1991). Some detailed structural information relating to the PSI reaction centre core has been obtained from the X-ray crystal structure determined at 6Å resolution (Krauss *et al* 1993) and more recently at 4Å (Schubert *et al* 1997). Although the resolution of the structure is relatively low sufficient data was obtained to assign 89 chlorophyll *a* molecules and most of the electron carriers. In addition 34 trans-membrane and 9 surface  $\alpha$ -helices have been identified (figure 1.8). Data on the organisation of the individual subunits within the complex and their orientation within the membrane has also been demonstrated. Topological studies, including theoretical predictions, protease treatments and salt washes have previously been employed with significant effect to determine which subunits are located on the stromal or luminal surface of the membrane and which parts of the polypeptide chain of integral subunits are exposed (Nechustai *et al* 1996). These studies reveal that at least 3 subunits, PsaC, D, and E are peripheral on the stromal side of the membrane. All three polypeptides have also been identified in the crystal structure. In the higher plant reaction center one subunit, PsaN is peripheral on the luminal surface. All other PSI subunits are integral membrane proteins although many have peripheral domains. In addition to high resolution

structural data chemical cross linking analysis can be employed to provide information concerning the relative position of PSI subunits within the complex. When coupled to existing PSI data, in particular topological data, cross linking studies allow reasonable models of PSI subunit organisation to be generated. One such model has been derived from the use of chemical cross linking in conjunction with diagonal electrophoresis (Jansson *et al*1996). In this model subunits PsaD, H, J and I are placed on one side of the complex while PsaE, F and J are on the other. Symmetry is also maintained with the placing of subunits G and K on opposite sides of the complex where they associate with light harvesting polypeptides. In keeping with other studies, LHCI polypeptides are found to be arranged as dimers although the existence of homodimer formation is not excluded.

#### **1.3.4 ATP Synthase**

During photosynthetic electron transport energy is captured in the form of a trans-membrane proton gradient, which is used to generate ATP from ADP and Pi by the action of the CF1 - CF0 ATP synthase. This thylakoid membrane protein complex is composed of more than 20 polypeptides arranged in a bipartite structure. A membrane intrinsic moiety, CF0, is responsible for proton translocation while CF1, the stroma exposed peripheral component performs the task of ATP synthesis. CF0 is made up of four polypeptides named I, II, III and IV. Three of these polypeptides, I to III are present in single copy per CF0. IV on the other hand is present in multiple copies. Five different polypeptides make up CF1:  $\alpha$ ,  $\beta$ ,  $\gamma$ ,  $\delta$  and  $\epsilon$ . Two of these,  $\alpha$  and  $\beta$ , form a large hetero-hexamer believed to be the main catalytic subunit. All other CF1 polypeptides are present in single copy. The catalytic mechanism of ATP synthesis has

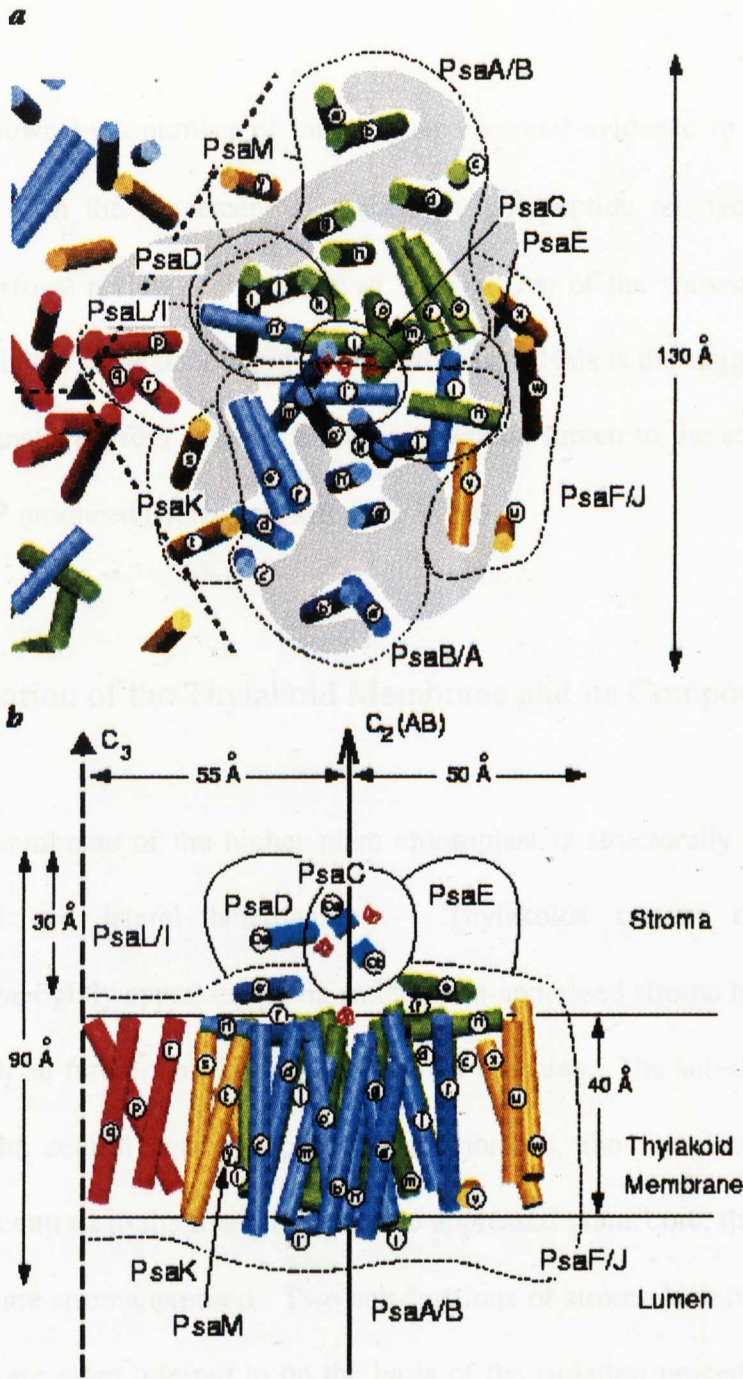


**Figure 1.8** Model showing the subunit organisation of PSI from the 4 Å resolution crystal structure. Above figure shows top view while bottom figure shows side view.

(from Schubert et al 1997)

recently been shown by a number of lines of experimental evidence to involve inter-subunit rotation with the movement of the CF1  $\gamma$  polypeptide relative to the  $\alpha_3\beta_3$  hetero-hexamer (for a review see Junge *et al* 1997). One of the consequences of the recent advances in the understanding of ATP synthase catalysis is the suggestion that the enzyme must translocate four protons from the thylakoid lumen to the stroma for each molecule of ATP produced (Berry and Rumberg 1996).

### 1.3.5 Organisation of the Thylakoid Membrane and its Components

The thylakoid membrane of the higher plant chloroplast is structurally complex with both transverse and lateral heterogeneity. Thylakoids consist of two main compartments, the tightly appressed grana and the non-appressed stroma lamellae. Each compartment can be further subdivided into distinct domains. The sub-domains of the grana include the central core of appressed membranes, the margins and the end membranes. In contrast to the membranes of the appressed grana core, the margins and end membranes are stroma exposed. Two sub-fractions of stroma lamellae can also be isolated. These are often referred to on the basis of the isolation procedure as T3 and Y100 (Jansson *et al* 1997). T3 represents the membrane fraction that connects the more extremely stromal exposed Y100 domains to the grana. Lateral heterogeneity of the thylakoid membrane extends to the distribution of the four supramolecular protein complexes (Anderson 1989). The appressed grana regions are enriched in PSII reaction centres while the stroma exposed lamellae, grana margins and grana end membranes contain most of the PSI reaction centres and ATP synthase (figure 1.9).. The cytochrome  $b_6f$  complex on the other hand is evenly distributed throughout the thylakoid membrane.

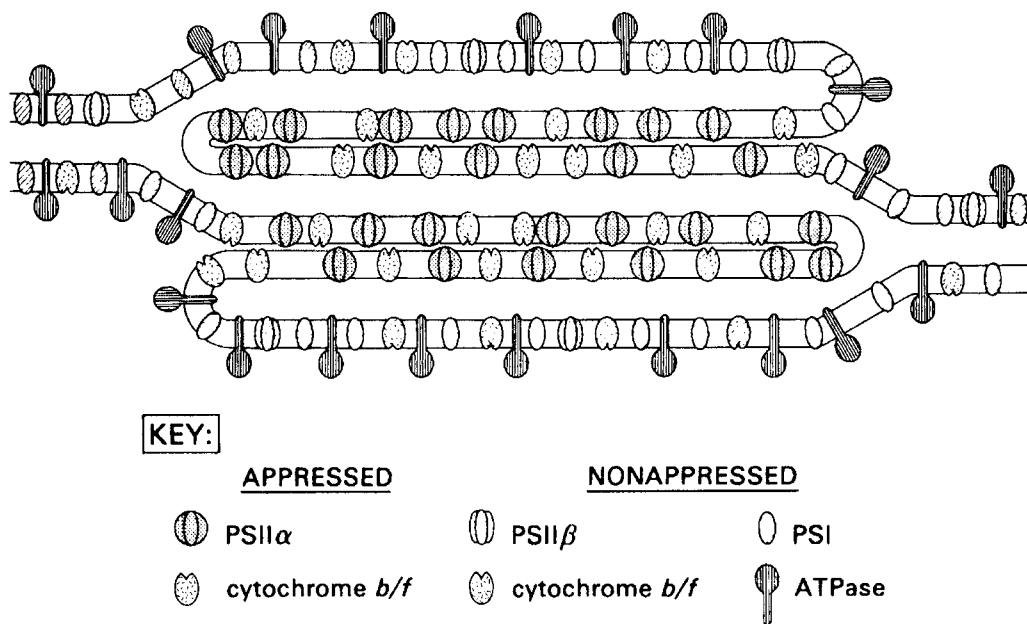


**Figure 1.9** Distribution of photosynthetic complexes within the thylakoid membrane (Anderson 1989)

The lateral heterogeneity found in the distribution of both the PSI and PSII reaction centres is also reflected in a structural and functional heterogeneity. PSII reaction centres exist in two subpopulations, PSII $\alpha$  and PSII $\beta$ . PSII $\alpha$  accounts for up to 80% of all PSII centres while PSII $\beta$  make up the remaining 20%. The main distinction between the two subpopulations is in the size of the peripheral antenna and the location of the centres within the thylakoid membrane. PSII $\beta$  reaction centres have significantly lower amounts of the peripheral light harvesting component, LHCII, and are located in the stroma lamellae and possibly the grana margins, while the PSII $\alpha$  centres occupy the appressed grana membranes (Wolenberger *et al* 1994, Guenther and Melis 1990). In addition the two subpopulations may be functionally dissimilar although this point remains contentious. It is clear that a population of PSII reaction centres exist which transfer electrons from QA to QB with significantly reduced efficiency (Graan and Ort

1986). These PSII-Q<sub>B</sub> nonreducing centres share some common features with PSII $\beta$ , including similar antenna size and their location within the thylakoid membrane (Melis 1991). However, differences in the population size of PSII $\beta$  and PSII-Q<sub>B</sub> nonreducing centres suggests that the relationship between the two is not strict. In order to account for the disparity between PSII $\beta$  and PSII-Q<sub>B</sub> nonreducing centres and to provide physiological meaning to the heterogeneity within PSII a unifying model, based on the turnover of damaged PSII centres, has been presented (Melis 1991) (figure 1.10). The 'PSII repair cycle model' suggests that damaged PSII centres migrate to the stroma following detachment from their peripheral LHCII component. Damaged PSII centres in the stroma lamellae undergo repair to form photochemically competent centres that are still unable to perform electron transfer from Q<sub>A</sub> to Q<sub>B</sub>. These centres are then activated to form PSII which are Q<sub>B</sub> reducing. Structural heterogeneity has also been demonstrated for the PSI reaction centre. A small fraction of PSI centres located within the appressed regions of the grana membranes have been shown to lack the light harvesting component Lhca1 as well as being deficient in the Lhca4 polypeptide (Jansson *et al* 1997). This is in contrast to the PSI centres located in stroma exposed membranes which carry a full complement of light harvesting polypeptides.

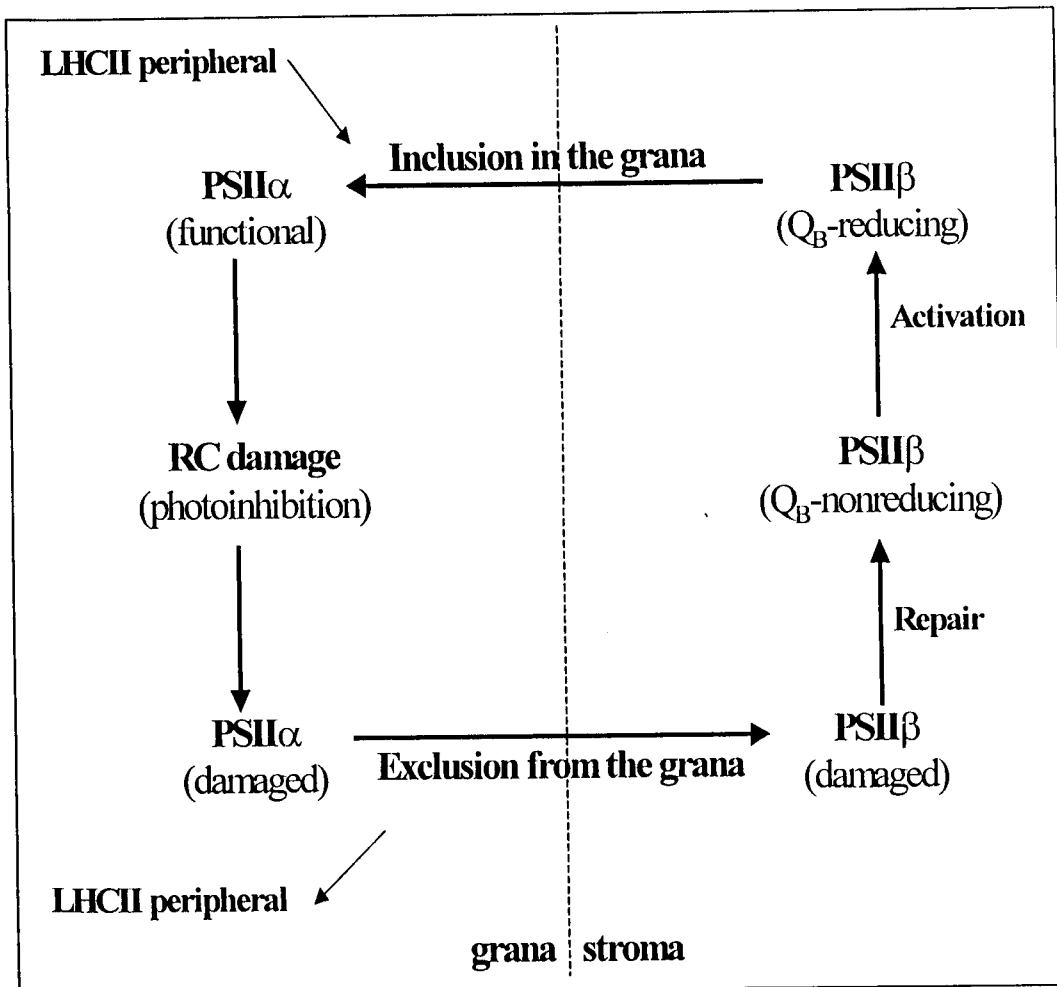


**Figure 1.10** Model of the PSII repair cycle (adapted from Melis 1991)

## 1.4 Photosynthetic Acclimation to Irradiance

Photosynthetic acclimation can be loosely defined as the modulation of the composition and function of the photosynthetic apparatus, following the selective synthesis and degradation of photosynthetic components, in response to sustained environmental stimuli. Such stimuli include light quality and quantity, temperature, nutrient and water availability and CO<sub>2</sub> supply. Although the main topic of this thesis involves the response to light quantity, or irradiance, the interplay between the various stimuli described above cannot be ignored since changes in irradiance in the field are likely to be accompanied by changes in most if not all other stimuli. This section however will deal with photosynthetic acclimation to irradiance referring to other stimuli only where appropriate. Short term regulation of photosynthesis, which differs from acclimation in that it involves the reallocation of existing photosynthetic components in response to transient changes in irradiance is covered in section 1.5.

The need to acclimate arises from the fact that plants often encounter variations in their light environment in the form of cloud cover, canopy gaps, seasonal change etc. Given their lack of motility plants must accommodate differing levels of irradiance to achieve the efficient utilisation of limiting light while avoiding the potentially damaging effects of excess irradiance.

### 1.4.1 Photosynthetic acclimation to constant growth irradiance

Changes in the photosynthetic apparatus are observed when plants are grown under environmental conditions that differ only in the levels of irradiance. For example changes in the light harvesting antenna of PSII have been reported for many plant species and these changes have been correlated with the ratio Chl *a/b*. Using semi-denaturing gel electrophoresis Leong and Anderson (1984) demonstrated that for pea grown in high light there was less LHCII relative to PSII when compared to plants grown at low light. This difference was consistent with the observed increase in Chl *a/b* for pea grown under the high light conditions. Such changes in the size of the PSII light harvesting antenna have been reported for a number of other plant species including Barley (De la Torre & Burkey 1990) and *A. macrohiza* (Chow *et al* 1987). However no differences in Chl *a/b* ratio were observed for *T. albiflora* when grown under low and high irradiance (Chow *et al* 1991). In Syrian Barley, which are naturally adapted to arid environments, there is a dramatic decrease in chlorophyll content when plants are grown under progressively higher light intensities at elevated temperatures (Havaux and Tardy 1999). This decrease takes place with with no apparent decrease in light harvesting antenna of PSII. A similar phenomenon has also been reported for *Guzmania monostachia* when grown at high light with significant decreases in chlorophyll content resulting in no change in chlorophyll *a/b* (Maxwell *et al* 1999). A decrease in thylakoid membrane content is however reported to account for the loss of chlorophyll in *Guzmania*. Changes in the size of the PSI light harvesting antenna on the other hand have been reported to remain constant in most cases (De la Torre & Burkey 1990, Leong and Anderson 1984).

It has been suggested that changes in reaction centre stoichiometry are influenced largely by changes in spectral quality (Anderson *et al* 1995). However it is clear from a number of studies that PSII/PSI can vary with changes in growth irradiance. When grown over a large range of irradiance pea showed significant differences in PSII content ranging from 1.4 mmol mol chl<sup>-1</sup> at 30  $\mu\text{mol quanta m}^{-2} \text{s}^{-1}$  to 5 mmol mol chl<sup>-1</sup> at 800  $\mu\text{mol quanta m}^{-2} \text{s}^{-1}$ . Although less dramatic, increases in PSII content have also been demonstrated for pea by Evans (1987) and for mustard by Wild *et al* (1986) at higher growth irradiance. Despite the changes in PSII content with growth light intensity little or no change in PSI content has so far been observed.

Significant increases in the amount of cytochrome *b<sub>6</sub>f* complex have been reported for several plant species, including pea and barley, when grown at higher irradiance (Leong & Anderson 1984, De la Torre & Burkey 1990). Higher rates of ATPase activity have also been reported (Chow and Hope 1987, De la Torre & Burkey 1990). In addition increased levels of Rubisco which correlate well with an increased capacity for CO<sub>2</sub> fixation are observed at higher growth light intensities for many plant species (Stitt 1986, Seeman *et al* 1989). The overall effect of the observed changes in the capacity for electron transport, CO<sub>2</sub> fixation and ATP synthesis may be to support higher rates of photosynthesis. The saturating rate of photosynthesis (P<sub>max</sub>) has indeed been shown to be elevated in response to growth at higher irradiance for some plant species including spinach (Anderson & Osmond 1987) and *Arabidopsis* (Walters and Horton 1994). However for some plant species there is no increase in P<sub>max</sub> with higher irradiance and P<sub>max</sub> has even been shown to decrease during growth at higher light intensities for *Castanospermum australe* (Anderson and Osmond 1987).

Anderson *et al* (1995) suggested that a general pattern of acclimation to growth irradiance could be described. At higher irradiance photosynthesis is limited at the level

electron transport and CO<sub>2</sub> fixation with maximal light capture more readily achieved than at lower irradiance where light harvesting becomes limiting. Therefore at higher irradiance plants have higher rates of photosynthesis which are supported by greater amounts of the electron transport components plastoquinone, cytochrome *b<sub>6</sub>f*, and plastocyanin as well as a higher content of the ATP synthase and CO<sub>2</sub> fixation enzyme Rubisco (reviewed in Anderson *et al* 1995). Since light harvesting is no longer limited at higher irradiance increased Chlorophyll *a/b* ratios, believed to be associated with a decrease in the size of the peripheral LHClI antenna, are also observed. Despite the emergence of patterns in the long term response to growth irradiance it is clear that some plant species have higher capacities for various aspects of photosynthetic acclimation than others. Murchie and Horton (1997) assessed the capacity for photosynthetic acclimation in a number of British plant species and identified two general strategies for acclimation: chloroplast level acclimation characterised by changes in Chl *a/b* and P<sub>max</sub> but with no change in chlorophyll content per unit leaf area and leaf level acclimation with changes in chlorophyll content per unit leaf area which correlated well with photosynthetic capacity. The capacity for acclimation was also linked to habitat distribution and it was suggested that chloroplast level acclimation was characteristic of plants naturally found in woodland shade.

#### **1.4.2 Photosynthetic acclimation to changes in growth irradiance**

Photosynthetic acclimation is a dynamic process which responds to changes in irradiance during growth by rapidly altering the composition of the photosynthetic apparatus. A transition from high to low irradiance (400 to 100  $\mu\text{mol quanta m}^{-2} \text{s}^{-1}$ ) with *Arabidopsis thaliana* for example was accompanied by a two-fold decrease in the

maximum rate of photosynthesis and a reduction in Chlorophyll *a/b* ratio from approximately 3.7 to 3.1 (Walters and Horton 1994). The decrease in maximum photosynthetic rate was completed in 48 hours while the reduction in Chlorophyll *a/b* ratio was achieved in 72 hours following an initial lag. The dynamic response to an increase in irradiance has been demonstrated with *Pisum sativum* (Chow and Anderson 1987). In this study a transition from 60 to 390  $\mu\text{mol quanta m}^{-2} \text{s}^{-1}$  was shown to elicit a two-fold elevation in the maximum rate of photosynthesis and an increase in Chlorophyll *a/b* ratio from 2.7 to 3.2. Both responses were reported to proceed with no apparent lag. In contrast *Spinacia oleracea* transferred from 30 to 1000  $\mu\text{mol m}^{-2} \text{s}^{-1}$  showed an increase in Chlorophyll *a/b* ratio from 2.7 to 3.1 in 72 hours with an apparent lag of 36-48 hours (Lindahl *et al* 1995). It has been suggested that the variable component of LHCII that is degraded following a transition to higher irradiance is enriched in the Lhcb2 gene product (Larsson *et al* 1987)

Changes in PSII content have also been shown to be modulated following a change in growth irradiance with both Barley (De la Torre and Burkey 1990) and Pea (Chow and Anderson 1987) showing significant increases following a change to higher irradiance. The changes in PSII content seemed to take place over a longer time scale (four days and ten days respectively) than Chl *a/b* and Pmax.

### **1.4.3 The regulatory mechanism of photosynthetic acclimation to irradiance**

The observed long term response of the photosynthetic apparatus to irradiance suggests that there must be an underlying regulatory mechanism for acclimation, the details of

which are at present poorly defined. This mechanism must include a sensor in order to sample the environment and a means of transducing any signal which may arise either directly from the sensor or at some other level. Finally the signal must elicit the coordinated synthesis and degradation of the photosynthetic machinery to bring about the appropriate state of acclimation. Two key hypothesis exist regarding the regulation of photosynthetic acclimation; molecular feedback (section 1.4.3.1) and 'excitation pressure' (section 1.4.3.2). Both postulates share many common features. In addition a role for the redox poise of intersystem electron transfer components has been implicated in providing the signal for acclimation (section 1.4.3.3). Finally, regulatory proteolysis of specific thylakoid components has been demonstrated (section 1.4.3.4).

#### **1.4.3.1 Molecular feedback**

The molecular feedback hypothesis was first proposed to account for the finding that several factors other than the light environment could bring about similar changes in the photosynthetic apparatus to those seen during acclimation to light quality and irradiance (Melis *et al* 1985). For example chlorophyll b mutations, altered CO<sub>2</sub> availability and sublethal doses of PSII herbicides were all shown to induce changes that mimic light acclimation. From these observations it was concluded that a regulatory feedback mechanism existed which controlled adjustments in the composition of the thylakoid membrane to correct imbalances in photosynthesis. The imbalance was said to occur at the level of electron transport with changes in redox poise favouring either linear or cyclic electron flow, the result being a shift in the ratio of ATP/NADPH. Changes in the photosynthetic metabolite pool would then serve to initiate a signal transmission process. The molecular feedback hypothesis as it was first proposed is concerned

mainly with acclimation to light quality and the authors accept that the response to irradiance is more difficult to fit within the scheme. The hypothesis has therefore been extended by Anderson *et al* (1995) to include multiple regulatory feedback mechanisms rather than a single common regulatory pathway. In addition, the scheme of Anderson *et al* includes the suggestion that photosystems I and II act as regulatory light sensors. This suggestion is strengthened by the finding that none of the photoreceptors currently identified in higher plants (i.e. the phytochrome family and blue light receptors) have any direct role in signalling for acclimation (Walters, unpublished data).

#### 1.4.3.2 'Excitation Pressure'

The 'Excitation Pressure' hypothesis is a variation on molecular feedback that accounts for the interplay between irradiance and temperature during photosynthetic acclimation. In a study using the green alga *Chlorella vulgaris*, Maxwell *et al* (1994) observed a 2-fold increase in chlorophyll *a/b* ratio and a significantly higher light saturated rate of O<sub>2</sub> evolution for cells grown at 5°C compared to 27°C at a constant growth irradiance of 150 μmol m<sup>2</sup> s<sup>-1</sup>. In addition an increase in xanthophyll cycle content and a decrease in chlorophyll content were observed during growth at 5°C. These observations suggested that acclimation to low temperature growth could mimic the effects of high light acclimation seen in other systems. Furthermore growth of cells at 5°C and a lower irradiance of 5 μmol m<sup>2</sup> s<sup>-1</sup> resulted in a similar pigment composition and P<sub>max</sub> level to cells grown at 27°C and 150 μmol m<sup>-2</sup> s<sup>-1</sup>. Cells grown at 5°C were also able to maintain PSII, or rather Q<sub>A</sub>, more oxidised than those grown at 27°C, when measured at low temperature. It was concluded therefore that *Chlorella* acclimated neither to

temperature nor irradiance *per se* but to the 'excitation pressure' on PSII as reflected in the redox state of  $Q_A$ . 'Excitation pressure' was defined as  $1-qP$  where  $qP$  is the photochemical fluorescence parameter which approximates to the redox state of  $Q_A$ . The relationship between low temperature and high irradiance in photosynthetic acclimation was therefore suggested to be derived from the fact that both stimuli give rise to high PSII 'excitation pressure' due to imbalances between energy supply through light harvesting and energy consumption through carbon fixation.. In the case of low temperature this imbalance results from the decrease in the rate of enzymatic reactions of the Calvin cycle at low temperature while light harvesting and photochemistry remain unaffected. The study was extended with the growth of *Chlorella* at low temperature and moderate irradiance ( $5^{\circ}\text{C}/150 \mu\text{mol m}^{-2} \text{s}^{-1}$ ) or high temperature and high irradiance ( $27^{\circ}\text{C}/2200 \mu\text{mol m}^{-2} \text{s}^{-1}$ ) to achieve the same high 'excitation pressure' of around 0.7 (Maxwell *et al* 1995a). In addition cells were also grown at a low PSII excitation pressure of 0.1-0.2 by providing either high temperature and moderate irradiance ( $27^{\circ}\text{C}/150 \mu\text{mol m}^{-2} \text{s}^{-1}$ ) or low temperature and low irradiance ( $5^{\circ}\text{C}/20 \mu\text{mol m}^{-2} \text{s}^{-1}$ ). Cells that were grown under conditions of high 'excitation pressure', when compared to those grown under conditions of low 'excitation pressure' exhibited a 2.4-fold higher chlorophyll *a/b* ratio and 3 fold higher light saturated rates of  $\text{O}_2$  evolution as well as an increased tolerance to photoinhibition. Since the growth conditions were selected to reflect only similarities in the redox state of  $Q_A$  and not temperature or irradiance the observations strengthened the suggestion that *Chlorella* undergo adjustments in photosynthesis in response to PSII 'excitation pressure'. Similar experiments were conducted to demonstrate the involvement of PSII redox state during photosynthetic acclimation using another green alga, *Dunaliella salina*. Cells were grown under several regimes of differing irradiance and temperature to achieve either high or low PSII 'excitation pressure' (Maxwell *et al* 1995b). Low PSII 'excitation pressure' was

then correlated with the abundance of LHCII apoprotein and mRNA. Furthermore the release of cells from high 'excitation pressure' during growth, in a process termed 'thermodynamic relaxation', resulted in a dramatic increase in LHCII apoprotein and mRNA accumulation. The results obtained with algae were interpreted in terms of a general signalling mechanism for photosynthetic acclimation to both irradiance and temperature. This signalling mechanism is reflected in the 'excitation pressure' of photosystem II and clearly incorporates the idea of molecular feedback. However the authors point out that the signal for acclimation is more likely to arise from changes in the redox poise of intersystem electron transport which accompany changes in PSII 'excitation pressure'. A role for PSII 'excitation pressure' has also been established in higher plants (Gray *et al* 1996, 1997). Using the same experimental approach that was applied to algae a number of growth regimes were defined for cultivars of wheat and rye whereby equivalent 'excitation pressure' was attained by altering both growth irradiance and temperature. As with the algae, it was shown that photosynthetic acclimation of the cereals responds to PSII 'excitation pressure' rather than irradiance or temperature alone. In contrast to the algae however there was no correlation between the redox state of PSII and the capacity for light harvesting. Instead correlation's were observed for  $P_{max}$  and the maximum capacity for non-photochemical quenching which contributed to an increased resistance to photoinhibition for plants grown at high 'excitation pressure'. An independent study using barley also concluded that there was no correlation between excitation pressure and PSII light harvesting (Montane *et al* 1998). In addition, correlation's were drawn between the accumulation of *Wcs19* mRNA, a gene previously shown to be expressed at low temperature, and high 'excitation pressure' regardless of whether the growth regime was based on low temperature or high light. Likewise the cereals grown at high excitation pressure exhibited a compact growth habit, usually associated with cold grown plants, at both low temperature and

moderate irradiance or moderate temperature and high irradiance. The 'excitation pressure' hypothesis is therefore extended to include the control of non-photosynthetic genes and plant morphology.

#### 1.4.3.3 Redox regulation of photosynthetic acclimation

The concept of redox regulation in photosynthetic acclimation is a key feature of both the molecular feedback hypothesis and the 'excitation pressure' hypothesis. Experiments carried out with the green alga, *Dunaliella tertiolecta*, have provided evidence that nuclear encoded photosynthetic genes are regulated by the redox poise of intersystem electron transport components in the chloroplast (Escoubas *et al* 1995). Using the electron transport inhibitor DBMIB, which blocks the oxidation of plastoquinol by the cytochrome *b<sub>6</sub>f* complex, the accumulation of LHCII apoprotein and mRNA is decreased during growth at low irradiance, effectively mimicking high light acclimation. Furthermore the use of the herbicide DCMU, which blocks the binding and therefore reduction of plastoquinone, results in an increase in LHCII apoprotein and mRNA accumulation during growth at high irradiance. The study also showed that irradiance dependence changes in the levels of LHCII are controlled at the level of *Lhcb* gene transcription. In conclusion the findings indicated that the levels of LHCII are regulated by the redox state of the plastoquinone pool which exerts control at the level of transcription. In a similar experiment using DCMU and DBMIB Pfannschmidt *et al* (1999) demonstrated that the redox state of the plastoquinone pool also regulates the transcription of reaction centre genes thereby controlling the stoichiometry of the two photosystems. The redox state of the plastoquinone pool has previously been shown to control the phosphorylation of peripheral LHCII during state transition (Allen 1992)

#### **1.4.3.4. Regulatory proteolysis of LHCII**

Increases in chlorophyll *a/b* ratio during prolonged exposure to high irradiance are associated with a decrease in the peripheral pool of LHCII (Leong and Anderson 1984). Recently a proteolytic activity associated with the thylakoid membranes of spinach has been shown to be involved in the degradation of LHCII following exposure to high irradiance (Lindahl *et al* 1995). With spinach both the increase in chlorophyll *a/b* ratio and the degradation of peripheral LHCII show a lag of around 48 hours following high light exposure. Interestingly, once the proteolysis has been initiated *in vivo* the activity will continue in the dark in isolated chloroplasts, the only requirement being for ATP upon which the protease is strictly dependant. Following a series of salt wash experiments it was established that the protease is bound extrinsically to the outer surface of the thylakoid membrane. However, the protease has yet to be isolated and therefore remains largely uncharacterised. It is known that the protease is of the serine/cysteine type although the possibility that LHCII is degraded by a Clp protease, recently shown to be associated with thylakoid membranes, has been excluded (Yang *et al* 1998). Two other types of protease, DegP and FtsH, have also been identified as thylakoid membrane components although there is currently no evidence linking these with the light induced degradation of LHCII (Lindahl *et al* 1996, Itzhaki *et al* 1998).

### **1.5 Short term regulation of photosynthesis**

When faced with long term increases in irradiance, photosynthetic acclimation provides a strategy for minimising the potential for photodamage. This strategy, which involves the selective synthesis and degradation of photosynthetic components, may take hours or even days to implement. The photosynthetic machinery of higher plants has therefore evolved a short-term strategy to avoid the damaging effects of excess irradiance. This short term strategy involves the reallocation of existing photosynthetic components in order to safely dissipate absorbed light energy which is in excess of that required for photosynthetic electron transport. Several distinct processes contribute to the short term regulation of photosynthesis but since they all result in a decrease in the fluorescence yield of *chlorophyll a* at room temperature they are collectively referred to as the process of non-photochemical quenching or qN. There are essentially three processes which contribute to qN. By far the most significant of these, in terms of photoprotection, is qE, or high energy quenching (section 1.5.1). qE is rapidly reversible whereas the component of qN known as qI relaxes more slowly and may even be irreversible under certain conditions (section 1.5.2). qT, the final component of non-photochemical quenching, which is related to the state transition, is covered in section 1.5.3.

### 1.5.1 High energy quenching: qE

High energy quenching, or qE, receives its name from the fact that it is entirely dependent upon the energisation of a trans-thylakoid proton gradient ( $\Delta pH$ ) and is therefore formed under conditions of excess irradiance (Briantais *et al* 1979). Its formation is both rapid and reversible and it functions to dissipate excess light energy following its safe conversion to heat. In addition to the dependence of qE on the

development of  $\Delta pH$ , its formation has also been correlated with the content of the xanthophyll carotenoid, zeaxanthin (Demmig-Adams and Adams 1992). Like  $qE$ , the formation of zeaxanthin requires excess irradiance and involves the two step de-epoxidation of violaxanthin in a process common to all plants known as the xanthophyll cycle (figure 1.11).

The dependence of the xanthophyll cycle on excess irradiance resides in the formation of a  $\Delta pH$  across the thylakoid membrane which stimulates the violaxanthin de-epoxidase enzyme. The association of xanthophyll cycle carotenoids with  $qE$  is a key piece of evidence in assigning the site of  $qE$ ; xanthophyll cycle carotenoids are found only in the bulk and minor LHCII complexes and not in the reaction centre core, strongly supporting the widely accepted belief that  $qE$  occurs within the PSII antenna. Further evidence supporting this suggestion includes the inhibition of  $qE$  during DCCD binding in the antenna and the effects on  $qE$  when various antenna components are absent (Horton *et al* 1996). Despite the extensive characterisation of the xanthophyll cycle its specific role in photoprotection remains debatable. The main controversy centres on whether zeaxanthin acts to directly quench excess irradiance within the PSII antenna or whether it plays a more peripheral role in energy dissipation. Initial objections to the idea that zeaxanthin acted directly as a quencher were based on the inability of simple energy transfer theory and measurements to show an allowed energy transfer step between excited chlorophyll and zeaxanthin. However the application of more advanced theory and the use of improved spectroscopic techniques have yielded energy values for the previously hidden ground state to S1 transition for both zeaxanthin and violaxanthin (Frank *et al* 1994). For violaxanthin the energy gap for the S1 state was found to be equivalent to 661 nm while the same energy gap for zeaxanthin was equivalent to 718 nm. Since light harvesting associated chlorophyll *a* has an emission at

around 718 nm it was concluded that zeaxanthin could in fact accept energy from excited chlorophyll *a*. Furthermore the probability of non-radiative decay from the zeaxanthin S1 state is high, making zeaxanthin an ideal direct quencher. Alternatively it has been suggested that, rather than acting directly to quench chlorophyll *a* fluorescence, the differences in polarity and conformation between zeaxanthin and violaxanthin provide an indirect role for the xanthophyll cycle in the dissipation of excess irradiance as heat (Ruban *et al* 1993a). It is proposed that quenching is induced by the protonation of the light harvesting antenna of PSII and that the formation of zeaxanthin serves as a regulator of proton induced conformational changes within LHCII. One line of evidence in favour of this suggestion has been provided by the isolation of chloroplasts from both dark adapted leaves, which contain very small amounts of zeaxanthin, and from light treated leaves, which have much higher levels of zeaxanthin (Noctor *et al* 1991). Both types of chloroplast were shown to have approximately the same saturated levels of qE. However the chloroplasts containing high levels of zeaxanthin had a lower pH requirement for qE formation indicating that although there is no absolute requirement for zeaxanthin in high energy quenching it does have an activating role. Quenching of *Chlorophyll a* fluorescence is consequently suggested to arise from the interactions between chlorophyll molecules within LHCII following proton induced conformational changes. It has also been suggested that the formation of zeaxanthin does not protect the photosynthetic apparatus from damage but protects thylakoid membrane lipids from photooxidation (Havaux and Niyogi 1999). Despite the controversy there is experimental evidence in favour of both chlorophyll-zeaxanthin and chlorophyll-chlorophyll interaction in the formation of a quencher for qE. A model for the molecular mechanism of qE has therefore been proposed in which both types of quenching may contribute to the formation of high energy quenching (Horton *et al* 1996). Based on both *in vitro* and *in vivo* data the model is centred on the possible existence of four

states of LHCII (figure 1.12). Each state differs in the extent to which they are associated with protons and xanthophyll cycle carotenoids and these differences determine the mechanism and therefore the level of quenching. Furthermore the transition between states depends upon whether excess irradiance results from a sudden increase or a more gradual rise in illumination. State I is unquenched since LHCII is unprotonated and binds violaxanthin. This state is most likely to prevail at low irradiance or in the dark. A gradual rise in irradiance would first favour the formation of state II, which is unprotonated but binds zeaxanthin. In state II there is a small amount of quenching via chlorophyll-zeaxanthin interaction. There is also an increased sensitivity of qE to  $\Delta pH$  making state II the light activated state. As the irradiance increases still further and the lumen pH continues to decrease LHCII becomes protonated giving rise to state IV which features strong chlorophyll-zeaxanthin quenching. When faced with a sudden increase in irradiance there is a transition from state I to state III in which violaxanthin is released from its binding site and LHCII becomes protonated. The result of state III formation is moderate quenching due to chlorophyll-chlorophyll interactions. More recently Ruban and Horton (1999) have demonstrated that the xanthophyll cycle regulates the kinetics of nonphotochemical energy dissipation

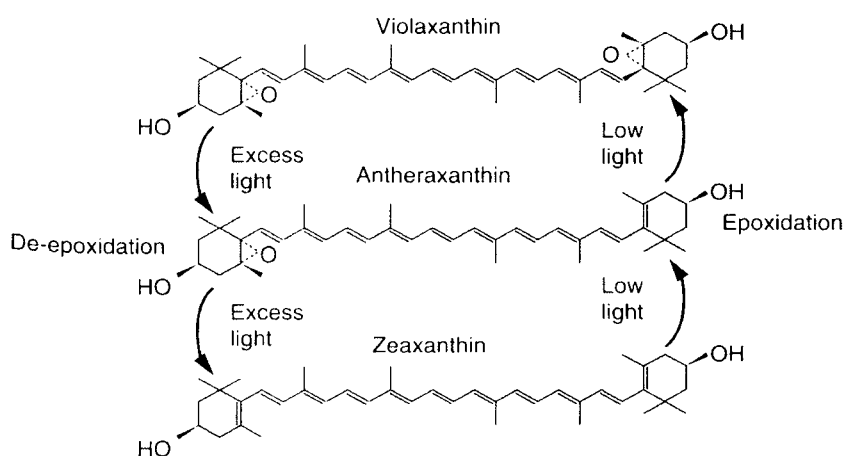


**Figure 1.11** The xanthophyll cycle (from Demmig-Adams 1990)

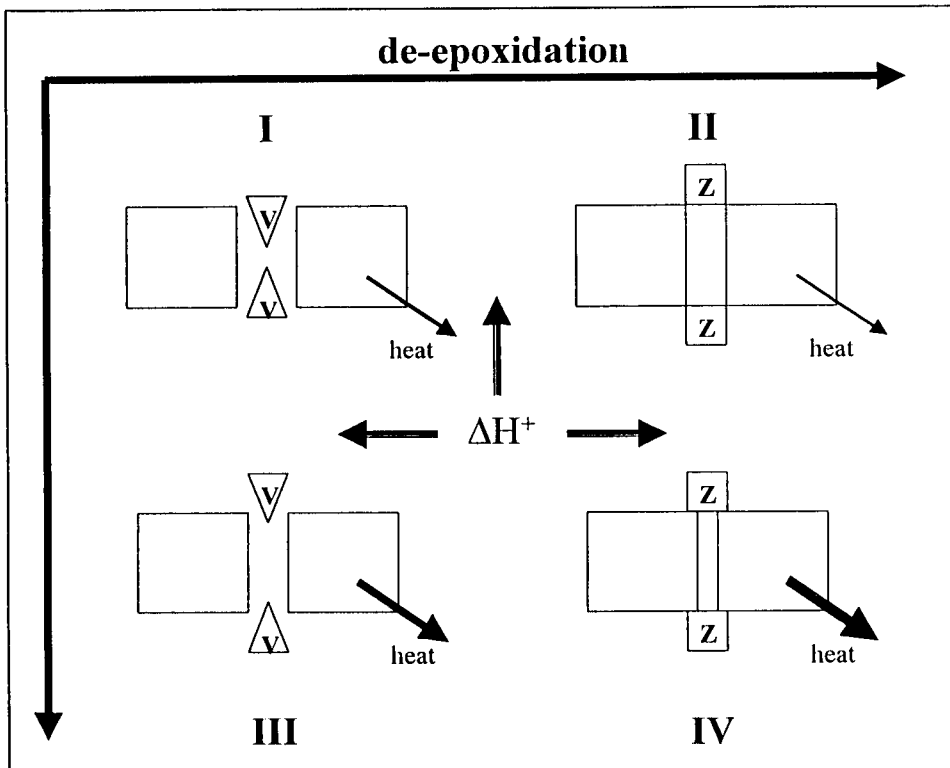


**Figure 1.12** The allosteric model for qE (from Horton *et al* 1996). Triangles represent violaxanthin while small squares represent zeaxanthin.

## 5.2 Slowly relaxing non-photochemical quenching: qI

In addition to qE a second component of non-photochemical quenching, qI, can be distinguished on the basis of its slow relaxation upon darkening. The extent to which qI contributes to total qN depends upon the conditions under which non-photochemical quenching is formed. Increasing levels of qI arise with increasing excess irradiance and following extended periods of excess irradiance. The nature of qI is not yet clearly resolved. It seems likely that part of qI is related to photoinhibition as evidenced by its association with the accumulation of inactive PSII centres (Oquist *et al* 1992). These

inactive centres may accumulate following high light induced damage (Cleland *et al* 1986) or they may be formed under conditions of extreme excess irradiance to act as quenchers giving qI a photoprotective role (Chow 1994). The elimination of a portion of qI following nigericin infusion suggest that qI may in part represent a more sustained form of qE (Ruban and Horton 1995). The sensitivity of qI to nigericin infusion decreases with increasing levels and duration of excess irradiance. Despite the sensitivity to nigericin it is not clear whether the trans-thylakoid proton gradient can account for the portion of qI that resembles qE. It has been suggested that stable forms of qE may arise from the maintenance of LHCII conformations which allow for heat dissipation long after the  $\Delta pH$  has subsided (Horton *et al* 1996). Such conformations may be maintained by protonated membrane domains that are insensitive to overall changes in  $\Delta pH$ . The advantage conferred by a sustained form of qE remains unclear since such a process is likely to lead to the loss of efficiency in conditions of fluctuating irradiance. One suggestion is that under conditions where the potential for extreme irradiance are high qI may enable qE to form more rapidly (Ruban *et al* 1993b).

### 1.5.3 State transition: qT

It is well established that qT arises as a result of the state transition in which peripheral LHCII becomes reversibly phosphorylated prior to its migration away from PSII (reviewed in Allen 1995). This process is believed to improve quantum efficiency under conditions of varying spectral quality by adjusting the absorption cross sections of each photosystem. There are however alternative suggestions for the physiological significance of the state transition including the provision for increased cyclic electron transport and the activation of PSII for degradation during photosynthetic acclimation.

The signal for state transition comes from the redox state of the plastoquinone pool which activates a LHCII specific protein kinase when reduced. In terms of photoprotection qT makes the least significant contribution to qN since it saturates at very low irradiance (Walters and Horton 1991).

## 1.6 Aims

The aim of this thesis was to carry out a detailed analysis of the capacity for photosynthetic acclimation to irradiance in *Arabidopsis thaliana* with the long-term objective of elucidating the underlying mechanisms that regulate the process. With the exception of Leong and Anderson (1984) a detailed analysis of light acclimation in a single plant species has so far been lacking. The initial objective for this projective was to demonstrate the ability of *Arabidopsis* to acclimate to a broad range of irradiance using Pmax and Chl *a/b* ratio as a simple index. The changes at the molecular level that underly the acclimation profile of Pmax and Chl *a/b* would then be established. This will be achieved by measuring the levels of chloroplast components at all growth irradiances including immunoblot analysis of all ten Chl *a/b* binding light harvesting polypeptides. In addition to a detailed analysis of the composition of the thylakoid membrane the functional consequences of photosynthetic acclimation will also be described. This will be achieved using the non-invasive technique of room temperature chlorophyll fluorescence. Finally the ability to respond to changes in growth irradiances are to be assessed using Pmax and Chl *a/b* to provide an indication of the state of acclimation and chlorophyll *a* fluorescence quenching data to assess the role of short term photosynthetic regulation. The choice of organism for this study was governed by the finding that *Arabidopsis* can acclimate well to moderately high and low irradiances

(Walters and Horton 1994) and by its amenability to genetic manipulation coupled to the fact that a genome sequencing project is currently underway. Although the genetic considerations are not directly relevant for this study they are vital for the long-term aims of the project.

## **Chapter Two**

### **Materials and Methods**

## 2 Materials and Methods

### 2.1 Plant Growth

Wild type seeds of *Arabidopsis thaliana* cv Landsberg erecta were obtained from the *Arabidopsis* stock centre (Nottingham). Seeds were spread thinly on a tray of moist Levington M2 compost (East Riding Horticulture, York, U.K.) and germinated in a plastic bag under moderate irradiance at 20 °C. Seedlings were then placed in individual pots and grown to maturity at 20 °C over a range of growth light intensities of constant light quality. The six growth irradiances used were 35, 100, 200, 400, 500 and 600  $\mu\text{mol quanta m}^{-2} \text{s}^{-1}$  provided by fluorescent tubes. Different light intensities were achieved by altering the distance of the plants relative to the growth light. The photoperiod was eight hours and started at 8 a.m. ending at 4 p.m. The dark period was therefore 16 hours. Lights were turned on and off without any time based ascent or descent in intensity. All plants, with the exception of those grown at 600  $\mu\text{mol m}^{-2} \text{s}^{-1}$  were grown in Steil growth cabinets. Plants grown at 600  $\mu\text{mol.m}^{-2}.\text{s}^{-1}$  were grown in a Sanyo growth cabinet. All plants were protected from irradiant heat with absorbant filters, built manually for the Steil cabinets and inbuilt for the Sanyo. All measurements described within this thesis were taken from mature leaf tissue. Because plants grown at different irradiances grow at different rates (i.e. growth at lower irradiance results in slower growth) the point of maturity was determined empirically. The definition of mature leaf tissue as applied to the work carried out here is leaf material that is fully expanded and that has a stable chlorophyll content, chlorophyll *a/b* ratio and maximum rate of oxygen evolution ( $P_{\text{max}}$ ). In addition plants were not used late in their development as they prepared for bolting. For plants grown at 35  $\mu\text{mol m}^{-2} \text{s}^{-1}$  the sampling period was between weeks 8 and 14, for 100  $\mu\text{mol m}^{-2} \text{s}^{-1}$  between weeks 7

and 12, for  $200 \mu\text{mol m}^{-2} \text{s}^{-1}$  between weeks 6 and 10, for  $400 \mu\text{mol m}^{-2} \text{s}^{-1}$  between weeks 5 and 9 and for  $600 \mu\text{mol m}^{-2} \text{s}^{-1}$  between 4 and 7 weeks. Plants were tested for circadian fluctuations in chlorophyll content, chlorophyll *a/b* and  $P_{\text{max}}$ . Although these parameters remained constant in mature leaf tissue throughout the light period plants were not sampled in the first or last hour of the light period. During transfer experiments plants were transferred and sampled as close to noon as possible. Oxygen evolution, chlorophyll content and chlorophyll *a/b* were all sampled in a single leaf disk with *in situ* fluorescence measurements sampled from the same batch of plants as the above parameters (chapter 3). Data for these parameters are averaged over at least 5 leaf disks taken from separate plants within a batch and replicated for 3 batches of plants grown at different times. Thylakoid membranes for western blot analysis (chapter 4) were also isolated from one batch of plants that the above measurements were sampled from. Relaxation kinetics of room temperature chlorophyll fluorescence quenching (chapter 5) were measured in at least 5 separate leaf disks taken from different plants within a batch and replicated for 2 batches of plants grown at different times to those described above. A further batch of plants separate from those already described above was sampled for Photosystem II content with replicates of between 6 and 10 leaf disks taken from separate plants (chapter 4). Thylakoid membranes were isolated from no less than 5 separate plants for Photosystem I estimation (chapter 4) from the same batch of plants used for photosystem II determination. Low temperature fluorescence measurements (chapter 4) were sampled from the same batch of plants as those described for photosystem determinations using at least 5 leaf disks taken from separate plants. During transfer experiments (chapter 6) chlorophyll content, chlorophyll *a/b* and  $P_{\text{max}}$  were sampled from the same leaf disks taken from at least 5 separate plants from 2 different batches. Separate batches of plants were used for the high to low and low to high transfers. Relaxation kinetics of room temperature chlorophyll fluorescence during

transfer experiments were measured in at least 5 separate leaf disks taken from different plants within 2 separate batches.

## 2.2 Chlorophyll determination

Chlorophyll content was determined according to Lichtenthaler and Wellburn (1983). Leaves were ground in 80% (v/v) acetone (BDH Merck Ltd.) and centrifuged at 1629 g for 5 minutes in a MSE Mistrall 1000 centrifuge. Using a Beckman DU650 spectrophotometer the absorbance of the supernatant was recorded at 663, 646 and 470 nm. The content of chlorophylls *a* and *b* were calculated as:

$$\text{Chl } a = 12.21 A_{663} - 2.81 A_{646}$$

$$\text{Chl } b = 20.13 A_{646} - 5.03 A_{663}$$

$$\text{where } A_{663} = A_{663} - A_{470} \text{ and } A_{646} = A_{646} - A_{470}.$$

## 2.3 Oxygen evolution

The light saturated rate of oxygen evolution ( $P_{\max}$ ) was measured using a Hansatech LD2 oxygen electrode. Using 1ml of air for calibration oxygen evolution from leaf disks was determined at 20°C at saturating  $\text{CO}_2$  (1%) and saturating non-photosynthetic irradiance. The saturating light intensity was determined separately for leaf disks from plants grown under each set of conditions. Plants were dark adapted at low-level irradiance ( $2 \mu\text{mol m}^{-2} \text{s}^{-1}$ ), provided by room lights, for at least 1 hour prior to measurement. Initially the dark respiration rate was measured as oxygen consumption.

Leaf disks were then exposed to moderate irradiance for between 5 and 15 minutes ( $100 - 600 \mu\text{mol m}^{-2} \text{s}^{-1}$ ) to obtain a steady level of oxygen evolution. The irradiance was then switched to that determined for each set of plants for oxygen evolution measurements. Data acquisition was carried out using "leaf disk" software (Hansatech Ltd). The maximum rate of oxygen evolution ( $P_{\text{max}}$ ) was then determined as the difference between dark oxygen consumption and oxygen evolution under saturating light and expressed on either a chlorophyll basis or a leaf area basis. Fluctuations in oxygen evolution were observed for plants particularly those grown under higher irradiance. The rate of oxygen evolution was therefore averaged over a 15 minute period of illumination. In order to determine the saturating non photoinhibitory light intensity for measurement of oxygen evolution for plants grown under the various irradiance leaf disks were subjected to increasing pulse light intensities for 15 minute periods (i.e. 15 minutes per leaf disk at one irradiance followed by 15 minutes irradiance on a second leaf disk at a higher irradiance etc). In this way light response curves were generated for plants grown at each irradiance from which the appropriate light intensity for measurement of oxygen evolution was selected.

## **2.4 PSII content**

PSII content was assayed by the oxygen yield per saturating flash method essentially according to Chow *et al* (1989). Measurement of oxygen evolution was carried out in a Hansatech LD2 leaf disk oxygen electrode. The chamber was maintained under conditions of saturating  $\text{CO}_2$  using matting dampened with bicarbonate buffer and at  $20^\circ\text{C}$  using a water cooling system. In order to detect small amounts of oxygen evolved in the nmole range the signal was amplified up to one hundred fold. The oxygen

electrode was therefore insulated by foam housing to minimise small effects of changes in ambient temperature which were seen to pose problems at the level of signal amplification used. In addition stray electrical fields from the pulse light created very high background noise when the signal was amplified therefore all electrical wires were insulated in aluminium foil and electrical tape. Prior to measurement leaf disks were incubated in the dark (within the leaf disk chamber) for 15 minutes to achieve steady state respiration. Saturating pulses of sufficient duration (0.1 sec) to turn PSII centres over once were applied at a rate of 5HZ. Background far-red illumination was also supplied to ensure that PSI turnover did not limit electron transport. Room temperature chlorophyll fluorescence was used to measure the redox state of photosystem II during measurement to enable a far red light range and light intensity to be selected which ensured PSII reaction centres remained oxidised. The photochemical quenching parameter  $qP$  was used as an indication of PSII redox state. Despite small decreases in  $qP$  during measurement (eg typically from 0.95 to 0.9) the values were still high enough to suggest that PSII was being maintained in an oxidised state ensuring that PSII content was not underestimated through missed turnover. Non photoinhibitory saturating light levels were determined individually for plants grown under all conditions. Leaf disks were subjected to increasing pulse light intensities for 15 minute periods (i.e. 15 minutes per leaf disk at one irradiance followed by 15 minutes irradiance on a second leaf disk at a higher irradiance etc). In this way light response curves were generated for plants grown at each irradiance from which the appropriate light intensity for measurement of oxygen evolution was selected. During measurement the dark respiration rate was first recorded before applying saturating pulses which were maintained for a period of up to 15 minutes while oxygen evolution was measured. 3 to 4 cycles of light and dark were applied with net oxygen evolution being taken as the difference between dark respiration rate of oxygen consumption and light rate of oxygen evolution. The oxygen yield per

flash then gave an estimate of the PSII content which was expressed per unit chlorophyll. Total chlorophyll content was measured from the same leaf disk used for oxygen evolution. Figure 2.1 shows a typical trace for oxygen evolution during a PSII assay on plants grown at  $600 \mu\text{mol m}^{-2} \text{s}^{-1}$ .

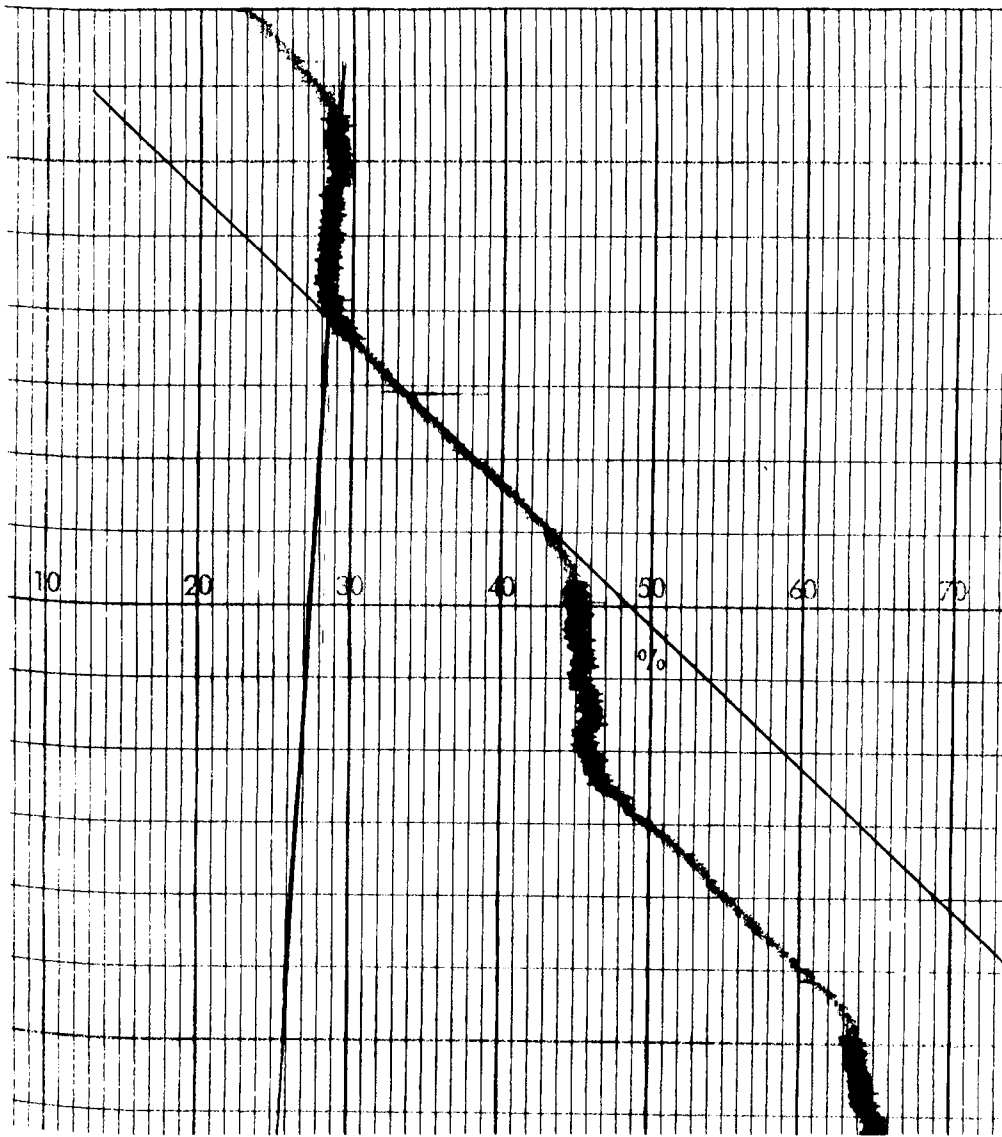


**Figure 2.1** Typical trace for a photosystem II assay by the method of oxygen yield per saturating flash. Thin lines on the trace show oxygen consumption during dark respiration while the thicker lines show oxygen evolution during a period of saturating flashes.

## 2.5 Thylakoid preparation

Thylakoid preparation was carried essentially according to Walters and Horton (1994). Prior to the isolation of thylakoid membranes plants were dark adapted for up to 4 hours under room lights ( $2 \mu\text{mol m}^{-2} \text{s}^{-1}$ ). The preparation was then carried out on ice. Leaves were homogenised in semi-frozen grinding media (0.33 M sorbitol, 5 mM  $\text{MgCl}_2$ , 5 mM EDTA, 10 mM HEPES pH 7.6). The homogenised solution was filtered through four layers of muslin followed by two layers of muslin and one layer of cotton wool. The filtrate was centrifuged at 4,000 g for 10 minutes. The pellet was resuspended in a small volume of wash buffer (0.33 M sorbitol, 1 mM  $\text{MgCl}_2$ , 1 mM EDTA, 50 mM HEPES pH 7.6) before being pelleted at 4,000 g for 10 minutes. The pellet was then osmotically shocked by resuspension in 5mM  $\text{MgCl}_2$  for at least 30 seconds before the addition of an equal volume of 0.66 M sorbitol. Thylakoids were either used fresh or immediately frozen in liquid nitrogen.

## 2.6 PSI content

The PSI content of freshly prepared thylakoid membranes was assayed by the reduced minus oxidised difference spectra of P700 following chemically induced redox changes (Whitmarsh and Ort 1984). A 1ml cuvette was prepared containing thylakoids (prepared as above) to a final concentration of between 10 and 20  $\mu\text{g/ml}$ , 10  $\mu\text{l}$  of 10 mM methyl viologen and made up to 1 ml with distilled  $\text{H}_2\text{O}$ . The sample was mixed and then firmly secured in the sample chamber of a DW2000 spectrophotometer (SLM/Aminco, Urbana) with the temperature controlled at  $15^\circ\text{C}$ . The DW2000 was set to dual wavelength mode with a measuring wavelength of 702 nm and a reference wavelength of 725 nm, using a slit width of 1.5 nm. After a steady baseline had been

established a 30 second burst of red light was applied in order to completely reduce P700. 5  $\mu\text{l}$  of 0.2 M ferricyanide was then carefully added and the sample was gently mixed taking care not to disturb the position of the cuvette. A steady P700 oxidised baseline was allowed to develop. The concentration of P700 was then calculated using a reduced minus oxidised extinction coefficient of  $64 \text{ mM}^{-1} \text{ cm}^{-1}$  and expressed per unit chlorophyll.

## **2.7 Gel electrophoresis**

### **2.7.1 SDS PAGE**

SDS-PAGE was run using a Biorad mini-protean gel system essentially according to Laemmli (1970). Thylakoid membrane samples were solubilised by the addition of a 1:1 volume of freshly prepared solubilisation buffer containing 18  $\mu\text{l}$  of 10% SDS, 3.2  $\mu\text{l}$  of 1M DTT, 0.001% bromophenol blue, 36  $\mu\text{l}$  of gel dissociation buffer (440 mM sucrose, 300 mM Tris-HCl pH 8.3, 3mM EDTA, 3mM PMSF), 42.8  $\mu\text{l}$  dH<sub>2</sub>O. For Western blot analysis 1  $\mu\text{g}$  chlorophyll equivalents were loaded onto a 15 % (w/v) acrylamide gel. Gels were run at 150 Volts for 2 hours at 4°C.

### **2.7.2 Western blotting**

Gels were blotted onto Hybond C nitrocellulose membrane (Amersham International p.l.c.) using a Biorad mini electroblotting cell in a transfer buffer containing 2mM Tris pH 8.3, 190 mM glycine, 20% methanol, 0.1% SDS. Blots were then blocked in TBS-tween (20 mM Tris pH7.5, 500mM NaCl, 0.1% tween 20) containing 5% milk powder. Three washes in TBS-tween followed before incubation with antibody diluted to the

appropriate concentration in antibody buffer (TBS-tween, 2% milk powder, 0.0025% Triton X-100) for 2.5 hours. The blot was then rinsed three times in TBS-tween followed by incubation with secondary antibody, anti rabbit IgG raised in Donkey (Amersham International Plc), at a concentration of 0.03% for 1 hour. Three washes in TBS tween followed by one wash in dH<sub>2</sub>O followed. Antibody detection was carried out using an ECL kit (Amersham International P.l.c.) according to the manufacturer's instructions.

## **2.8 Rubisco content**

Soluble protein was extracted from frozen leaf disks by grinding in 1 ml of extraction buffer (1.2g Tris pH 8.0, 0.004g EDTA, 4 mls of 0.5 M MgCl<sub>2</sub> made up to 100 mls with boiled H<sub>2</sub>O) in the presence of a small volume of PVPP. Leaf disks were ground to a powder while still frozen and then allowed to thaw. A 200 µl aliquot was taken for chlorophyll determination (section 2.2). 1 µg chlorophyll equivalents were then solubilised and resolved on SDS PAGE as described in section 2.7.1. Following coomassie staining the relative band density of the Rubisco large subunit was determined by densitometric scanning using Optimas software.

## **2.9 Room temperature chlorophyll fluorescence**

Dark relaxation kinetics of room temperature chlorophyll fluorescence was determined according to Walters and Horton (1991). A PAM 101 chlorophyll fluorimeter (Heinz Waltz, Kings Lynn) was attached to a leaf disk chamber by a branched fibreoptic providing pulse light, actinic light and measuring beam. The pulse light was supplied

by a Schott LK 1500 lamp (Schott Glass Ltd, Stafford) while a custom built lamp supplied the actinic light. The chamber was maintained at 20°C under conditions of saturating CO<sub>2</sub> and the leaf disk was kept moist during the measurement. Data was collected using Fip software (Q<sub>A</sub>-Data Oy, Turku, Finland). Leaf disks were dark adapted for up to 2 hours under room lights and for 15 minutes in the chamber before measurement. Figure 2.1 shows a typical trace. A baseline was briefly recorded before the measuring beam was switched on to record F<sub>o</sub>. The measuring beam was set as high as possible without inducing a secondary rise in fluorescence. The intensity of the measuring beam was determined separately for plants grown at each irradiance. After 30 seconds a 1 second saturating pulse of 3000 μmol quanta m<sup>-2</sup> s<sup>-1</sup> was applied to record F<sub>m</sub>. A 30 minute period of actinic illumination followed during which time the 1 second pulse was applied every 3 minutes. The intensity, duration and frequency of the pulse light were empirically selected to give saturation without inducing fluorescence quenching for plants grown at all irradiance. After 30 minutes of actinic illumination the chamber was darkened and a far red light applied during which time F<sub>o</sub>' was sampled. Saturating pulses were then applied every 2 minutes initially and then every 3 minutes for a total of 45 minutes in order to record the relaxation kinetics of fluorescence quenching.

Analysis of the data allowed the fluorescence quenching parameters, φPSII, qP and qN to be determined. qP was calculated as  $(F_m' - F_s) / (F_m' - F_o')$  where F<sub>s</sub> represents steady state fluorescence following actinic illumination. φPSII was calculated as the product of qP and F<sub>v</sub>'/F<sub>m</sub>'. qN was calculated as  $F_m / (F_m' - 1)$ . In addition plotting F<sub>m</sub>/(F<sub>m</sub>' - 1) against time gave rise to the dark relaxation kinetics of chlorophyll fluorescence quenching which showed at least 2 distinct phases (Figure 2.2). Regression analysis of the dark kinetics gave rise to a value for qI, the slowly relaxing component of qN and qE.

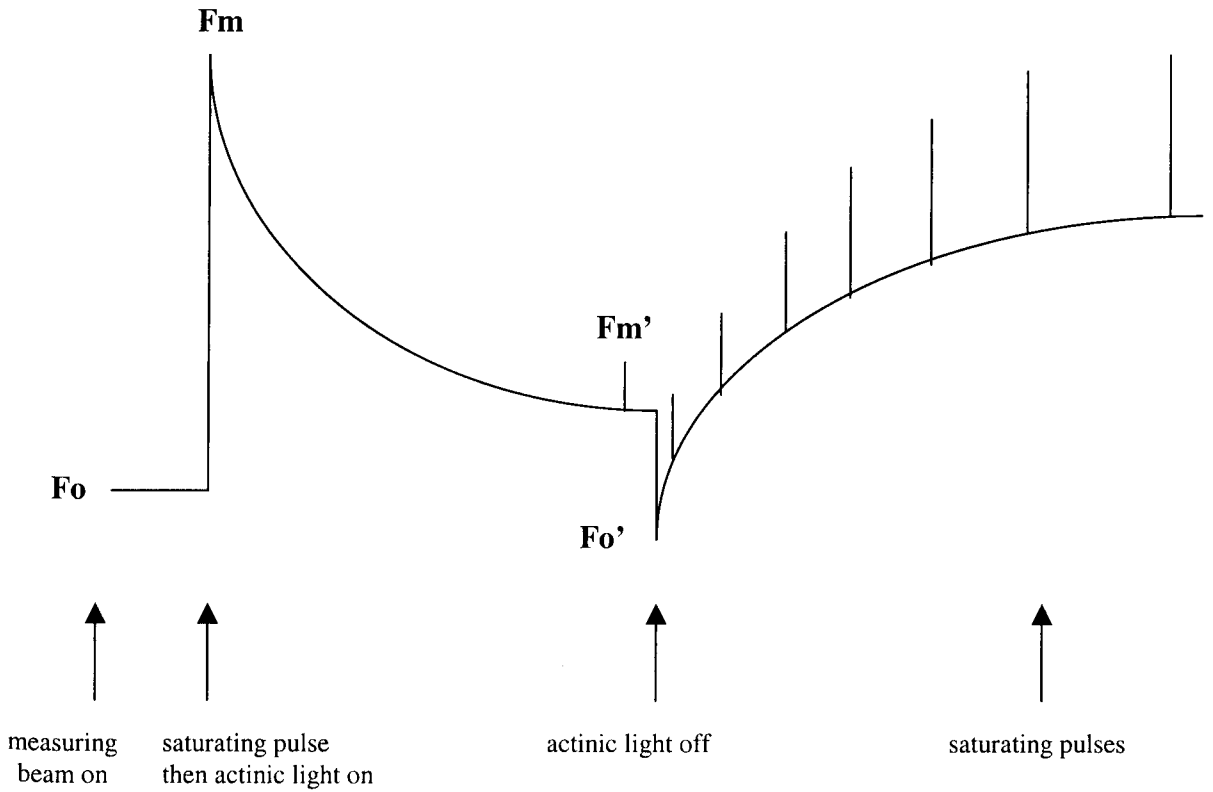


**Figure 2.1** Schematic representation of a fluorescence trace indicating the use of pulse and actinic lights and showing dark relaxation of quenching.

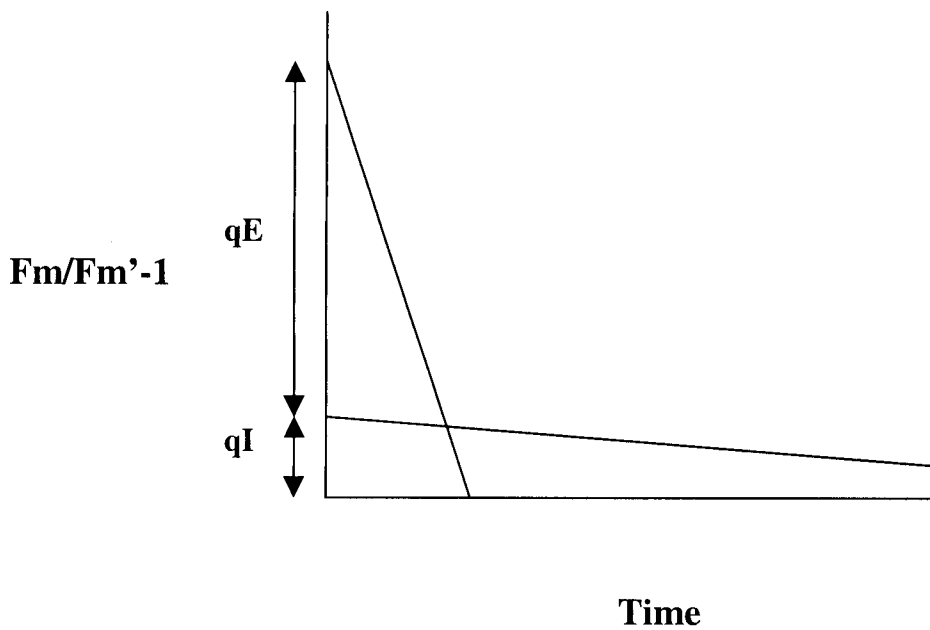


**Figure 2.2** Schematic representation showing a plot of  $F_m/F_m' - 1$  against time for the dark relaxation kinetics of chlorophyll fluorescence quenching. Lines were fitted to a slowly relaxing phase ( $qI$ ) and faster relaxing phase ( $qE$ ).

### 2.9.1 *in situ* measurements

*In situ* measurements of room temperature chlorophyll fluorescence were used to determine  $qP$  and  $\phi PSII$ . Measurements were taken in the growth cabinets using a Waltz portable fluorimeter (Heinz Waltz, Kings Lynn). Actinic irradiance was supplied by the cabinet's growth light and care was taken not to shade or disturb the leaves during measurement. The temperature in the chamber was maintained at 20°C and the  $CO_2$  concentration was ambient. The measuring beam, saturating pulse and far red lights required to sample  $F_o$ ,  $F_m'$ ,  $F_s$  and  $F_o'$  were all supplied by a single fibre optic. The saturating pulse was  $3000 \mu\text{mol quanta m}^{-2} \text{s}^{-1}$ . During the sampling of  $F_o'$  the growth lights in the cabinet were briefly turned off. The parameters  $qP$  and  $\phi PSII$  were calculated as described in section 2.9.

### 2.9.2 Measurement of state transition

The state transition was detected by recording PSII fluorescence at room temperature in attached leaves of *Arabidopsis thaliana*. 650 nm and 740 nm lights were used to preferentially excite PSII and PSI respectively. PSII fluorescence was recorded using a PAM 101 chlorophyll fluorimeter (Heinz Waltz, Kings Lynn). Leaves were illuminated with PSII and PSI light for 20 minutes until a steady state level of fluorescence had been reached, this was close to the  $F_o$  level and was designated state 1. The PSI light was turned off resulting in a rise in fluorescence as PSII became reduced. The fluorescence then declines reaching a minimum level after approx 10 minutes as PSII became oxidised. The PSI light was then turned back on resulting in a small decline of fluorescence.

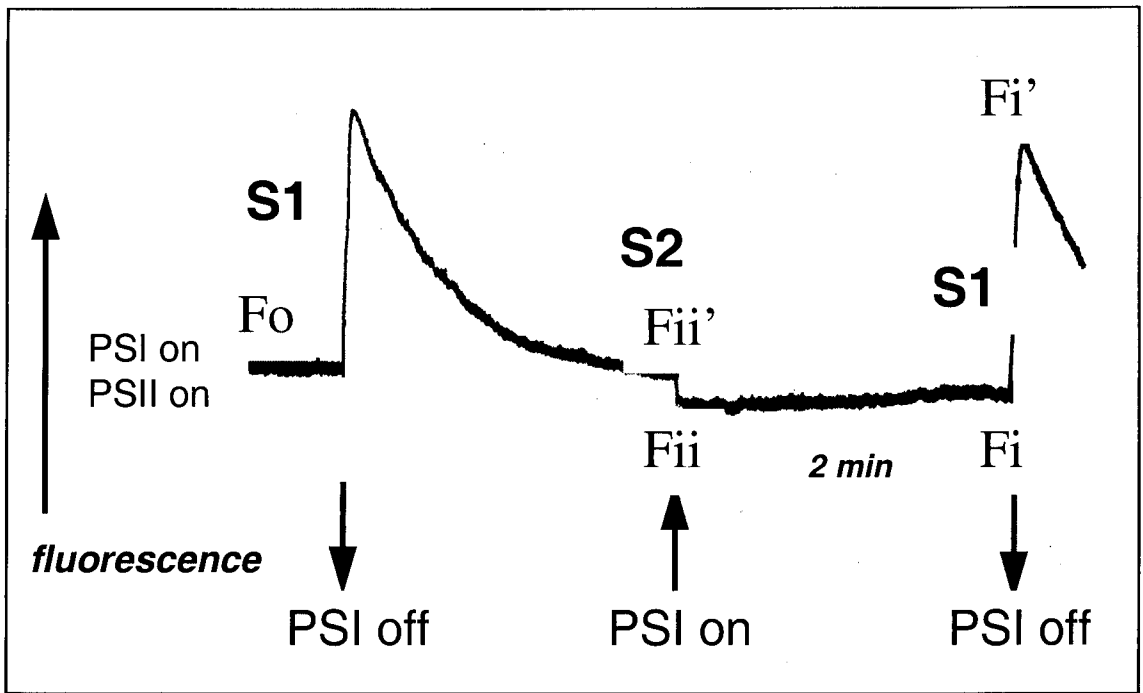


**Figure 2.3** Typical trace showing state transition measurement. States 1 and 2 are indicated along with the light regime used.

## 2.10 Low temperature chlorophyll fluorescence

77K fluorescence emission spectra were measured essentially according to Ruban and Horton (1992). 1cm diameter leaf disks were frozen in liquid nitrogen and homogenised in 2 mls of grinding buffer (section 2.5). Homogenised and diluted leaf disks were placed in a custom built holder between two pieces of glass, while still frozen, and immersed in liquid nitrogen in a cryostat. The samples were then excited with a broad band light with  $\lambda_{max}$  of 430 nm. The broad band excitation had an intensity of  $80 \mu\text{mol quanta m}^{-2} \text{s}^{-1}$  and was provided by 150 W tungsten lamp with corning filters (4-96 and 5-57) defining the range. The light was passed through a heat absorbing filter. Chlorophyll fluorescence detection was via a 1024-channel silicon diode (model no.

1455 using a Monospec 27 monochromater). Analysis was via a PARC multi-channel 1461 analyser and OMAvision software (EG&G instruments Corp, Princeton).

## 2.11 HPLC analysis of carotenoid composition

Pigments for HPLC analysis were extracted from leaf disks by grinding in the presence of ethanol and diethyl ether (BDH Merck Ltd.). The resulting solution was filtered twice through a plugged Pasteur pipette before being dried under gaseous nitrogen. Samples were stored at -20°C and redissolved in acetone before use. HPLC analysis of carotenoid content was carried out according to Johnson *et al* (1993). The solvent system used was 0-60 % (v/v) ethyl acetate (Fischer Scientific Ltd) in acetonitrile (BDH Merck Ltd) / water (9:1) at 1 ml/min for 16 minutes. A constant flow of 60% (v/v) ethyl acetate was maintained for 9 minutes followed by a 60-100% (v/v) gradient for 5 minutes. Carotenoid content was calculated from the chromatogram peak at 447 nm for Lutein, antheroxanthin and  $\beta$ -carotene (cis isomers), 455nm for zeaxanthin,  $\beta$ -carotene and chlorophyll *b*, 441 nm for neoxanthin, 437nm for violaxanthin, 431nm for chlorophyll *a*. Values for chlorophyll were adjusted by a factor of 1.512 and 1.99 for chlorophylls *b* and *a* respectively.

## **Chapter Three**

# **Acclimation to Growth Irradiance: Changes in Chlorophyll Content, P<sub>max</sub>, *in situ* Chlorophyll Fluorescence**

### 3.1 Introduction

Plants grown at different irradiance show marked variations at both the molecular and whole plant levels, with changes in the composition of the thylakoid membrane and in overall plant morphology having been observed for several species. At the whole plant level a number of photomorphogenic responses have been described many of which are associated with shade avoidance (Smith 1982). These responses are manifest in the development of stem, leaf and root and are under the control of a host of photoreceptors including the phytochromes and the blue light receptors, which respectively respond to changes in the ratio of red to far red light and the fluorese rate of blue light. Natural shade environments have altered levels of both spectral quality and irradiance. It is therefore difficult to assign any aspect of shade avoidance as being a response to either property of the shade environment. For example, blue light receptors have been shown to control both hypocotyl and petiole extension in response to irradiance, in particular the fluorese rate of blue light (Liscum and Hangarter 1991, Walters and Horton 1994). However hypocotyl extension is also known to be under the control of phytochrome (Robson *et al* 1993) and therefore responds to changes in spectral quality as well as irradiance.

Chloroplast changes at the molecular level, which include electron transfer components, ATP synthase and chlorophyll *a/b* ratio as well as Pmax and Rubisco content, are for many plant species responses to irradiance alone (reviewed in Anderson *et al* 1995). Spectral quality on the other hand is believed to exert control over the relative levels of the two reaction centres with little effect on other chloroplast components. However, for a number of plant species reaction centre stoichiometry is also modulated by

irradiance with PSII content in particular being regulated in an antagonistic manner to light quality (Anderson *et al* 1988, Murchie and Horton 1998). Despite the opposing effects of light quality and quantity on reaction centre content two parameters, the ratio of chlorophyll *a/b* and Pmax, provide a convenient index of the extent to which a plant has acclimated to growth irradiance.

The majority of studies on photosynthetic acclimation to growth irradiance, which have been conducted using a number of different plants species, have concentrated on the effects of high and low irradiance by comparing just two growth light regimes, with the exception of Leong and Anderson (1984). There is consequently a need to examine in detail the effects of an extensive range of growth irradiance. Previous studies with *Arabidopsis thaliana* (L.) Heynh. cv. Landsberg *erecta* have shown that this winter annual is able to successfully acclimate to both low ( $100 \mu\text{mol. m}^{-2}. \text{s}^{-1}$ ) and moderately high ( $400 \mu\text{mol. m}^{-2}. \text{s}^{-1}$ ) irradiance (Walters and Horton 1994). This chapter describes the response of *A. thaliana* to a wider range of growth irradiance including very low and very high growth light regimes using chlorophyll *a/b* ratio and Pmax as an index of acclimation. In addition *in situ* measurements of room temperature chlorophyll fluorescence and a description of plant morphology are provided.

## **3.2 Results**

### **3.2.1 Plant growth and morphology**

*Arabidopsis thaliana* plants grown over a range of irradiance are shown in figure 3.1. A

A number of significant differences are evident in overall leaf morphology. Leaves from plants grown at higher irradiance are larger and thicker than those grown at lower irradiance although high light grown plants tend to have more curled leaf edges. Curled leaf edges are particularly pronounced at  $600 \mu\text{mol m}^{-2} \text{s}^{-1}$ . In addition high light grown plants have shorter petioles. The overall result of the altered leaf morphology observed for *A. thaliana* over the range of growth irradiance is a more compact and well ordered rosette formation at higher light intensities. The rate of plant growth was markedly slower for low light grown plants with  $35 \mu\text{mol m}^{-2} \text{s}^{-1}$  taking 80-90 days to reach maturity in contrast to 25-30 for plants grown at  $600 \mu\text{mol m}^{-2} \text{s}^{-1}$ . As a result of decreased growth rate lower light grown plants bolted later than those grown at higher irradiance.

### 3.2.2 Chlorophyll content

A comparison of the total chlorophyll content per unit leaf area for *Arabidopsis thaliana* grown at different growth irradiance is shown in table 3.1. Plants grown at  $100 \mu\text{mol m}^{-2} \text{s}^{-1}$  show a slight decrease in chlorophyll content compared to those grown at all other irradiance. Despite this there is no discernible trend for changes in chlorophyll content with growth irradiance. This similarity in chlorophyll content means that the measurement of any parameter expressed on a chlorophyll basis will show the same pattern of change with growth irradiance when expressed per unit leaf area.

Although the total chlorophyll content remains constant within a limited range, the ratio of chlorophyll *a* to chlorophyll *b* shows significant growth irradiance dependant changes

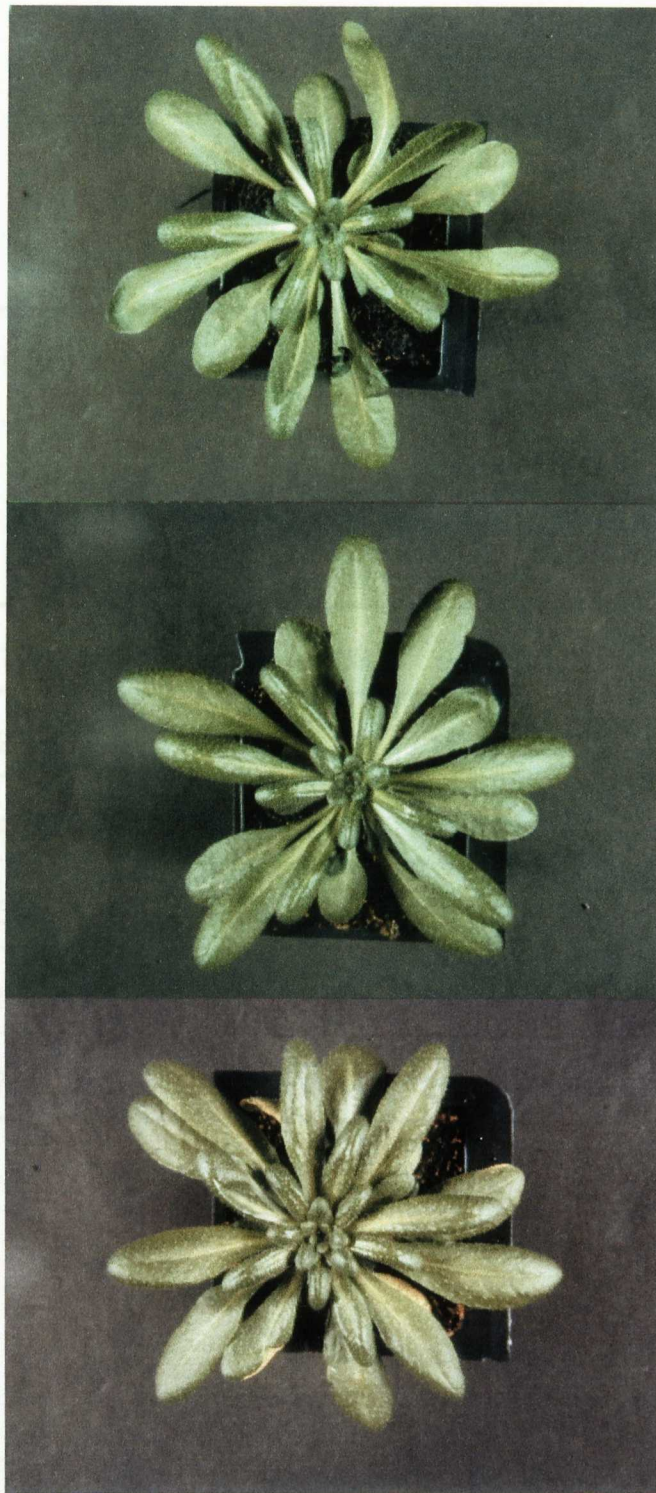


**Figure 3.1** *Arabidopsis thaliana* grown under three different light regimes which differ only in their level of irradiance. Top image represents plants grown at  $100 \mu\text{mol m}^{-2} \text{s}^{-1}$ , middle image represents plants grown at  $200 \mu\text{mol m}^{-2} \text{s}^{-1}$ , bottom image represents plants grown at  $400 \mu\text{mol m}^{-2} \text{s}^{-1}$ .

<b>Growth irradiance</b> ( $\mu\text{mol quanta m}^{-2} \text{ s}^{-1}$ )	<b>Chl <i>a/b</i></b>	<b>Chl content</b> ( $\mu\text{g chl cm}^{-2}$ )	<b>Pmax/A</b> ( $\mu\text{molO}_2\text{m}^{-2}\text{s}^{-1}$ )	<b>Pmax/Chl</b> ( $\mu\text{molO}_2 \text{ mol Chl s}^{-1}$ )
<b>35</b>	3.17 $\pm$ 0.03	23.36 $\pm$ 0.88	6.95 $\pm$ 0.51	26.68 $\pm$ 1.38
<b>100</b>	3.23 $\pm$ 0.04	21.03 $\pm$ 0.89	11.86 $\pm$ 0.41	51.10 $\pm$ 2.41
<b>200</b>	3.48 $\pm$ 0.06	25.80 $\pm$ 0.73	15.03 $\pm$ 0.63	52.60 $\pm$ 2.18
<b>400</b>	3.57 $\pm$ 0.06	26.66 $\pm$ 2.64	17.34 $\pm$ 1.39	63.90 $\pm$ 9.98
<b>500</b>	4.14 $\pm$ 0.13			84.29 $\pm$ 6.73
<b>600</b>	4.75 $\pm$ 0.10	23.28 $\pm$ 1.44	28.67 $\pm$ 1.99	113.69 $\pm$ 13.82

**Table 3.1** Chlorophyll content, Chlorophyll *a/b* ratio and Pmax per leaf area and per unit Chlorophyll for *Arabidopsis thaliana* grown at different irradiance. Growth irradiance are given as  $\mu\text{mol quanta m}^{-2} \text{ s}^{-1}$ . Means  $\pm$  se of at least 15 samples taken from separate plants in 3 separate experiments using different batches of plants. Oxygen evolution, chlorophyll content and chlorophyll *a/b* were all determined in the same leaf sample. (Data for plants grown at 500  $\mu\text{mol m}^{-2} \text{ s}^{-1}$  provided courtesy of Dr. Robin Walters)

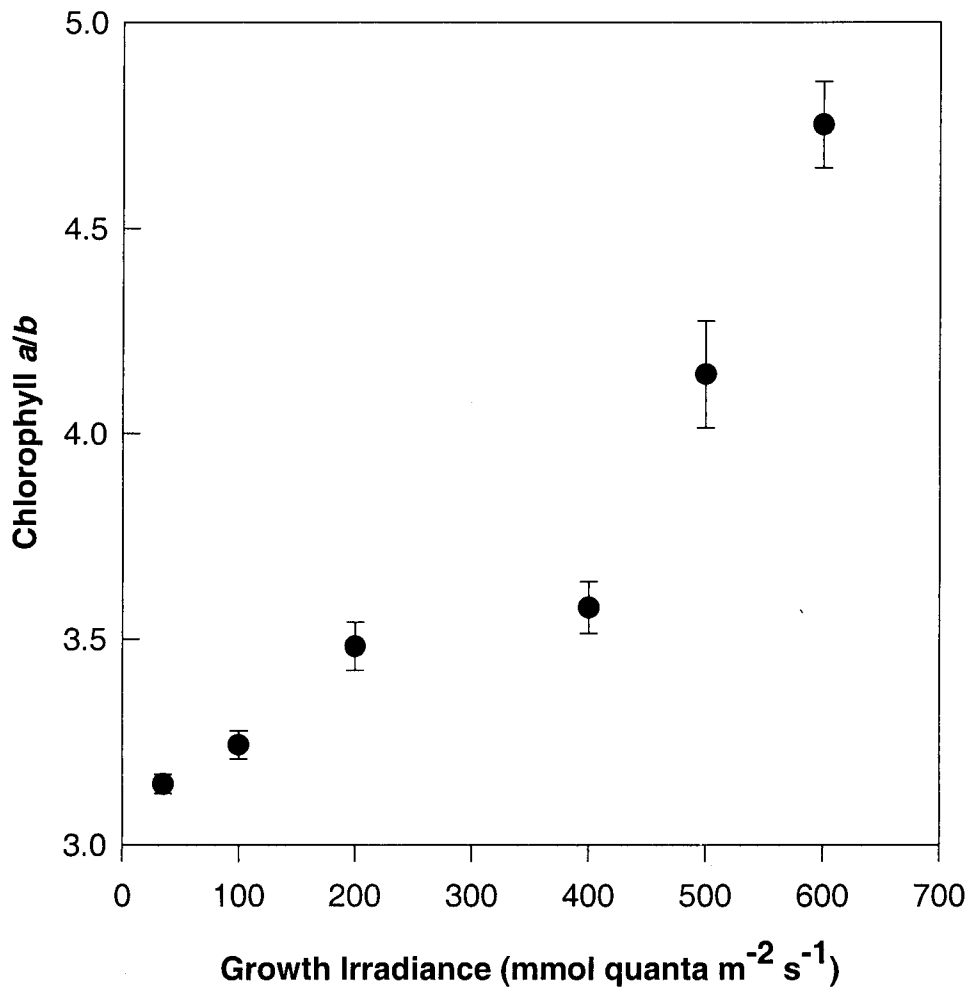


**Figure 3.2** Relationship between Chlorophyll *a/b* ratio and growth irradiance for *Arabidopsis thaliana*. Means  $\pm$  se of at least 15 samples taken from separate plants in 3 separate experiments using different batches of plants. Oxygen evolution, chlorophyll content and chlorophyll *a/b* were all determined in the same leaf sample. (Data for plants grown at 500  $\mu\text{mol m}^{-2} \text{s}^{-1}$  provided courtesy of Dr. Robin Walters)

with an overall increase at higher light intensities (table 3.1). As shown in figure 3.2 the relationship between growth irradiance and Chl *a/b* ratio is non-linear. A discontinuous response of Chl *a/b* ratio to growth irradiance has previously been demonstrated for pea (Leong and Anderson 1984). As with pea the Chl *a/b* ratio of *Arabidopsis* increases more sharply at lower irradiance decreasing beyond 200  $\mu\text{mol. m}^{-2}. \text{s}^{-1}$ . While pea shows a linear response at all irradiance above 200  $\mu\text{mol. m}^{-2}. \text{s}^{-1}$  *Arabidopsis* plants show a sharp increase in Chl *a/b* ratio between 400 and 600  $\mu\text{mol. m}^{-2}. \text{s}^{-1}$ .

### 3.2.3 Photosynthetic capacity

Measurement of the light saturated rate of photosynthesis under conditions of saturating  $\text{CO}_2$  ( $P_{\text{max}}$ ), as determined by the level of oxygen evolution, measures a plants photosynthetic capacity.  $P_{\text{max}}$  for *Arabidopsis* grown at different irradiance are shown in table 3.1 and figures 3.3 and 3.4. As expected from the similarity in total chlorophyll per unit leaf area the pattern of change in  $P_{\text{max}}$  is similar when expressed on both a leaf area basis and per unit chlorophyll.  $P_{\text{max}}$  is strongly influenced by growth light intensity with an overall increase in photosynthetic capacity at higher irradiance. Such changes in  $P_{\text{max}}$  must be supported by changes in electron transport capacity and carbon fixation. As with the Chl *a/b* ratio the response to growth irradiance of  $P_{\text{max}}$  is non-linear with a steeper increase at light intensities of up to 200  $\mu\text{mol. m}^{-2}. \text{s}^{-1}$  and between 400 and 600  $\mu\text{mol. m}^{-2}. \text{s}^{-1}$ . Figure 3.5 shows the relationship between the Chl *a/b* ratio and  $P_{\text{max}}$  per unit chlorophyll over the range of growth irradiance. There is a high correlation coefficient ( $r^2 = 0.95$ ) between these two parameters.

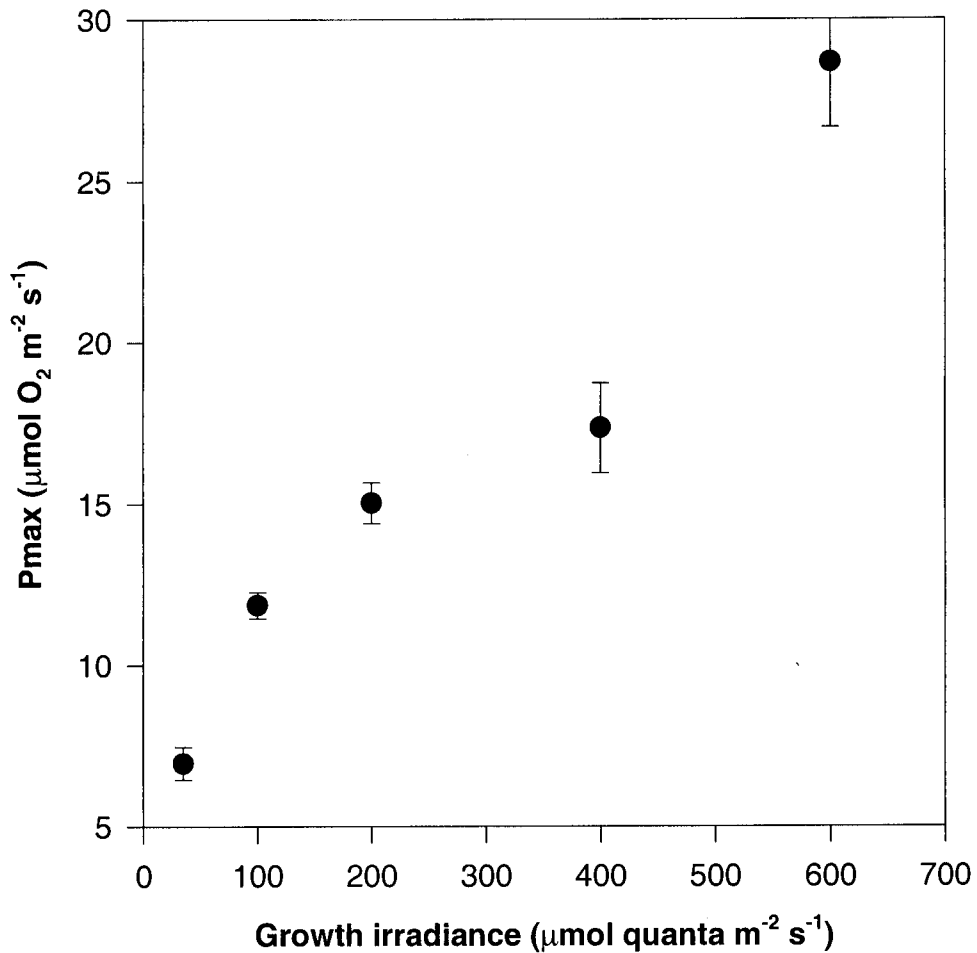


**Figure 3.3** Relationship between Pmax per unit area and growth irradiance for *Arabidopsis thaliana*. Means  $\pm$  se of at least 15 samples taken from separate plants in 3 separate experiments using different batches of plants. Oxygen evolution, chlorophyll content and chlorophyll *a/b* were all determined in the same leaf sample.. (Data for plants grown at 500  $\mu\text{mol m}^{-2} \text{s}^{-1}$  provided courtesy of Dr. Robin Walters)

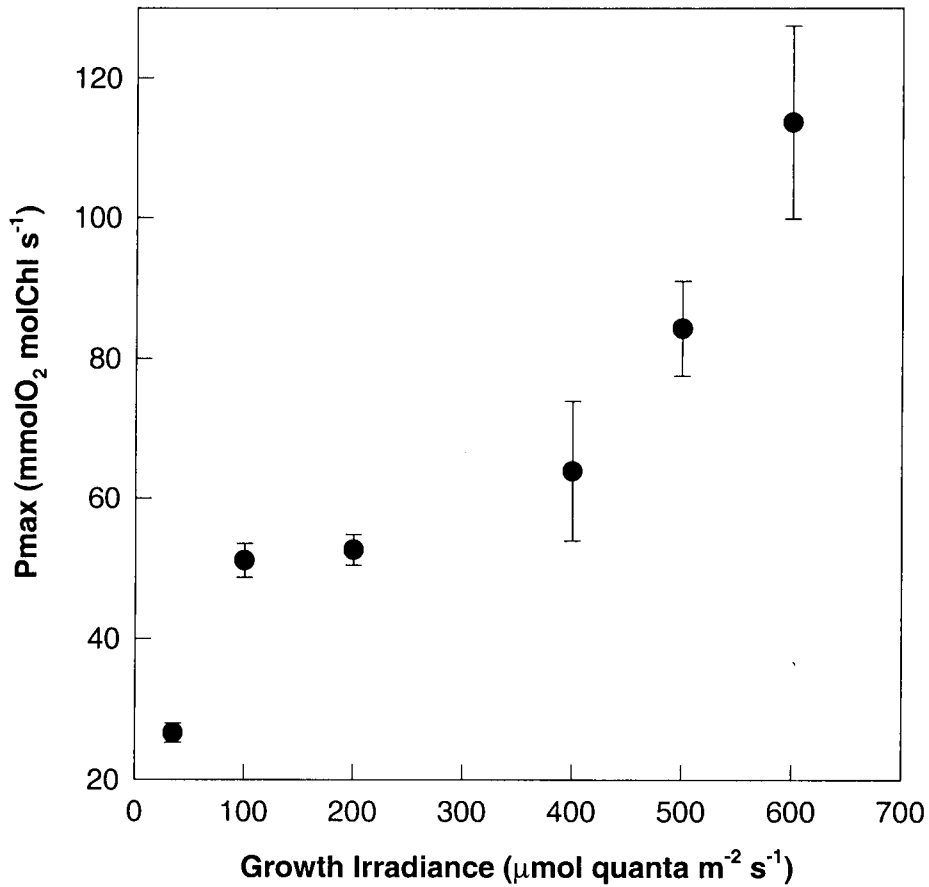


**Figure 3.4** Relationship between Pmax per unit Chlorophyll and growth irradiance for *Arabidopsis thaliana*. Means  $\pm$  se of at least 15 samples taken from separate plants in 3 separate experiments using different batches of plants. Oxygen evolution, chlorophyll content and chlorophyll *a/b* were all determined in the same leaf sample.. (Data for plants grown at  $500 \mu\text{mol m}^{-2} \text{s}^{-1}$  provided courtesy of Dr. Robin Walters)

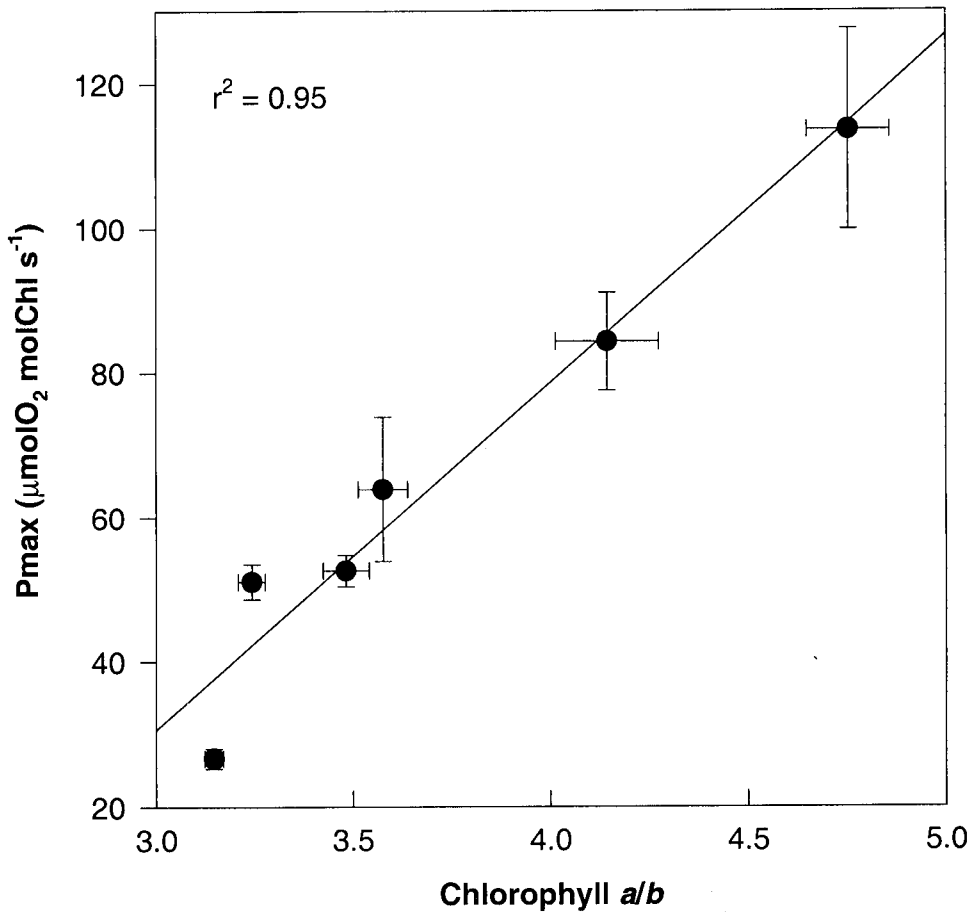


**Figure 3.5** Relationship between Pmax per unit Chlorophyll and Chlorophyll *a/b* ratio for *Arabidopsis thaliana* grown over a range of irradiance. Means  $\pm$  se of at least 15 samples taken from separate plants in 3 separate experiments using different batches of plants. Oxygen evolution, chlorophyll content and chlorophyll *a/b* were all determined in the same leaf sample.

### 3.2.4 Room temperature Chlorophyll fluorescence (*in situ*)

Room temperature chlorophyll fluorescence can be used as a non-invasive probe of plant physiology. Two fluorescence parameters,  $qP$  and  $\phi PSII$ , have been measured *in situ* for *A. thaliana* grown over a range of irradiance.  $qP$  determines the amount of absorbed excitation energy that is used for photochemistry and is an approximation of the proportion of open PSII reaction centres. Values of  $qP$  can range between 0 and 1 with higher values being indicative of more highly oxidised reaction centres.  $\phi PSII$  is a measure of the quantum efficiency of PSII and is the product of  $qP$  and  $Fv'/Fm'$  (for measuring principles see section 3.9). Values for  $\phi PSII$  range between 0 and 0.83, these tend to decrease as non-photochemical quenching increases and the efficiency of PSII light harvesting is down regulated. At higher irradiance further decreases in  $\phi PSII$  may also be attributed to decreases in  $qP$ .

In order to determine  $qP$  and  $\phi PSII$  at the growth irradiance and temperature under conditions of ambient  $CO_2$ , room temperature chlorophyll fluorescence was measured *in situ* for *Arabidopsis thaliana* grown at different irradiance. As shown in figures 3.6 and 3.7 both  $qP$  and  $\phi PSII$  are consistently high for plants grown at all light intensities.

## 3.3 Discussion

*Arabidopsis thaliana* grown at different irradiance show changes in leaf morphology, growth rate and composition of the photosynthetic apparatus. Increases in growth rate at higher irradiance, which led to decreases in the time taken for flowering, can be simply

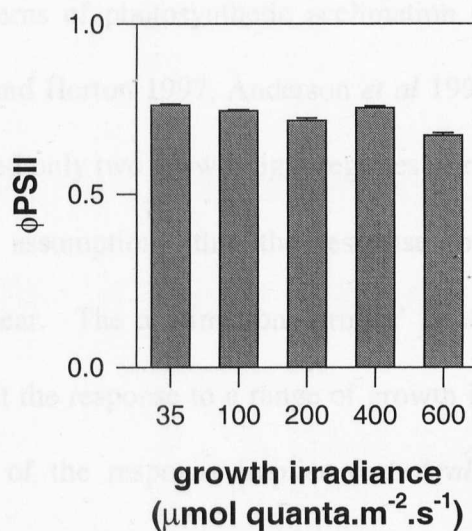
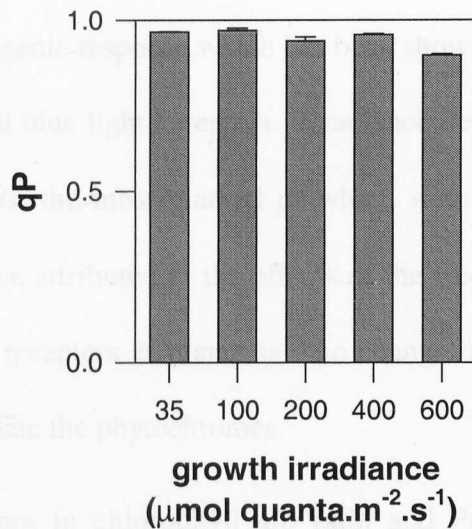


**Figure 3.6 (top) and Figure 3.7 (below)** Relationship between qP (top) and  $\phi\text{PSII}$  (below) as measured *in situ* and growth irradiance for *Arabidopsis thaliana*. Means  $\pm$  se of at least 15 samples taken from separate plants in 3 separate experiments using different batches of plants ( i.e. those batches used for determining oxygen evolution, chlorophyll content and chlorophyll *a/b*)

explained in terms of the increased availability of energy for growth at high light intensities. Changes in the leaf morphology of *Arabidopsis* with growth irradiance are part of the photomorphogenic response which has been shown to be under the regulation of the phytochromes and blue light receptors. Irradiance dependant photomorphogenic responses in *Arabidopsis*, the most marked of which were leaf thickness and petiole extension, are likely to be attributed to the effects of the fluorescence rate of blue light acting on the blue light receptors as plants saw no change in the ratio of red to far red light which might stimulate the phytochromes.

As stated earlier, changes in chlorophyll *a/b* ratio and Pmax provide an index for changes in the composition of the photosynthetic apparatus. During acclimation to growth irradiance *Arabidopsis* showed an increase in both Chl *a/b* ratio and Pmax at higher light intensities. Previous studies with a number of different plant species have established similar patterns of photosynthetic acclimation to irradiance (Walters and Horton 1994, Murchie and Horton 1997, Anderson *et al* 1995). However, the majority of these studies have used only two growth light regimes to represent high and low light environments with the assumption that the response to a range of growth light irradiance would be linear. The acclimation 'profile' of *Arabidopsis* presented here clearly demonstrates that the response to a range of growth irradiance is discontinuous. This non-linear nature of the response implies that *Arabidopsis* employs different strategies for acclimation to low and high irradiance. Despite this, high values for qP and  $\phi$ PSII suggest that *Arabidopsis* is able to fully acclimate to each growth irradiance regardless of the strategy involved.

## **Chapter Four**

# **Acclimation to Growth Irradiance: Changes in the Composition of the Photosynthetic Apparatus**

## 4.1 Introduction

The previous chapter demonstrates the ability of *Arabidopsis thaliana* to acclimate to a range of growth irradiance using Pmax and the chlorophyll *a/b* ratio as a simple index. In this chapter changes in the composition of the photosynthetic apparatus are assessed in an attempt to understand the molecular basis of photosynthetic acclimation to irradiance.

Changes in Pmax have previously been associated with changes in the content of the CO<sub>2</sub> fixing enzyme, Rubisco (Bjorkman 1981). With *Arabidopsis*, growth at two different light intensities resulted in a change in Pmax that was directly attributed to changes in the levels of Rubisco per unit chlorophyll (Walters and Horton 1994). To determine whether the same relationship exists across a wider range of growth irradiance Rubisco content has been assessed for *Arabidopsis* plants grown over the same irradiance range as those previously described in chapter 3 (section 4.2). However, due to the logistical problems associated with the growth of plants at a number of different light intensities data for plants grown at 500  $\mu\text{mol m}^{-2} \text{s}^{-1}$  are limited to Pmax and chlorophyll *a/b* ratio only (chapter 3).

A number of acclimation studies have addressed the effects of the growth light environment on reaction centre levels (reviewed in Anderson *et al* 1995). In most cases, including work with *Arabidopsis* (Walters and Horton 1994), it has been concluded that changes in reaction centre levels are associated mainly with differences in the spectral quality of the growth light, with light intensity having little or no effect. Again many of the earlier studies, with the exception of pea, have concentrated on a limited range of growth light environments. In addition reliable methods for the assay of both PSII and

PSI have proven difficult to establish. This chapter describes the functional assay of both PSII and PSI reaction centres for *Arabidopsis* grown over a range of irradiance.

Since reaction centre levels are generally assumed to remain relatively constant with growth irradiance differences in the ratio between chlorophylls *a* and *b* are thought to be associated with changes in the photosystem antenna and in particular LHCII. Direct evidence for changes in LHCII with growth irradiance have been obtained for both pea and *Arabidopsis* using semi-denaturing gel electrophoresis (Leong and Anderson 1984, Walters and Horton 1995). Despite this a comprehensive study of the effects of growth irradiance on the composition of the light-harvesting antenna of both photosystems is currently lacking. It is not known whether PSI light harvesting and the minor PSII light harvesting components undergo changes during acclimation to growth irradiance. Using a unique set of antibodies raised against the ten known chlorophyll *a/b* binding proteins this chapter describes the effects of a range of growth light intensity on the light harvesting antenna of PSI and PSII. Finally low temperature fluorescence spectra, which often reflect differences in light harvesting, are presented for plants grown at all irradiance.

## **4.2 Results**

### **4.2.1 Rubisco content**

Rubisco subunits are highly abundant (up to 40% of total soluble protein). They may therefore be cleanly resolved when stained with Coomassie-blue. When the small subunit of Rubisco is resolved from total soluble protein, extracted from *Arabidopsis* leaves at different growth irradiance and loaded on a chlorophyll basis, the relative

density of each band provides an estimate of the change in Rubisco content per unit chlorophyll. Figure 4.1 shows the relative band density of the Rubisco small subunit per unit chlorophyll for *Arabidopsis* grown at the previously defined growth light intensities. An increase in Rubisco content is observed from 35 to 100  $\mu\text{mol m}^{-2} \text{s}^{-1}$  and again from 100 to 200  $\mu\text{mol m}^{-2} \text{s}^{-1}$ . A slight decrease can then be seen between 200 and 400  $\mu\text{mol m}^{-2} \text{s}^{-1}$  followed by a significant increase from 400 to 600  $\mu\text{mol m}^{-2} \text{s}^{-1}$ .

Overall the trend for change in Rubisco content with growth irradiance for *Arabidopsis* is similar to the discontinuous response of  $P_{\text{max}}$ . Rubisco content may therefore make a significant contribution to the determination of maximum rate of photosynthesis. However the regression coefficient (figure 4.2,  $r^2 = 0.81$ ) for relative Rubisco content per unit chlorophyll and  $P_{\text{max}}$  per unit chlorophyll may not be high enough to directly attribute changes in  $P_{\text{max}}$  to differences in Rubisco content, the relationship failing to hold strongly at both 400 and 600  $\mu\text{mol m}^{-2} \text{s}^{-1}$ .

#### 4.2.2 PSII content

The PSII content of *Arabidopsis* leaves was assayed using the oxygen yield per flash method (Chow *et al* 1989). Leaf disks are subjected to saturating light flashes of sufficient duration to provide a single turnover of PSII reaction centres while background far red illumination ensures that PSI turnover does not become limiting. The oxygen yield per flash then gives an estimate of the number of functional PSII centres expressed on a chlorophyll basis. Care is taken to ensure that the single turnover flashes are sufficiently saturating without being photoinhibitory for plants grown at any given irradiance.

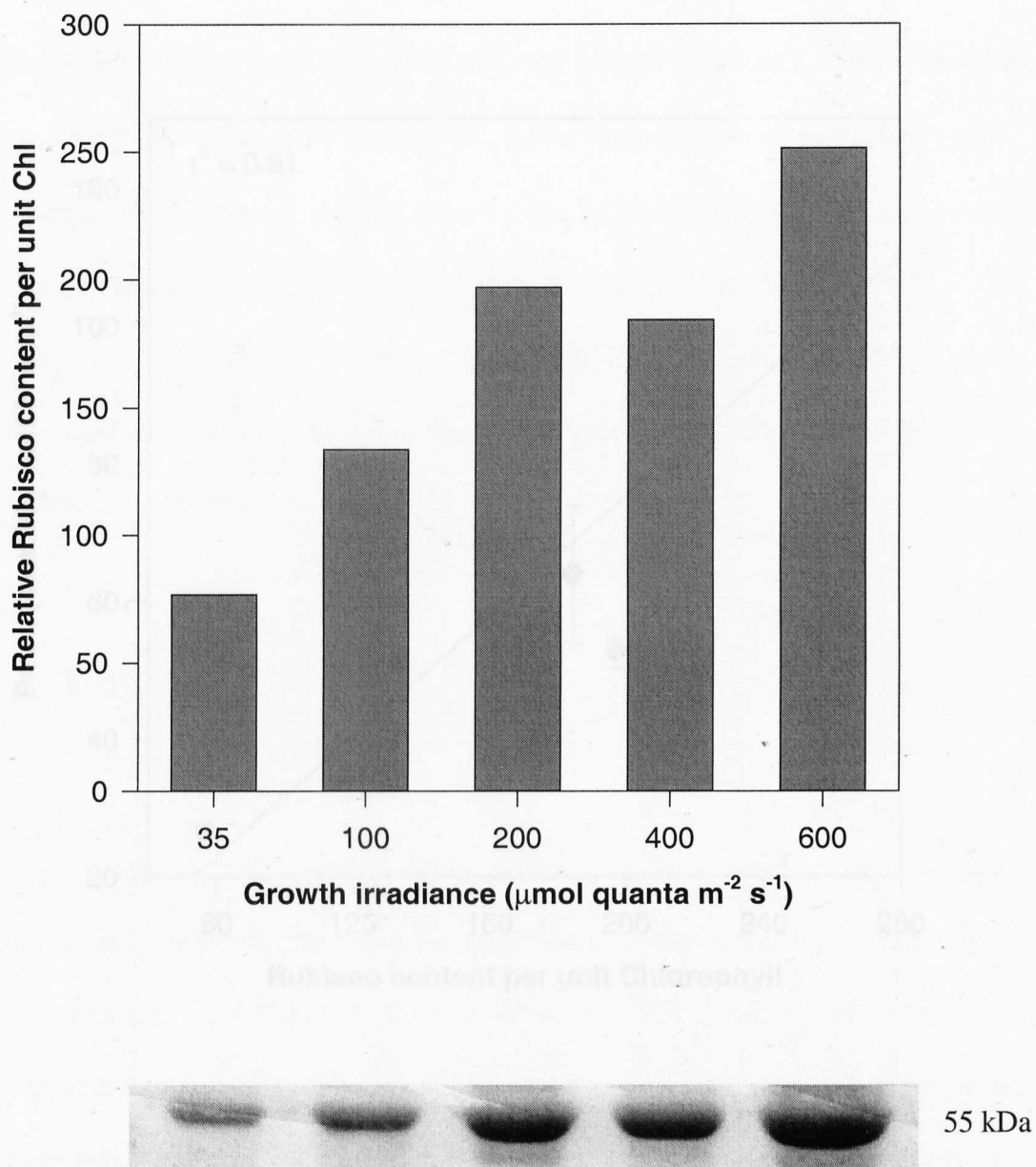


**Figure 4.1** Rubisco large subunit bands and relative band density from coomassie stained SDS PAGE of total soluble protein from *Arabidopsis thaliana* grown over a range of irradiance. Data presented are from a single experiment though the same trend was observed for 5 separate experiments using different plants. Gels loaded on a chlorophyll basis (2 mg chlorophyll per lane). The chlorophyll content was determined from the same leaf sample used for protein isolation.

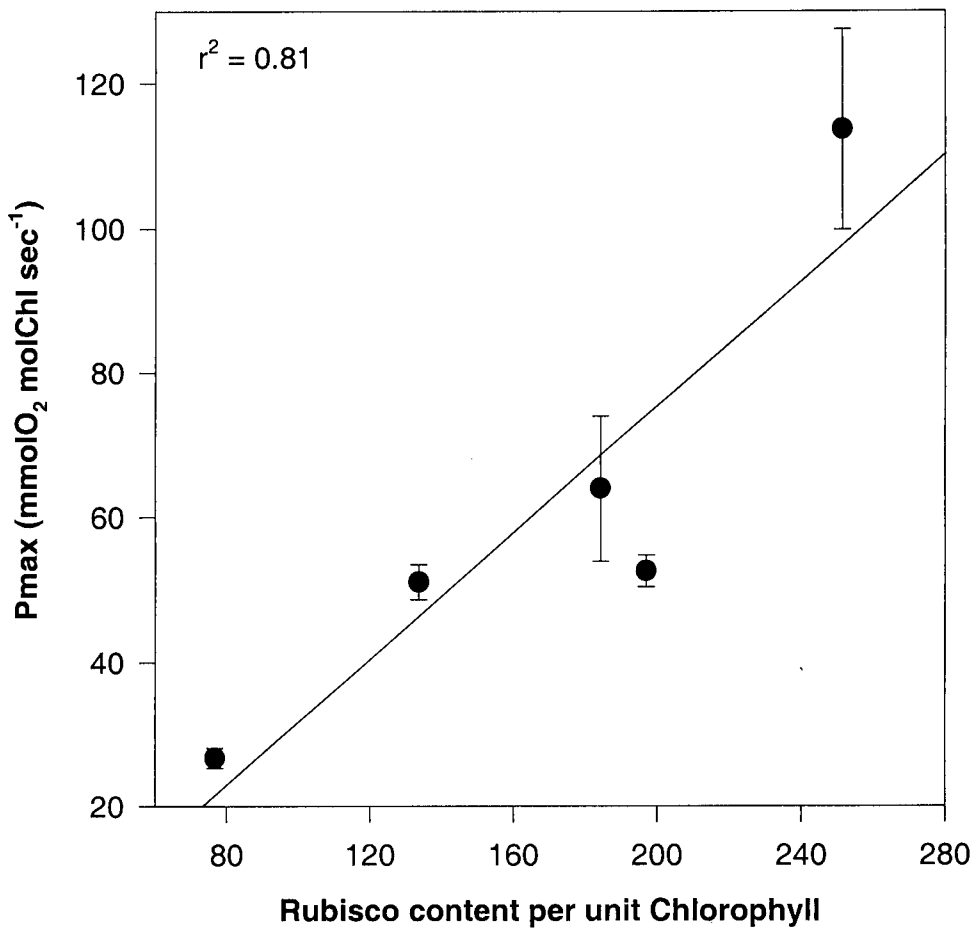


**Figure 4.2** Relationship between Pmax per unit Chlorophyll and Rubisco content per unit chlorophyll for *Arabidopsis thaliana* grown over a range of irradiance. Means  $\pm$  se of 15 replicates from 3 separate batches of plants for Pmax. Rubisco content based on a single experimant from a single plant. Fitted line represents first order regression.

Functional PSII content for *Arabidopsis* grown at the defined range of irradiance is shown in Figure 4.3. From these data it is clear that PSII content per unit chlorophyll is changing in the same discontinuous manner as that observed for Pmax and chlorophyll *a/b* ratio with increases from 35 to 100 and 100 to 200  $\mu\text{mol m}^{-2}\text{s}^{-1}$  followed by a levelling off at 400  $\mu\text{mol m}^{-2}\text{s}^{-1}$  before increasing significantly at 600  $\mu\text{mol m}^{-2}\text{s}^{-1}$ . Since changes in chlorophyll content per unit leaf area are limited across the growth range the same trend in PSII content per unit leaf area would be anticipated. The observation that substantial variations in the levels of PSII are seen at different growth irradiance suggests that changes in thylakoid membrane components other than LHCI must contribute to the final chlorophyll *a/b* ratio.

#### 4.2.3 PSI content

The PSI content of *Arabidopsis* thylakoid membranes was assayed spectrophotometrically from the change in absorbance at 702nm relative to 725nm upon chemical reduction of P700. Figure 4.4 shows the PSI content, expressed on a chlorophyll basis, of *Arabidopsis* thylakoid membranes taken from plants grown over the defined irradiance range. Little change in the levels of PSI can be observed between 100 and 600  $\mu\text{mol m}^{-2}\text{s}^{-1}$  with an increase of just 0.2mM PSI per mole chlorophyll at 400 and 600  $\mu\text{mol m}^{-2}\text{s}^{-1}$  growth relative to plants grown at 100 and 200  $\mu\text{mol m}^{-2}\text{s}^{-1}$ . PSI levels show a dramatic increase at the lowest growth irradiance with almost double the amount of photosystem per unit chlorophyll. The same trend should be observed per unit leaf area given the relative consistency in chlorophyll content on a leaf area basis.

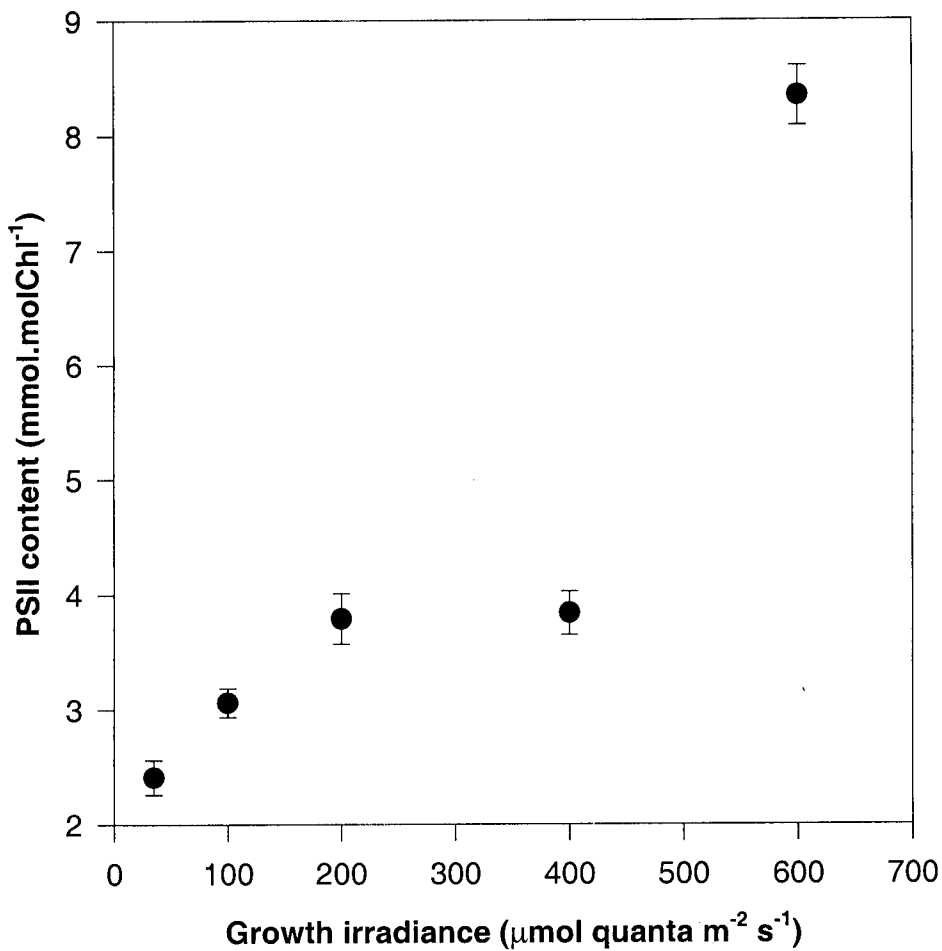


**Figure 4.3** Relationship between PSII content and irradiance for *A.thaliana* grown over a range of irradiance. PSII content measured using the oxygen yield per saturating flash method. Means  $\pm$  se of at least 5 thylakoid preparations taken from separate plants. PSI, PSII content and 77k fluorescence spectra measured from the same batch of plants.

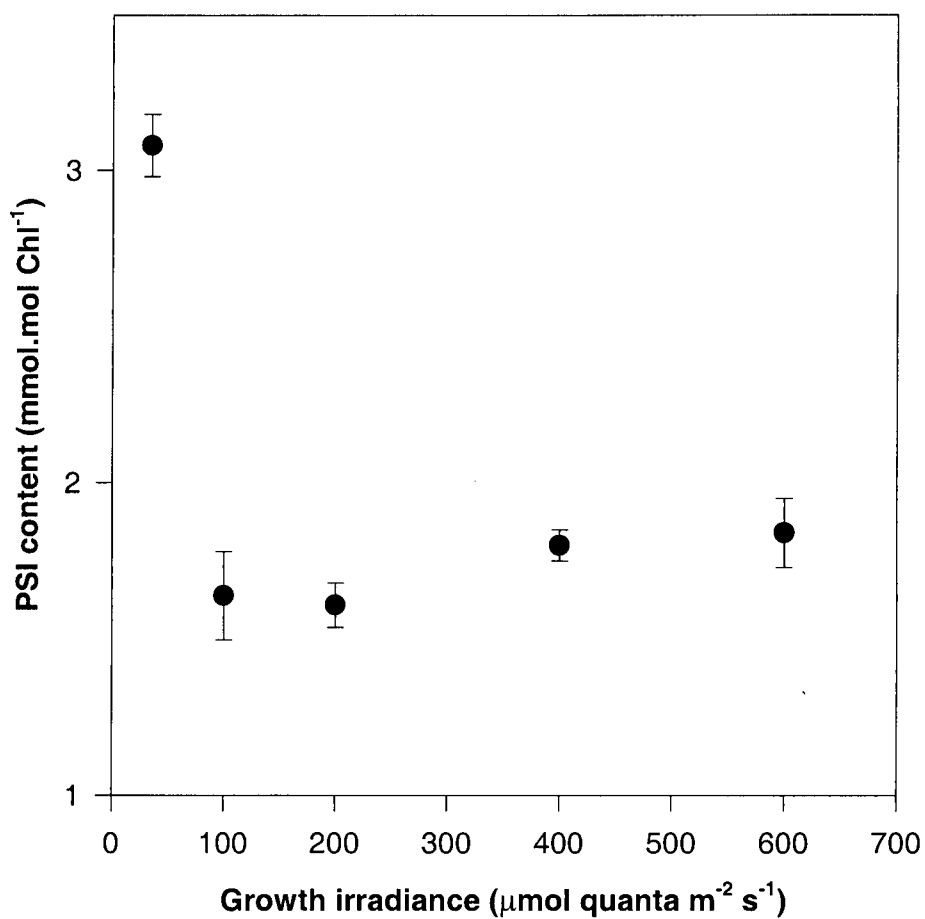


**Figure 4.4** Relationship between PSI content and irradiance for *A.thaliana* grown over a range of irradiance. PSI content measured using oxideised minus reduced difference spectra for P700. Means  $\pm$  se of at least 5 thylakoid preparations taken from separate plants. PSI, PSII content and 77k fluorescence spectra measured from the same batch of plants.

Changes in the levels of the two photosystems with growth irradiance gives rise to alterations in the ratio of PSII to PSI. The differences in PSII/PSI are marked at both the highest and lowest growth irradiance with elevated levels of PSII giving rise to a higher ratio at  $600\mu\text{mol m}^{-2} \text{s}^{-1}$  and higher levels of PSI combining with lower levels of PSII to produce a lower ratio at  $35 \mu\text{mol m}^{-2} \text{s}^{-1}$ .

#### **4.2.4 Light harvesting polypeptide composition**

##### **4.2.4.1 Immunoblotting**

Semi-quantitative immunoblotting was carried out for all ten known chlorophyll *a/b* binding light harvesting polypeptides from *Arabidopsis* plants grown at the defined range of growth irradiance. Equivalent amounts of solubilised thylakoid membranes, loaded on a chlorophyll basis, were resolved for plants grown under each light intensity by SDS gel electrophoresis. Membrane proteins were then transferred to nitro-cellulose membrane for detection with a unique set of monospecific antibody raised against the chlorophyll *a/b* binding proteins. Detection was completed by enhanced chemiluminescence followed by densitometric scanning to provide a measure of the relative band density for each polypeptide. Data for the light harvesting polypeptides of photosystems I and II are shown in figures 4.6 through 4.15. Blots for each polypeptide are shown along with the relative band density before and after normalisation on reaction centre content. The reproducibility of such blots is made difficult by a number of factors including loading inaccuracies, incomplete membrane transfer and uneven binding of primary and secondary antibody (Jansson *et al* 1997). Data presented here

are therefore based on single blots although the same trends have been observed for at least two blots for most polypeptides.

#### 4.2.4.2 PSII light harvesting polypeptide composition.

Immunoblot analysis of the six chlorophyll *a/b* binding light harvesting polypeptides of PSII are shown in figures 4.6 through 4.11. Figures 4.6, 4.7 and 4.8 show the relative polypeptide levels for Lhcb1, 2 and 3 respectively, all of which are believed to make up mixed trimers of bulk LHCII. All three polypeptides show a decrease per reaction centre with increasing growth irradiance. Such decreases in LHCII are likely to make significant contributions to the observed pattern of change in the chlorophyll *a/b* ratio with growth irradiance. However the changes in bulk LHCII are clearly insufficient to account for the full extent of the change in chlorophyll *a/b* ratio particularly at the highest growth irradiance where relatively small differences are seen between 400 and 600  $\mu\text{mol m}^{-2} \text{s}^{-1}$ .

The relative polypeptide composition of the three minor light harvesting polypeptides, Lhcb4, 5 and 6, are shown in figures 4.9, 4.10 and 4.11 respectively. Data for Lhcb4, which cross-reacts with Lhca2, are the sum of two bands which increase and decrease in a reciprocal manner with increasing irradiance. The nature of the doublet, which is separated by 1 or 2 kDa, is unknown but since both bands are detected by the antibody it is assumed that two forms of the polypeptide are present. Possibilities for the existence of two forms of Lhcb4 include differentially expressed gene products or alternative splicing. Alternatively an apparently higher molecular weight form of the polypeptide may arise as a result of a post translation modification. Lhcb4 has been shown to be phosphorylated under conditions of cold stress (Testi *et al* 1996). Minor light harvesting

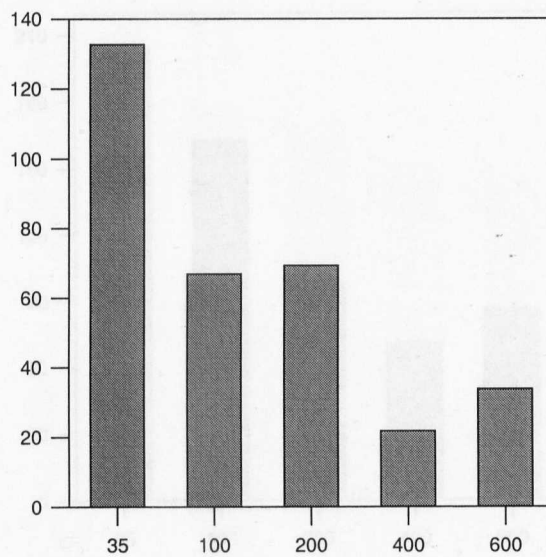
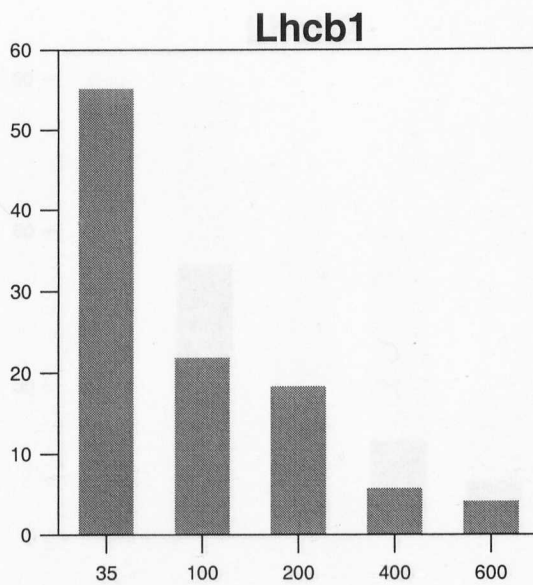


**Figure 4.5** Immunoblot and densitometric analysis of the Lhcb1 polypeptide content of *A.thaliana* grown over a range of irradiance. Top bar chart represents data expressed per unit PSII. Lower bar chart represents unnormalised data. X-axis; Growth Irradiance ( $\mu\text{mol. m}^{-2}. \text{s}^{-1}$ ). Y-axis; Relative Band Density. Data presented are for single blots using thylakoid membranes from a single plant. The same trends have been observed at least twice using the same thylakoid preparation. SDS-Page loaded on a chlorophyll basis (1  $\mu\text{g}$  Chlorophyll per lane)

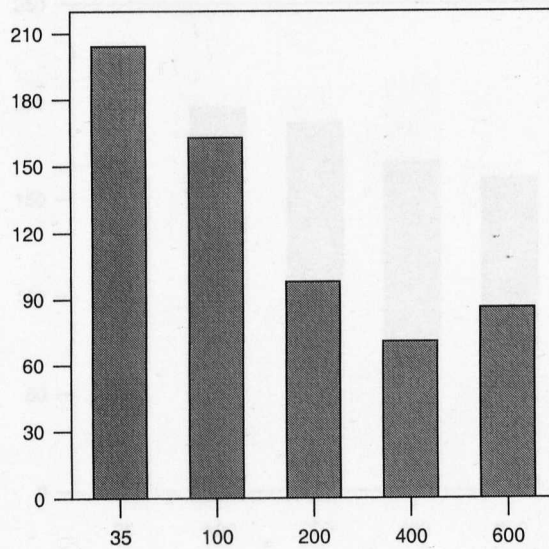
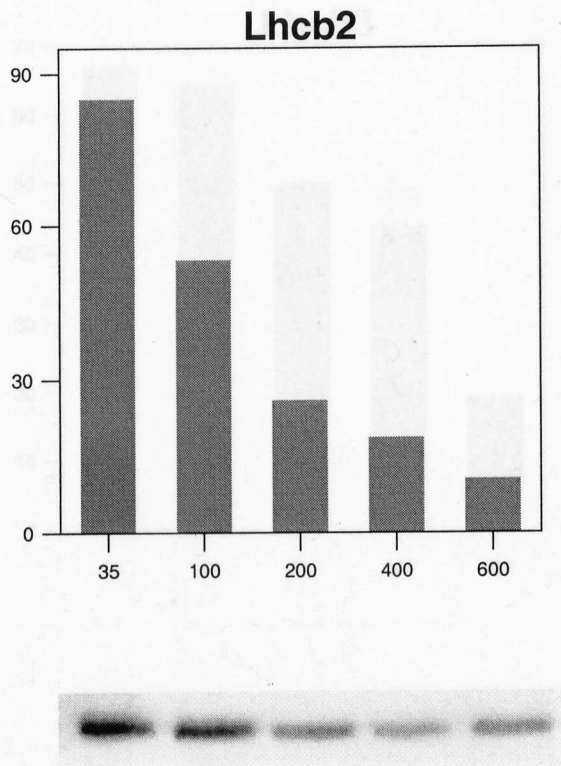


**Figure 4.6** Immunoblot and densitometric analysis of the Lhcb2 polypeptide content of *A.thaliana* grown over a range of irradiance. Top bar chart represents data expressed per unit PSII. Lower bar chart represents unnormalised data. X-axis; Growth Irradiance ( $\mu\text{mol. m}^{-2}. \text{s}^{-1}$ ). Y-axis; Relative Band Density. . Data presented are for single blots using thylakoid membranes from a single plant. The same trends have been observed at least twice using the same thylakoid preparation. SDS-Page loaded on a chlorophyll basis ( $1 \mu\text{g}$  Chlorophyll per lane)

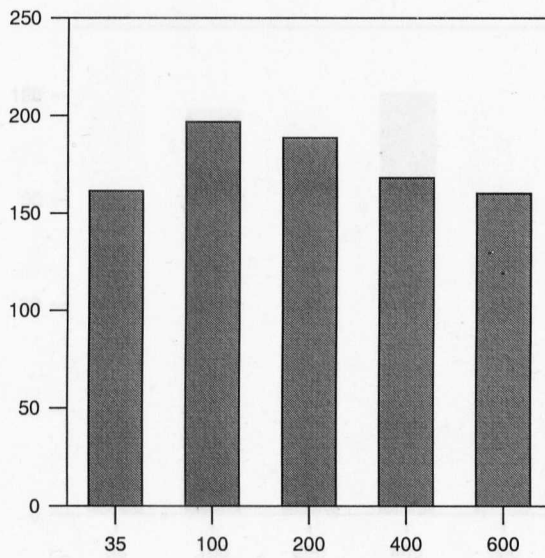
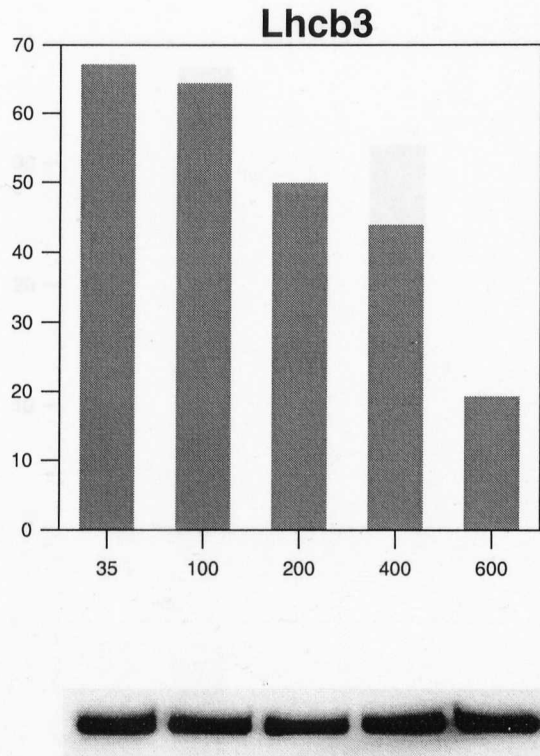


**Figure 4.7** Immunoblot and densitometric analysis of the Lhcb3 polypeptide content of *A.thaliana* grown over a range of irradiance. Top bar chart represents data expressed per unit PSII. Lower bar chart represents unnormalised data. X-axis; Growth Irradiance ( $\mu\text{mol. m}^{-2} \cdot \text{s}^{-1}$ ). Y-axis; Relative Band Density . . Data presented are for single blots using thylakoid membranes from a single plant. The same trends have been observed at least twice using the same thylakoid preparation. SDS-Page loaded on a chlorophyll basis (1  $\mu\text{g}$  Chlorophyll per lane)

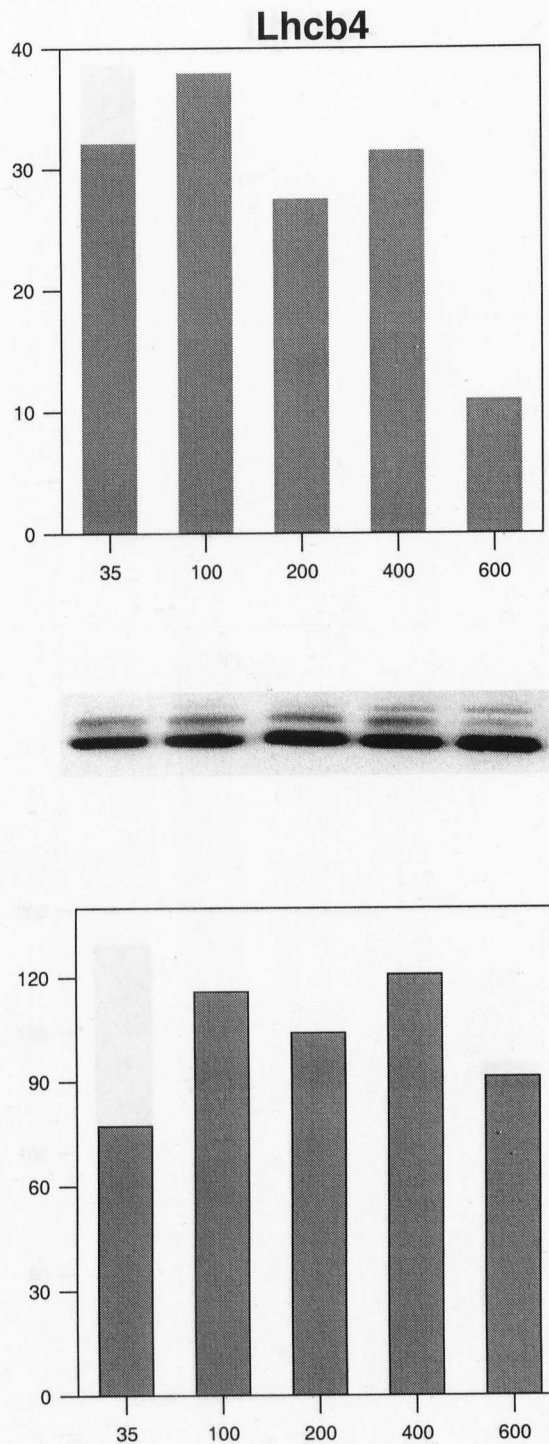


**Figure 4.8** Immunoblot and densitometric analysis of the Lhcb4 polypeptide content of *A.thaliana* grown over a range of irradiance. Top bar chart represents data expressed per unit PSII. Lower bar chart represents unnormalised data. X-axis; Growth Irradiance ( $\mu\text{mol. m}^{-2}. \text{s}^{-1}$ ). Y-axis; Relative Band Density. NB. Lowest band is Lhca1. . Data presented are for single blots using thylakoid membranes from a single plant. The same trends have been observed at least twice using the same thylakoid preparation. SDS-Page loaded on a chlorophyll basis (1  $\mu\text{g}$  Chlorophyll per lane)

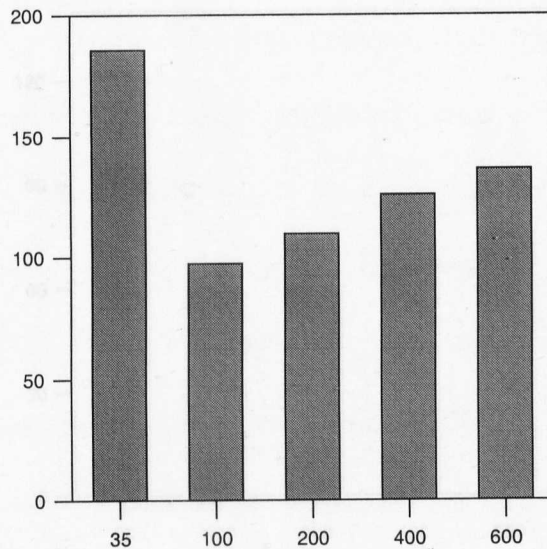
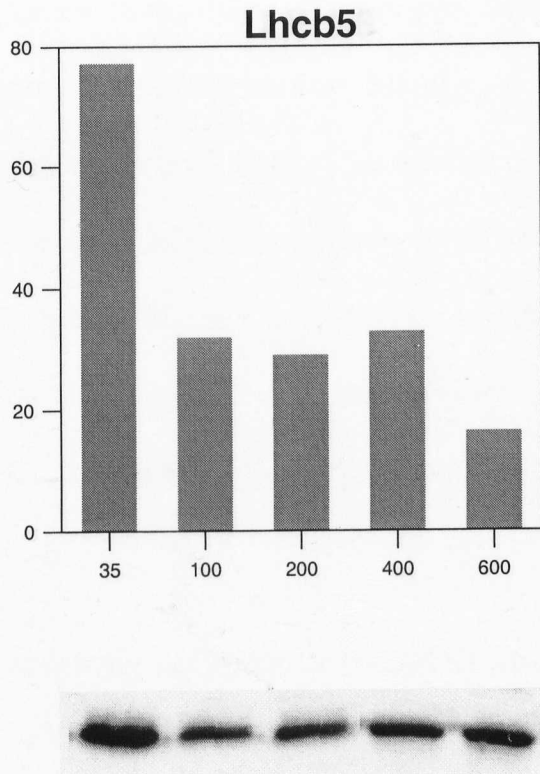


**Figure 4.9** Immunoblot and densitometric analysis of the Lhcb5 polypeptide content of *A.thaliana* grown over a range of irradiance. Top bar chart represents data expressed per unit PSII. Lower bar chart represents unnormalised data. X-axis; Growth Irradiance ( $\mu\text{mol. m}^{-2} \text{s}^{-1}$ ). Y-axis; Relative Band Density . . Data presented are for single blots using thylakoid membranes from a single plant. The same trends have been observed at least twice using the same thylakoid preparation. SDS-Page loaded on a chlorophyll basis ( $1 \mu\text{g}$  Chlorophyll per lane)

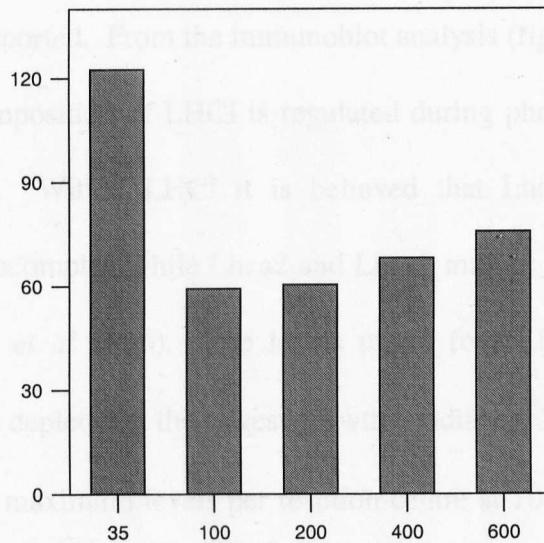
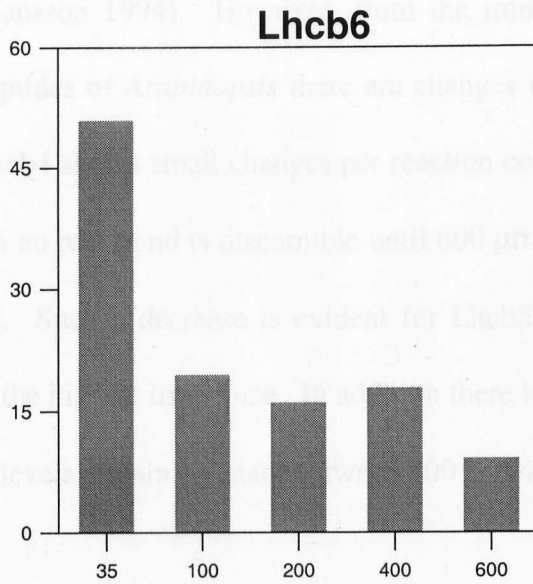


**Figure 4.10** Immunoblot and densitometric analysis of the Lhcb6 polypeptide content of *A.thaliana* grown over a range of irradiance. Top bar chart represents data expressed per unit PSII. Lower bar chart represents unnormalised data. X-axis; Growth Irradiance ( $\mu\text{mol. m}^{-2}. \text{s}^{-1}$ ). Y-axis; Relative Band Density. . Data presented are for single blots using thylakoid membranes from a single plant. The same trends have been observed at least twice using the same thylakoid preparation. SDS-Page loaded on a chlorophyll basis (1  $\mu\text{g}$  Chlorophyll per lane)

polypeptides of PSII are often assumed to be present in a fixed 1:1 stoichiometry with the reaction centre (Jansson 1994). However, from the immunoblot analysis of the minor antenna polypeptides of *Arabidopsis* there are changes in all three proteins with growth irradiance. Lhcb4 shows small changes per reaction centre between 35 and 400  $\mu\text{mol m}^{-2} \text{s}^{-1}$  although no real trend is discernible until 600  $\mu\text{mol m}^{-2} \text{s}^{-1}$  where there is a substantial decrease. Such a decrease is evident for Lhcb5 and Lhcb6 per reaction centre when grown at the highest irradiance. In addition there is a significant increase at 35  $\mu\text{mol m}^{-2} \text{s}^{-1}$  while levels remain constant between 100 and 400  $\mu\text{mol m}^{-2} \text{s}^{-1}$ .

#### 4.2.4.3 PSI light harvesting polypeptide composition

Changes in the levels of PSI light harvesting polypeptides with growth irradiance have not previously been reported. From the immunoblot analysis (figures 4.12 through 4.15) it is clear that the composition of LHCI is regulated during photosynthetic acclimation to growth irradiance. Within LHCI it is believed that Lhca1 and Lhca4 form a functional dimeric subcomplex while Lhca2 and Lhca3 may or may not form a dimeric subcomplex (Jansson *et al* 1996). The levels of all four LHCI polypeptides when normalised on PSI are depleted at the lowest growth irradiance, 35  $\mu\text{mol m}^{-2} \text{s}^{-1}$ . Lhca1 and Lhca4 then reach maximum levels per reaction centre at 100 and 200  $\mu\text{mol m}^{-2} \text{s}^{-1}$  before decreasing at 400 and again at 600  $\mu\text{mol m}^{-2} \text{s}^{-1}$ . Levels of Lhca4 in particular are low at 600  $\mu\text{mol m}^{-2} \text{s}^{-1}$ . Changes in the levels of Lhca2 and 3 are not clearly defined between 100 and 600  $\mu\text{mol m}^{-2} \text{s}^{-1}$  although there does seem to be a reciprocal relationship between the change in the two polypeptides from 100 to 400

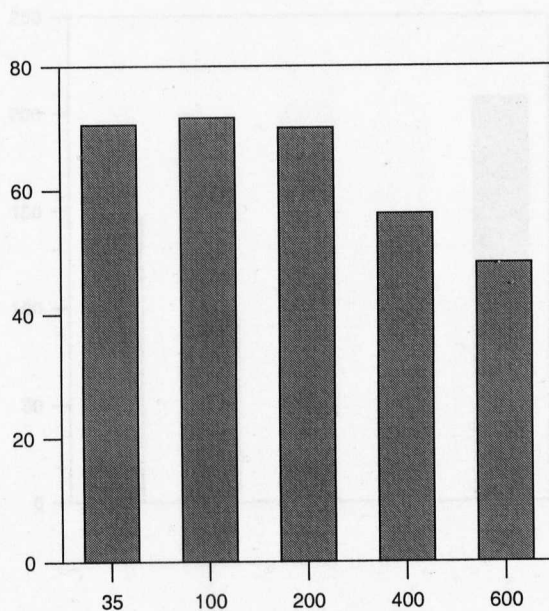
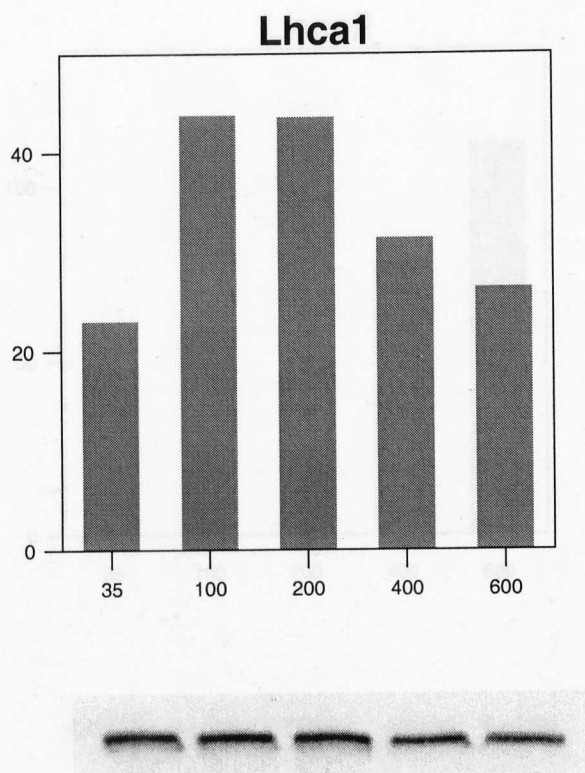
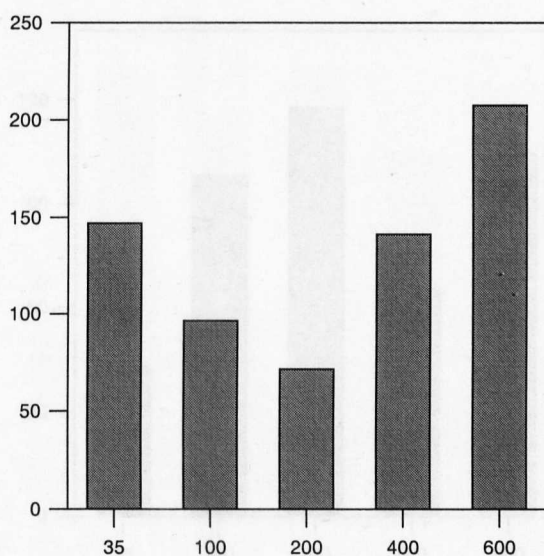
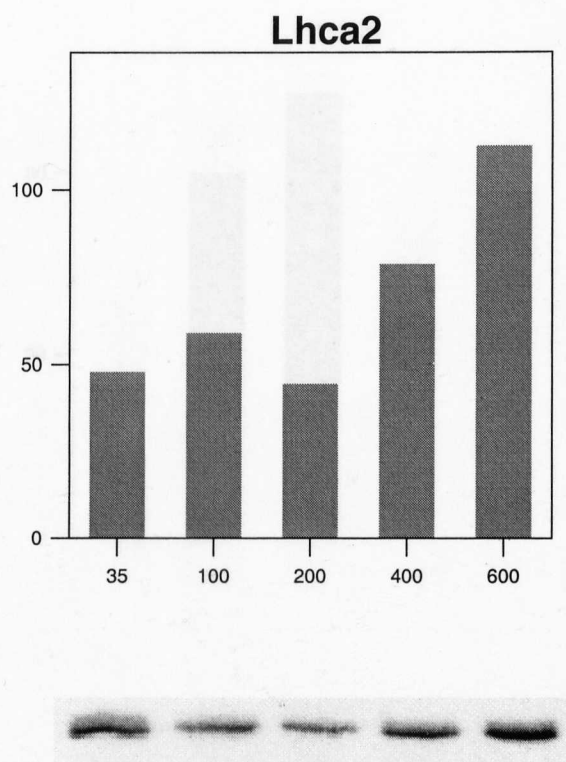
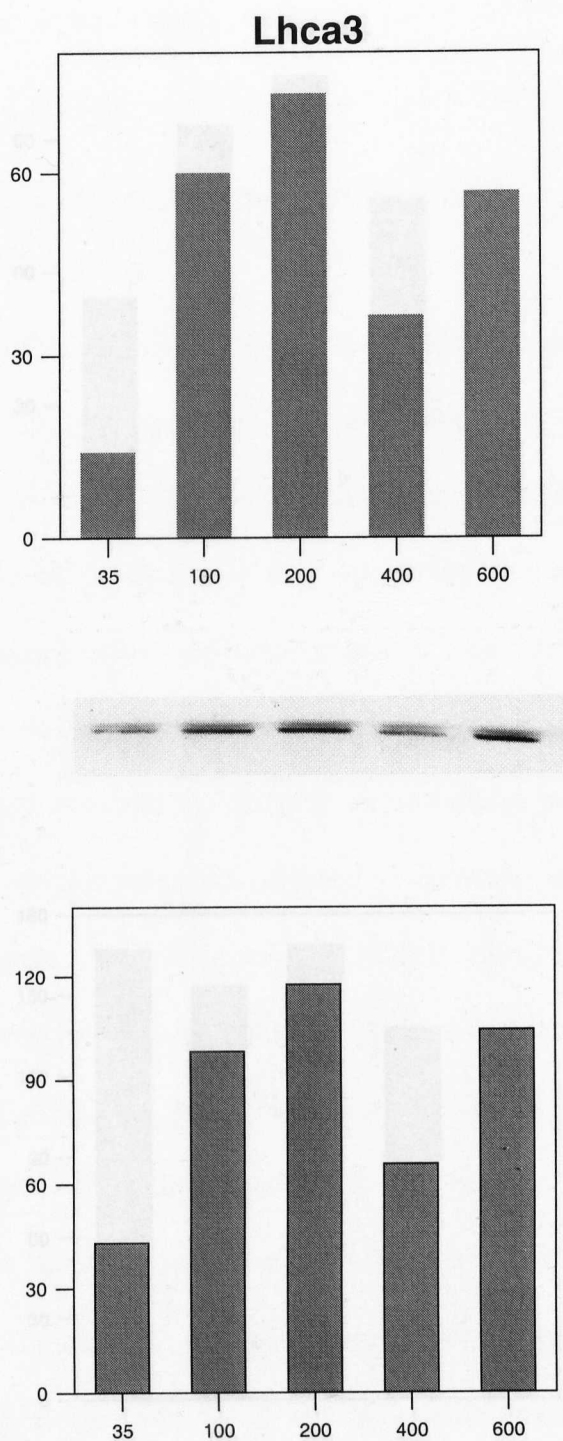


Figure 4.11 Immunoblot and densitometric analysis of the Lhca1 polypeptide content

**Figure 4.11** Immunoblot and densitometric analysis of the Lhca1 polypeptide content of *A.thaliana* grown over a range of irradiance. Top bar chart represents data expressed per unit PSI. Lower bar chart represents unnormalised data. X-axis; Growth Irradiance ( $\mu\text{mol. m}^{-2}. \text{s}^{-1}$ ). Y-axis; Relative Band Density. . Data presented are for single blots using thylakoid membranes from a single plant. The same trends have been observed at least twice using the same thylakoid preparation. SDS-Page loaded on a chlorophyll basis (1  $\mu\text{g}$  Chlorophyll per lane)



**Figure 4.12** Immunoblot and densitometric analysis of the Lhca2 polypeptide content of *A.thaliana* grown over a range of irradiance. Top bar chart represents data expressed per unit PSI. Lower bar chart represents unnormalised data. X-axis; Growth Irradiance ( $\mu\text{mol. m}^{-2}. \text{s}^{-1}$ ). Y-axis; Relative Band Density. . Data presented are for single blots using thylakoid membranes from a single plant. The same trends have been observed at least twice using the same thylakoid preparation. SDS-Page loaded on a chlorophyll basis ( $1 \mu\text{g}$  Chlorophyll per lane)



**Figure 4.13** Immunoblot and densitometric analysis of the Lhca3 polypeptide content of *A.thaliana* grown over a range of irradiance. Top bar chart represents data expressed per unit PSI. Lower bar chart represents unnormalised data. X-axis; Growth Irradiance ( $\mu\text{mol. m}^{-2} \cdot \text{s}^{-1}$ ). Y-axis; Relative Band Density. . Data presented are for single blots using thylakoid membranes from a single plant. The same trends have been observed at least twice using the same thylakoid preparation. SDS-Page loaded on a chlorophyll basis (1  $\mu\text{g}$  Chlorophyll per lane)

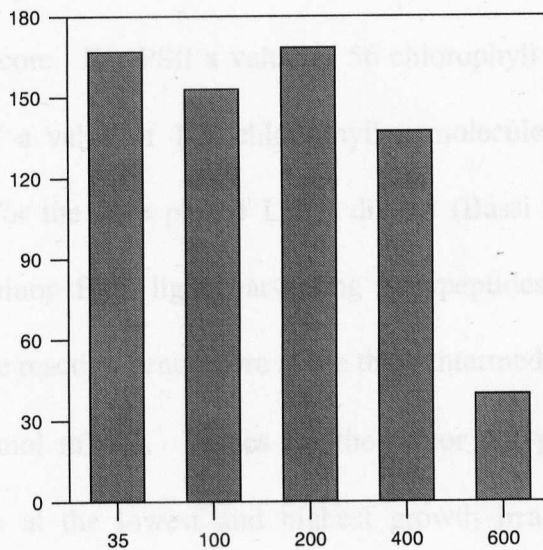
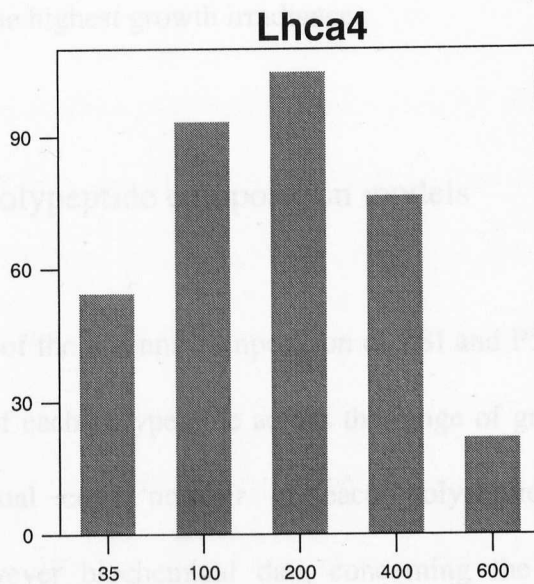


**Figure 4.14** Immunoblot and densitometric analysis of the Lhca4 polypeptide content of *A.thaliana* grown over a range of irradiance. Top bar chart represents data expressed per unit PSI. Lower bar chart represents unnormalised data. X-axis; Growth Irradiance ( $\mu\text{mol. m}^{-2}. \text{s}^{-1}$ ). Y-axis; Relative Band Density. . Data presented are for single blots using thylakoid membranes from a single plant. The same trends have been observed at least twice using the same thylakoid preparation. SDS-Page loaded on a chlorophyll basis (1  $\mu\text{g}$  Chlorophyll per lane)

$\mu\text{mol m}^{-2} \text{ s}^{-1}$  with no change in the sum of the two. An overall increase in both Lhca2 and 3 is observed at the highest growth irradiance.

#### 4.2.4.4 Antenna polypeptide composition models

Immunoblot analysis of the antenna composition of PSI and PSII gives an indication of the relative amount of each polypeptide across the range of growth irradiance but says nothing of the actual copy number of each polypeptide associated with the photosystems. However biochemical data concerning the amount of chlorophyll associated with thylakoid membrane components is available and from the known amounts of each reaction centre and the ratio of chlorophyll *a* to *b* at any given growth irradiance it is possible to model the distribution of antenna polypeptides. For every 1000 chlorophylls a known number of chlorophyll *a* molecules are subtracted to account for the PSII and PSI core. For PSII a value of 56 chlorophyll *a* molecules per core is assumed and for PSI a value of 179 chlorophyll *a* molecules and 30 chlorophyll *b* molecules accounts for the core plus 4 LHCI dimers (Bassi *et al* 1996). It is then assumed that the minor PSII light harvesting polypeptides are present in a 1:1 stoichiometry with the reaction centre core at the three intermediate growth irradiance of 100, 200 and 400  $\mu\text{mol m}^{-2} \text{ s}^{-1}$ . Values for the minor polypeptides associated with reaction centre cores at the lowest and highest growth irradiance are increased or decreased relative to the value at intermediate irradiance in accordance with the immunoblot data. Having allocated chlorophylls for the reaction centres plus the PSII minor antenna the remainder is allocated to LHCII trimers, the levels of which should be in agreement with the relative values indicated by the immunoblot data. Differences in the levels of the PSI light harvesting polypeptides must also be corrected for where

indicated by the immunoblot data. Finally the overall chlorophyll *a/b* ratio for the model must agree with the measured chlorophyll *a/b* ratio.

Data for the models of antenna polypeptide distribution for plants grown at each of the defined growth irradiance are shown in table 4.1. The amount of chlorophyll *a* associated with the PSII core reflects the PSII content as described in section 4.3. As mentioned above, the minor light harvesting polypeptides of PSII are assumed to be present in a 1:1 stoichiometry with the reaction centre core. According to the immunoblot data the levels of Lhcb4, 5 and 6 remain constant at the three intermediate growth irradiance. It has therefore been assumed that the minor light harvesting polypeptides are all present in a 1:1 stoichiometry with the PSII core at 100, 200 and 400  $\mu\text{mol.m}^{-2}.\text{s}^{-1}$ . In accordance with the immunoblot data a 1:1 stoichiometry has also been assigned for Lhcb4 at 35  $\mu\text{mol.m}^{-2}.\text{s}^{-1}$ . However, at the highest growth irradiance the immunoblot analysis indicates that Lhcb4 levels have been reduced to 0.35 per PSII. The immunoblot analysis also indicates changes in the number of Lhcb5 and Lhcb6 associated with PSII at both the highest and lowest growth irradiance. Interestingly these changes are of the same magnitude for these two polypeptides which, from these data, are suggested to be present as 2 copies per PSII at the lowest growth irradiance and 0.5 copies per PSII at the highest growth irradiance. The amounts of chlorophyll *a* and *b* associated with the minor light harvesting polypeptides at each growth irradiance has been assigned on the basis of existing biochemical and structural data.

The remaining chlorophylls were assigned to LHCI and the PSI core as well as to the peripheral LHCII trimers associated with PSII. For the latter this was done in strict agreement with the immunoblot data although assigning the actual number of LHCII trimers per PSII was done within the constraints of the known overall chlorophyll *a/b* ratio and in consideration of the assignment of LHCI and the PSI core chlorophylls.

per 1000 Chl	35 $\mu\text{mol.m}^{-2}.\text{s}^{-1}$	100 $\mu\text{mol.m}^{-2}.\text{s}^{-1}$	200 $\mu\text{mol.m}^{-2}.\text{s}^{-1}$	400 $\mu\text{mol.m}^{-2}.\text{s}^{-1}$	600 $\mu\text{mol.m}^{-2}.\text{s}^{-1}$
<b>PSII</b>	<b>2.41</b> 135 Chla, 0 Chlb	<b>3.06</b> 171 Chla, 0 Chlb	<b>3.79</b> 212 Chla, 0 Chlb	<b>3.84</b> 215 Chla, 0 Chlb	<b>8.35</b> 467 Chla, 0 Chlb
<b>Lhcb4</b>	<b>1 per PSII</b> 17 Chla, 5 Chlb	<b>1 per PSII</b> 21 Chla, 6 Chlb	<b>1 per PSII</b> 27 Chla, 8 Chlb	<b>1 per PSII</b> 27 Chla, 8 Chlb	<b>0.35 per PSII</b> 20 Chla, 6 Chlb
<b>Lhcb5</b>	<b>2 per PSII</b> 34 Chla, 14 Chlb	<b>1 per PSII</b> 121 Chla, 9 Chlb	<b>1 per PSII</b> 27 Chla, 12 Chlb	<b>1 per PSII</b> 27 Chla, 12 Chlb	<b>0.5 per PSII</b> 29 Chla, 13 Chlb
<b>Lhcb6</b>	<b>2 per PSII</b> 24 Chla, 24 Chlb	<b>1 per PSII</b> 15 Chla, 15 Chlb	<b>1 per PSII</b> 19 Chla, 19 Chlb	<b>1 per PSII</b> 19 Chla, 19 Chlb	<b>0.5 per PSII</b> 21 Chla, 21 Chlb
<b>Bulk LHClI</b>	<b>5 trimers</b> 253 Chla, 181 Chlb	<b>3.5 trimers</b> 225 Chla, 161 Chlb	<b>2.4 trimers</b> 191 Chla, 136 Chlb	<b>2.3 trimers</b> 188 Chla, 134 Chlb	<b>0.8 trimer</b> 149 Chla, 106 Chlb
<b>PSI + LHCl monomer</b>	<b>3.08</b> <b>2 per PSI</b> 291 Chla, 22 Chlb	<b>1.64</b> <b>7-8 per PSI</b> 313 Chla, 43 Chlb	<b>1.61</b> <b>8 per PSI</b> 304 Chla, 45 Chlb	<b>1.80</b> <b>7 per PSI</b> 307 Chla, 44 Chlb	<b>1.84</b> <b>2-3 per PSI</b> 152 Chla, 16 Chlb
<b>Total Chl</b>	754 Chla 246 Chlb	766 Chla 234 Chlb	780 Chla 220 Chlb	783 Chla 217 Chlb	838 Chla 162 Chlb
<b>Chl a/b</b>	<b>3.07</b>	<b>3.27</b>	<b>3.55</b>	<b>3.61</b>	<b>5.17</b>

**Table 4.1** Model showing the antenna polypeptide distribution for *A.thaliana* grown over a range of irradiance. The numbers of each component within the model are based on existing biochemical data along with the immunoblot data presented in this chapter and in accordance with the measured chlorophyll a/b ratio (see chapter 1)

Since little biochemical data is available for the amount of chlorophyll bound by LHCI polypeptides these data are potentially the least accurate in the model. PSI core and LHCI data have however been assigned according to the known levels of P700 and the immunoblot data for LHCI polypeptides but the actual amounts of chlorophyll a and b have been fitted to the known overall chlorophyll *a/b* ratio.

PSI is assumed to be associated with 8 LHCI monomers at a growth irradiance of 200  $\text{mmol.m}^{-2}.\text{s}^{-1}$  and the immunoblot data indicates that 7 or 7-8 monomers of LHCI per reaction center are also present at the two other intermediate growth irradiances. There may however be differences in the monomer composition of LHCI across the intermediate growth light range. The amount of LHCI associated with the PSI core shows significant decreases at both the highest and lowest growth irradiances with values of 2 and 2-3 monomers per PSI at 35 and 600  $\text{mmol.m}^{-2}.\text{s}^{-1}$  respectively. The light-harvesting antenna of PSI at the highest growth irradiance is particularly deficient in the Lhca4 polypeptide.

Having assigned chlorophylls to all other thylakoid components the remainder could be used to provide accurate values for the number of LHCII trimers associated with the PSII core. The LHCII values shown in table 4.1 show excellent agreement with the immunoblot data and, along with all other data provide reasonable values for the overall chlorophyll *a/b* ratio. These values show a decrease with increasing growth irradiance and range from 5 trimers per PSII at 35  $\text{mmol.m}^{-2}.\text{s}^{-1}$  to 0.8 trimers per PSII at the 600  $\text{mmol.m}^{-2}.\text{s}^{-1}$ .

#### 4.2.5 77k Fluorescence emission spectra

Low temperature fluorescence emission spectra provide an indication of differences in both the composition and function of the PSI and PSII reaction center and their associated light-harvesting antenna. The 77k emission spectra for Arabidopsis grown over the defined range of growth irradiance are shown in figure 4.16. Spectra were recorded in leaf disks that had been ground in an appropriate buffer in the presence of liquid nitrogen in order to effectively dilute the sample and minimize the risk of fluorescence reabsorption, a phenomenon often seen in leaf disks due to high concentration of chlorophyll *a*. Data from plants grown all 5 growth irradiances were normalized on the small satellite peak at around 770nm. The normalized data show significant decreases in PSII emission with increasing growth irradiance. This decrease may reflect changes in the composition and levels of the PSII antenna although a contribution from fluorescence reabsorption can not be ruled out. In addition there is a decrease in emission from the PSI peak for plants grown at 600  $\text{mmol}\cdot\text{m}^{-2}\cdot\text{s}^{-1}$ . The difference spectra for plants grown at 600 and 200  $\text{mmol}\cdot\text{m}^{-2}\cdot\text{s}^{-1}$  (pink line) suggests that the loss of PSI emission at the highest growth irradiance is the result of decreased emission from the shorter wave length emitters. This is unusual as plants grown at 600  $\text{mmol}\cdot\text{m}^{-2}\cdot\text{s}^{-1}$  are depleted in the content of Lhca4 which is believed to be a part of the LHCI-730 complex which emits at longer wavelengths. As with the PSII emission the possibility of reabsorption exists although this is less likely for PSI since the reabsorption phenomenon affects shorter wavelength emission primarily.

### 4.3 Discussion

Changes in the maximum rate of photosynthesis and chlorophyll *a/b* ratio have provided a simple index for photosynthetic acclimation to irradiance in *Arabidopsis* (chapter 3). The aim of this chapter was to explain the underlying molecular basis of the acclimation profile seen in chapter 3.

Previous studies, one of which involved *Arabidopsis thaliana* grown at two different irradiances (Walters and Horton 1994), have attributed changes in P<sub>max</sub> with changes in the levels of Rubisco. In order to determine the extent to which changes in Rubisco contribute to changes in P<sub>max</sub> over a wide range of growth irradiance Rubisco large subunit levels were determined following SDS page of total soluble protein. The results of this study indicated a good correlation between Rubisco content and P<sub>max</sub> over the full range of growth irradiance. However the correlation coefficient was not sufficiently high to suggest that changes in P<sub>max</sub> could be exclusively attributed to changes in the levels of Rubisco. The correlation between Rubisco content and P<sub>max</sub> was lowest at a growth irradiance of 400 and 600  $\mu\text{mol}\cdot\text{m}^{-2}\cdot\text{s}^{-1}$ . One possible explanation for the weaker correlation at higher growth irradiance is that the band density for the Rubisco large subunit is so great, particularly at 600  $\mu\text{mol}\cdot\text{m}^{-2}\cdot\text{s}^{-1}$ , that it has begun to exceed the linear range for densitometric scanning. It should be noted that while this study measured the levels of Rubisco in relation to P<sub>max</sub>, increases in electron transport components and ATPase might also be expected to support higher maximum rates of photosynthesis.

Large changes in the ratio Chl *a/b* were seen for *Arabidopsis thaliana* grown over a wide range of irradiance in chapter 3. Changes in the levels of any component that binds chlorophyll will contribute to the overall Chl *a/b* ratio. Despite this previous studies have only concentrated on the contribution made by the reaction centers and the

PSII peripheral light harvesting antenna, LHCII. The minor light harvesting antenna of PSII and the PSI light harvesting antenna have been assumed to remain in a fixed stoichiometry with the reaction center core during photosynthetic acclimation to growth irradiance. Furthermore since the majority of studies have found little evidence for reaction center modulation, changes in Chl *a/b* ratio have generally been ascribed to changes in LHCII. One of the aims of this chapter was to reevaluate the assumption that changes in Chl *a/b* ratio during photosynthetic acclimation reflect changes in LHCII. To achieve this the levels of all known chlorophyll containing components, including the reaction centers and all ten chlorophyll *a/b* binding light harvesting polypeptides was measured over the defined range of growth irradiance.

PSII levels were measured using the oxygen yield per flash method. This method provides a measure of functional, oxygen evolving complexes. Despite conflicting reports suggesting that PSII levels may or may not change during acclimation to growth irradiance (Murchie & Horton 1998, Anderson *et al* 1995) it is clear from this study that PSII levels in *Arabidopsis* may be modulated over a wide range of growth irradiance. The overall magnitude of this change is large, ranging from around 2 mmol PSII per mol Chl at the lowest growth irradiance to 8 mmol PSII per mol Chl at the highest growth irradiance. The only previous study to measure changes in PSII content over a sufficiently large range of growth irradiance reported bilinear changes of between 2 and 5 mmol PSII per mol Chl for pea (Leong and Anderson 1984). In this study the change in PSII content over the full range of irradiance mirrors the overall change in Chl *a/b* ratio over the same range of irradiance. One reason why most previous studies have concluded that changes in the levels of PSII with growth light intensity are limited may lie in the range of growth irradiance used. Almost all previous studies have chosen just two growth light environments to reflect high and low light conditions. For example Walters and Horton (1994) saw little change in PSII content when measured at 100 and

400  $\mu\text{mol}\cdot\text{m}^{-2}\cdot\text{s}^{-1}$  with *Arabidopsis thaliana*. This same conclusion may also be drawn from this study when considering the same two growth irradiances. It is only at the two extreme growth irradiances, 35 and 600  $\mu\text{mol}\cdot\text{m}^{-2}\cdot\text{s}^{-1}$ , that the significant changes in PSII become apparent. This is particularly true at 600  $\mu\text{mol}\cdot\text{m}^{-2}\cdot\text{s}^{-1}$  where changes are so great that they must contribute significantly to the overall Chl *a/b* ratio.

As with PSII, previous studies have concluded that the levels of PSI remain constant with growth irradiance. However this study clearly shows that PSI levels, as measured by P700 reduction, may be modulated in response to growth irradiance. Again the changes take place at the extremes of the irradiance range with a doubling in PSI content at the lowest light intensity. It is possible therefore that, like PSII, changes in PSI content have been masked by the choice of the growth light environment. The reason for the significant changes in reaction center content at the extreme light intensities is unclear. It could be speculated that the dramatic increase in PSI content at low light serves to provide extra ATP through cyclic electron transport. Plants grown at 35  $\mu\text{mol}\cdot\text{m}^{-2}\cdot\text{s}^{-1}$  grown very slowly and are likely to be close to their compensation point. Plants grown under such conditions are likely to be less interested in CO<sub>2</sub> fixation for biomass production and more interested in generating ATP for housekeeping functions. Previous studies have demonstrated significant changes in LHCII content with growth irradiance (Leong and Anderson 1984, Walters and Horton 1995) leading many authors to assume that changes in Chl *a/b* ratio reflect changes in LHCII alone. The large changes in reaction center content discussed above suggest that changes in other thylakoid membrane components may also contribute to the overall Chl *a/b* ratio. Furthermore, measurement of the minor PSII light harvesting components of PSII and the PSI light harvesting antenna with growth irradiance is currently lacking. The immunoblot analysis described in this chapter suggests that changes in all ten light harvesting polypeptides may play a role in photosynthetic acclimation to growth

irradiance as well as contributing to the overall Chl *a/b* ratio. Large decreases, on a reaction center basis, in the three polypeptides believed to make up LHCII, i.e. Lhcb1, 2 and 3, with increasing growth irradiance are likely to make the most significant contribution to the Chl *a/b* ratio. These changes also serve to reduce the absorption cross section of PSII thereby minimizing the risk photodamage at higher light intensities. However the three minor light harvesting antenna of PSII, Lhcb4, 5 and 6, are all modulated in response to growth irradiance when expressed per unit PSII. As with the reaction center content, the changes in the minor light-harvesting antenna are all seen at the two extreme growth irradiance. For example, all three polypeptides are significantly reduced at the highest growth irradiance. However since the PSII content is dramatically increased at high light it is not known whether the levels of minor light harvesting antenna are associated with all PSII reaction centers or whether some reaction centers simply do not associate with these polypeptides. Nevertheless, either possibility remains equally intriguing. In addition, Lhcb5 and 6 are dramatically increased at the lowest growth irradiance. Since PSII levels are lowest at this growth irradiance it seems likely that these polypeptides are enriched in each reaction center. However the possibility that PSI binds some of these polypeptides, since PSI levels double at this growth irradiance, can not be ruled out.

Changes in the levels of the PSI light-harvesting antenna, LHCI, are also revealed by the immunoblot analysis. There are overall decreases in the content of LHCI per PSI at both the highest and lowest growth irradiance. Furthermore there are changes in the individual polypeptide composition of LHCI across the full range of irradiance. Such changes in the light-harvesting antenna of PSI have not previously been reported. Of particular interest is the significant decrease in Lhca4 at the highest growth irradiance. Not only is this decrease the most marked it may also have consequences for processes like the state transition (discussed in chapter 5).

## **Chapter Five**

# **Acclimation to Growth Irradiance: Chlorophyll Fluorescence and Carotenoid Content**

## 5.1 Introduction

Chapter 4 showed the changes in the molecular composition of the photosynthetic apparatus that gave rise to the acclimation profile for *Arabidopsis thaliana* over a range of growth irradiance (chapter 3). This chapter investigates the photosynthetic performance of plants grown over the same range of irradiance using room temperature chlorophyll *a* fluorescence as a non-invasive physiological probe. Using modulated fluorimetry along with saturating light pulses it is possible to calculate the contribution of both photochemical (qP) and non-photochemical (qN) processes to the decrease in maximal fluorescence yield known as quenching (reviewed in Horton and Bowyer 1990). Furthermore the product of  $F_v'/F_m'$  and qP gives the quantum efficiency of PSII ( $\phi_{PSII}$ ) from which the apparent electron transport rate may be calculated. Chlorophyll *a* fluorescence measurements of leaf disks from plants grown at the five defined growth irradiance were taken at actinic light intensities ranging from 25 to 1800  $\mu\text{mol m}^{-2} \text{s}^{-1}$  to provide light response curves for  $\phi_{PSII}$ , qP and qN. In addition the relaxation of non-photochemical quenching in the dark was monitored to resolve kinetically distinct phases of qN which have been attributed to energy dependant quenching (qE) and slowly relaxing quenching (qI) (Walters and Horton 1991). These data should provide an indication of whether *Arabidopsis thaliana* grown at higher irradiance are able to maintain an expected higher PSII quantum efficiency with increasing actinic light intensities. Furthermore since  $\phi_{PSII}$  is affected by both photochemical and non-photochemical components it is possible to assess whether the expected elevated levels of  $\phi_{PSII}$  for higher light plants are the result of enhanced photochemistry due to changes at the molecular level or whether a higher capacity for energy dependant non-

photochemical quenching is also observed. Such increases in the capacity for non-photochemical quenching have previously been observed for pea indicating that such processes are themselves subject to light acclimation (Park et al 1996). In addition where the rates of PSII electron transport cannot be accounted for by either photosynthetic acclimation or changes in non-photochemical processes it may be possible to infer alternative electron sinks.

Changes in the composition of the thylakoid membrane may have implications for the state transition. Therefore in addition to assessing whether acclimation affects the short term regulation of photosynthesis chlorophyll *a* fluorescence has also been used to measure the magnitude of the state transition for plants grown at all light intensities.

In addition to chlorophyll *a* fluorescence data, this chapter provides a detailed analysis of the carotenoid composition of plants grown at all five light intensities. As outlined in section 1.5.1 strong correlations exist between the formation of zeaxanthin, following the reversible de-epoxidation of violaxanthin, and the formation and levels of qE with the formation of zeaxanthin increasing the binding affinity of the xanthophyll cycle carotenoids for light harvesting complexes (Ruban *et al* 1999). However the relationship between zeaxanthin formation and energy dependant fluorescent quenching has been shown to be non-linear for a number of C3 and C4 plant species varying between leaves sun and shade leaves (Brugnoli *et al* 1998). In addition the xanthophyll cycle pool size has been shown to increase following high light growth with the majority of additional carotenoid being bound by LHCII (Verhoeven *et al* 1999). This chapter will therefore address whether such correlations exist for *A. thaliana* grown at a number of different irradiances.

## 5.2 Photochemical quenching

The utilisation of absorbed energy through PSII photochemistry and subsequent electron transport result in a decrease in the maximum yield of fluorescence known as photochemical quenching (qP). Values for qP range between 0 and 1 with 1 being the maximum level of quenching and 0 the minimum. Saturating light pulses or treatment with PSII herbicides that block electron transport result in the closure of the reaction centre. In this state  $Q_A$ , the first stable electron acceptor of PSII, is reduced and qP tends toward 0, while in dark adapted leaves the fluorescence yield reaches a maximum. Hence qP reflects the redox state of PSII with lower values indicating more highly reduced centres.

Figure 5.1 shows the relationship between qP and actinic light intensity for *A. thaliana* grown over the defined range of irradiance. Overall, plants grown at lower irradiance have both an earlier onsets in the decrease in qP and a steeper decline with increasing irradiance. Furthermore qP saturates at a lower value and lower actinic irradiance while plants grown at 400 and 600  $\mu\text{mol m}^{-2} \text{s}^{-1}$  apparently fail to reach their minimum value even at the highest actinic light intensity. These data indicate that plants acclimated to higher irradiance maintain PSII in a more oxidised state when subjected to increasing actinic light intensities.

Interestingly, while plants grown at 400  $\mu\text{mol m}^{-2} \text{s}^{-1}$  show a similar acclimation profile to those grown at 200  $\mu\text{mol m}^{-2} \text{s}^{-1}$  with a similar photosynthetic composition, the light response curve for qP is more closely related to 600  $\mu\text{mol m}^{-2} \text{s}^{-1}$ .

Since the photochemical quenching parameter (qP) approximates to the redox state of  $Q_A$ , the first stable electron acceptor of PSII, it has been suggested that this parameter can be used to estimate the 'PSII excitation pressure', a parameter that has been

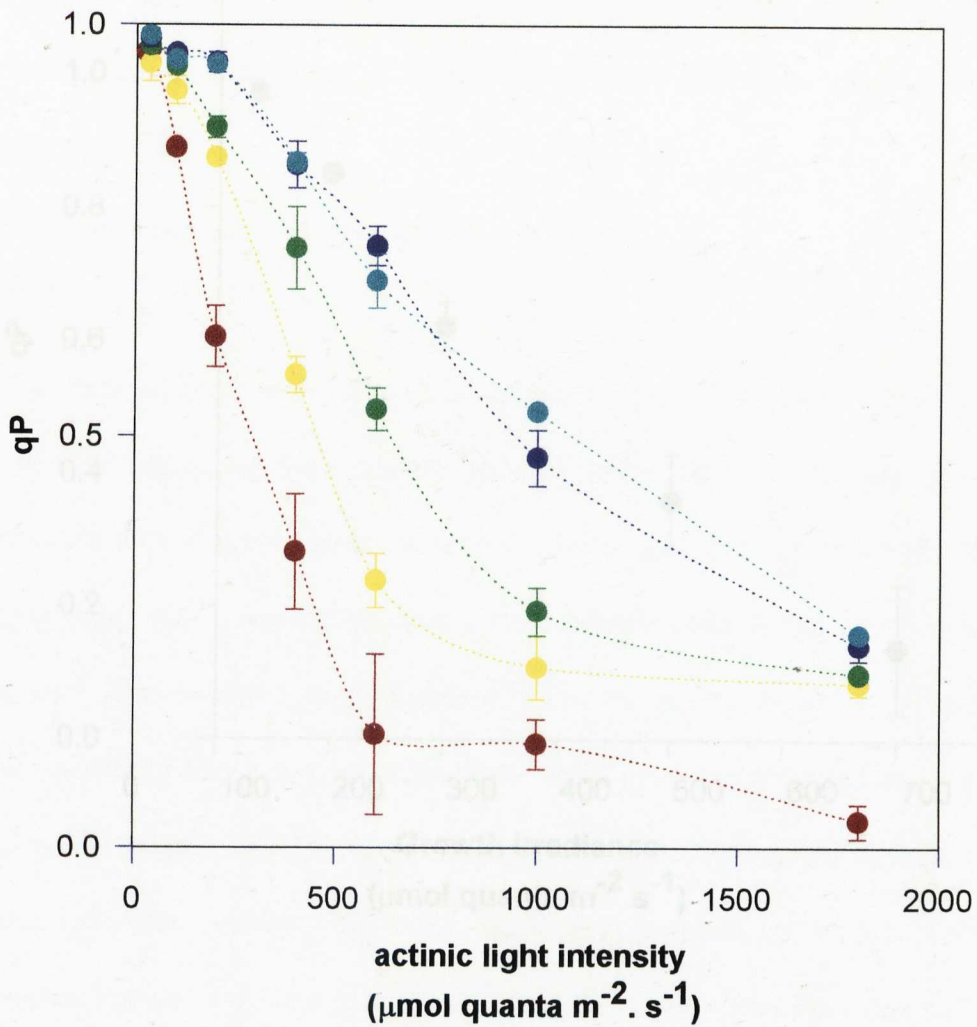
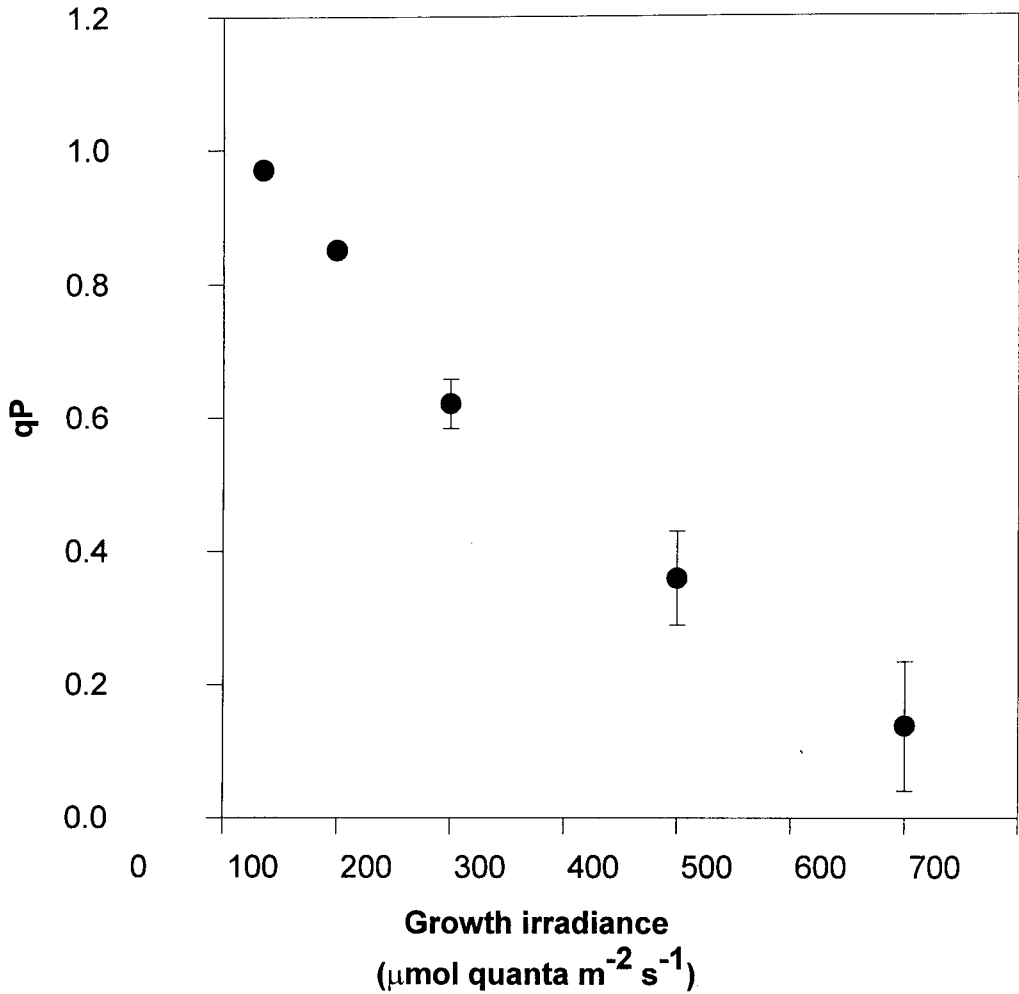


Figure 5.1. qP values for plants grown at 35  $\mu\text{mol m}^{-2} \text{s}^{-1}$  measured at the growth irradiance of all other plants. Means  $\pm$  se of at least 6 replicates from separate plants

**Figure 5.1** Relationship between qP and actinic light intensity for *A.thaliana* grown over a range of irradiance. Growth lights: red 35 $\mu\text{mol m}^{-2} \text{s}^{-1}$  , yellow 100 $\mu\text{mol m}^{-2} \text{s}^{-1}$  , green 200 $\mu\text{mol m}^{-2} \text{s}^{-1}$  , blue 400 $\mu\text{mol m}^{-2} \text{s}^{-1}$  , cyan 600 $\mu\text{mol m}^{-2} \text{s}^{-1}$ . Means  $\pm$  se of at least 6 replicates from separate plants grown in 2 batches. qP, qN, qE, qI, PPSII and electron transport rate are all calculated from the same leaf sample.



**Figure 5.2**  $qP$  values for plants grown at  $35 \text{ mmol m}^{-2} \text{ s}^{-1}$  measured at the growth irradiance of all other plants. Means  $\pm$  se of at least 6 replicates from separate plants grown in 2 batches.  $qP$ ,  $qN$ ,  $qE$ ,  $qI$ , PPSII and electron transport rate are all calculated from the same leaf sample.

correlated with some aspects of photosynthetic acclimation to both irradiance and temperature (see section 1.4.3.2). Using fluorescence data obtained from *Arabidopsis* plants grown at the lowest growth irradiance ( $35 \mu\text{mol m}^{-2} \text{s}^{-1}$ ) the predicted 'excitation pressure' has been estimated as the qP value at all other growth irradiance (figure 5.2). The predicted 'excitation pressure' for *Arabidopsis* plants across the defined range of growth irradiance is clearly not discontinuous as might have been expected from the acclimation profile

### 5.3 Non-photochemical quenching

When a dark adapted leaf receives a saturating pulse of light, which removes photochemical quenching, the maximum yield of fluorescence is observed. If the same leaf is treated with an actinic light for several minutes and then supplied with the same saturating pulse that gave the maximum fluorescence yield it can be seen that the fluorescence yield is significantly decreased from the maximum value. The second form of quenching which is seen in the light when qP is removed is known as non-photochemical quenching (qN). The total value of qN is determined by a number of thylakoid processes (section 1.5). The relationship between qN and its two main components, known as qE and qI, and actinic light intensity have been determined for *A.thaliana* grown over the defined range of irradiance.

#### 5.3.1 Total qN

Total qN was determined for plants grown at each irradiance following a minimum of 45 minutes treatment at each actinic light intensity. It can be seen from figure 5.3 that for plants grown at higher irradiance qN onset occurs at higher actinic irradiance. In

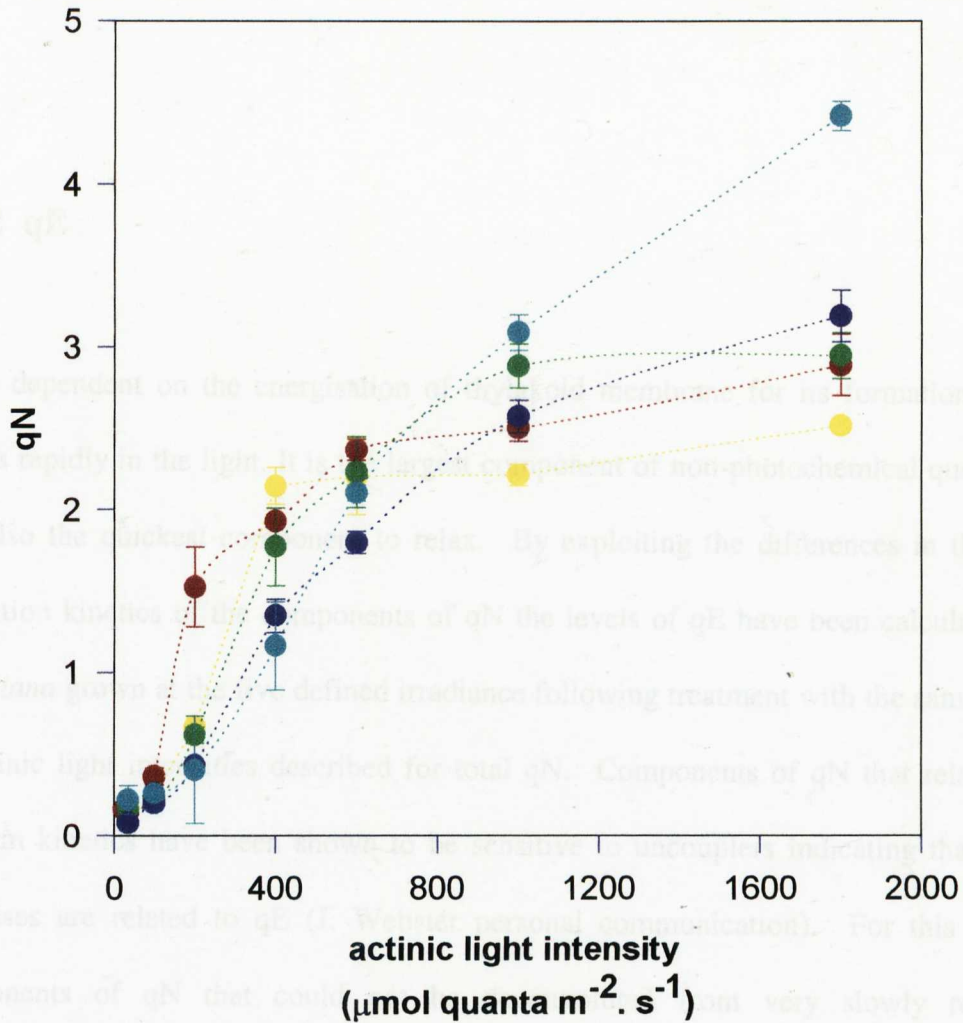


**Figure 5.3** Relationship between  $qN$  and actinic light intensity for *A.thaliana* grown over a range of irradiance. Growth lights: red  $35\mu\text{mol m}^{-2} \text{s}^{-1}$  , yellow  $100\mu\text{mol m}^{-2} \text{s}^{-1}$  , green  $200\mu\text{mol m}^{-2} \text{s}^{-1}$  , blue  $400\mu\text{mol m}^{-2} \text{s}^{-1}$  , cyan  $600\mu\text{mol m}^{-2} \text{s}^{-1}$ . Means  $\pm$  se of at least 6 replicates from separate plants grown in 2 batches.  $qP$ ,  $qN$ ,  $qE$ ,  $qI$ , PPSII and electron transport rate are all calculated from the same leaf sample.

addition plants grown at higher irradiance have higher maximum values of  $q_N$  which saturate at higher actinic light intensities with plants grown at  $600 \mu\text{mol m}^{-2} \text{s}^{-1}$  apparently failing to saturate even at the highest actinic light intensity. In general plants grown at lower irradiance have higher values of  $q_N$  at all actinic light intensities until they reach saturation.

### 5.3.2 $q_E$

$q_E$  is dependent on the energisation of thylakoid membrane for its formation which occurs rapidly in the light. It is the largest component of non-photochemical quenching and also the quickest component to relax. By exploiting the differences in the dark relaxation kinetics of the components of  $q_N$  the levels of  $q_E$  have been calculated for *A.thaliana* grown at the five defined irradiance following treatment with the same range of actinic light intensities described for total  $q_N$ . Components of  $q_N$  that relax with medium kinetics have been shown to be sensitive to uncouplers indicating that these processes are related to  $q_E$  (J. Webster personal communication). For this reason components of  $q_N$  that could not be deconvoluted from very slowly relaxing components of  $q_N$  (15 minutes or more) have been assigned as  $q_E$ . Figure 5.4 shows the relationship between  $q_E$  and actinic light intensity for plants grown over the defined range of irradiance. Similar trends are observed for  $q_E$  as those described for total  $q_N$  with an earlier onset of  $q_E$  for plants grown at lower irradiance.  $q_E$  values remain higher for lower light grown plants until they saturate. As with  $q_N$ , saturation of  $q_E$  takes place at lower actinic light intensities and has lower saturating values for plants grown at lower irradiance. However these trends do not hold for plants grown at 400

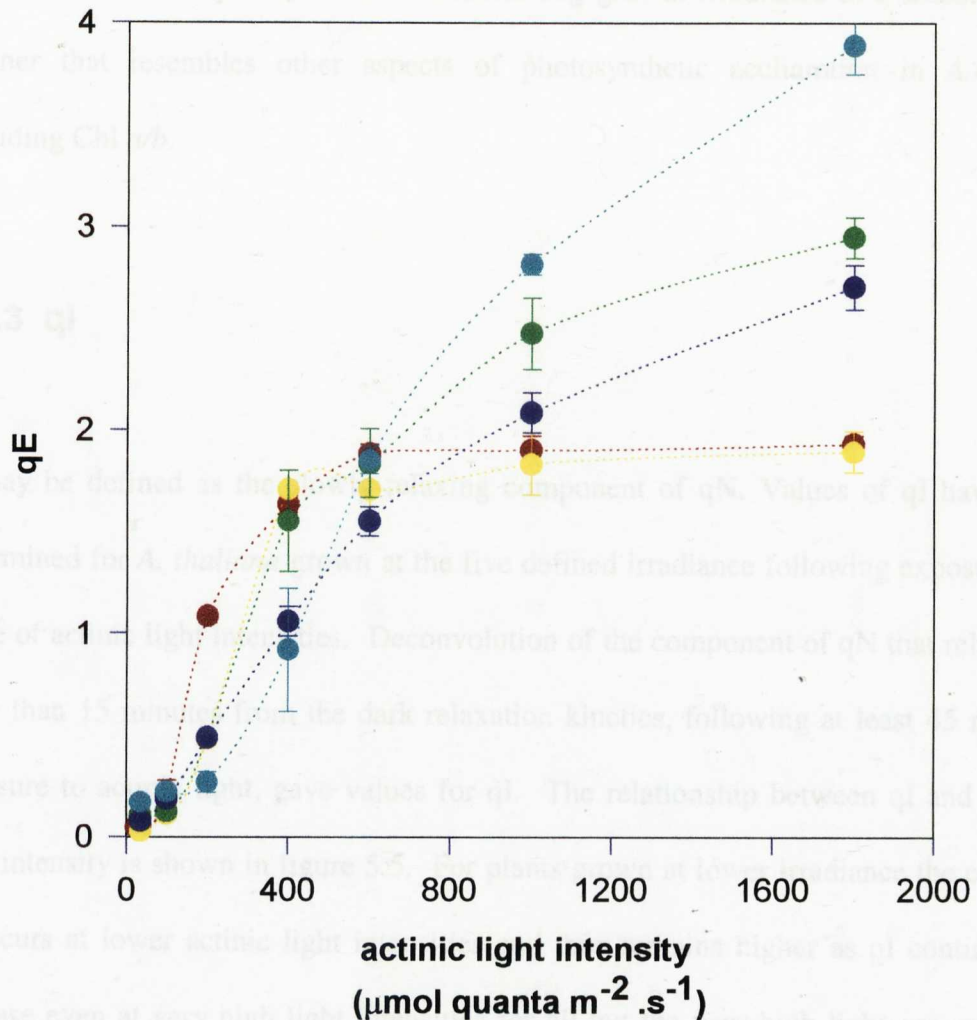


**Figure 5.4** Relationship between qE and actinic light intensity for *A.thaliana* grown over a range of irradiance. Growth lights: red  $35\mu\text{mol m}^{-2} \text{ s}^{-1}$  , yellow  $100\mu\text{mol m}^{-2} \text{ s}^{-1}$  , green  $200\mu\text{mol m}^{-2} \text{ s}^{-1}$  , blue  $400\mu\text{mol m}^{-2} \text{ s}^{-1}$  , cyan  $600\mu\text{mol m}^{-2} \text{ s}^{-1}$  Means  $\pm$  se of at least 6 replicates from separate plants grown in 2 batches. qP, qN, qE, qI, PPSII and electron transport rate are all calculated from the same leaf sample.

$\mu\text{mol m}^{-2} \text{s}^{-1}$  which have lower values of  $qE$  than plants grown at  $200 \mu\text{mol m}^{-2} \text{s}^{-1}$  at higher actinic light intensities. As expected  $qE$  constitutes a large part of  $qN$  although saturating values of  $qE$  make up a significantly smaller fraction of total  $qN$  for plants grown at lower irradiance when compared with those grown at higher irradiance. The maximum value of  $qE$  increases with increasing growth irradiance in a discontinuous manner that resembles other aspects of photosynthetic acclimation in *A.thaliana* including Chl *a/b*.

### 5.3.3 $qI$

$qI$  may be defined as the slowly relaxing component of  $qN$ . Values of  $qI$  have been determined for *A. thaliana* grown at the five defined irradiance following exposure to a range of actinic light intensities. Deconvolution of the component of  $qN$  that relaxed in more than 15 minutes from the dark relaxation kinetics, following at least 45 minutes exposure to actinic light, gave values for  $qI$ . The relationship between  $qI$  and actinic light intensity is shown in figure 5.5. For plants grown at lower irradiance the onset of  $qI$  occurs at lower actinic light intensities and then remains higher as  $qI$  continues to increase even at very high light intensities for all but the very high light grown plants ( $600 \mu\text{mol m}^{-2} \text{s}^{-1}$ ) which show little increase in  $qI$  beyond actinic light intensities of  $400 \mu\text{mol m}^{-2} \text{s}^{-1}$ . It can be seen that  $qI$  continues to increase for lower light grown plants beyond the saturating actinic light intensities for  $qE$ .

## 5.4 $\Phi\text{PSII}$

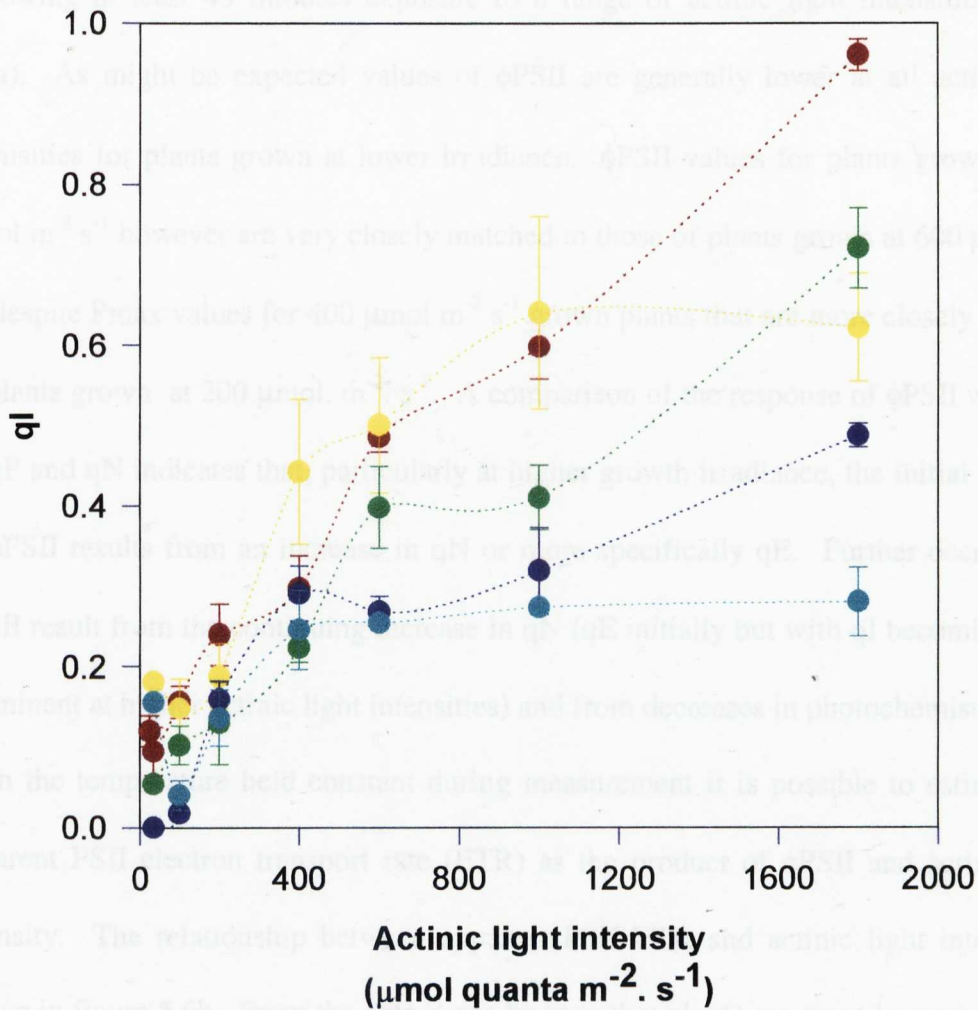


**Figure 5.5** Relationship between  $qI$  and actinic light intensity for *A. thaliana* grown over a range of irradiance. Growth lights: red  $35 \mu\text{mol m}^{-2} \text{s}^{-1}$ , yellow  $100 \mu\text{mol m}^{-2} \text{s}^{-1}$ , green  $200 \mu\text{mol m}^{-2} \text{s}^{-1}$ , blue  $400 \mu\text{mol m}^{-2} \text{s}^{-1}$ , cyan  $600 \mu\text{mol m}^{-2} \text{s}^{-1}$ . Means  $\pm$  se of at least 6 replicates from separate plants grown in 2 batches.  $qP$ ,  $qN$ ,  $qE$ ,  $qI$ , PPSII and electron transport rate are all calculated from the same leaf sample.

$\phi\text{PSII}$  is a measure of the quantum efficiency of PSII. It is calculated as the product of  $qP$  and  $F_v'/F_m'$ . It follows therefore that reductions in  $\phi\text{PSII}$  may result from increasing non-photochemical quenching, decreasing photochemistry or a combination of both.  $\phi\text{PSII}$  has been measured for plants grown at the five defined growth irradiance following at least 45 minutes exposure to a range of actinic light intensities (figure 5.6a). As might be expected values of  $\phi\text{PSII}$  are generally lower at all actinic light intensities for plants grown at lower irradiance.  $\phi\text{PSII}$  values for plants grown at  $400 \mu\text{mol m}^{-2} \text{s}^{-1}$  however are very closely matched to those of plants grown at  $600 \mu\text{mol m}^{-2} \text{s}^{-1}$  despite  $P_{\text{max}}$  values for  $400 \mu\text{mol m}^{-2} \text{s}^{-1}$  grown plants that are more closely matched to plants grown at  $200 \mu\text{mol m}^{-2} \text{s}^{-1}$ . A comparison of the response of  $\phi\text{PSII}$  with that of  $qP$  and  $qN$  indicates that, particularly at higher growth irradiance, the initial decrease in  $\phi\text{PSII}$  results from an increase in  $qN$  or more specifically  $qE$ . Further decreases in  $\phi\text{PSII}$  result from the continuing increase in  $qN$  ( $qE$  initially but with  $qI$  becoming more prominent at higher actinic light intensities) and from decreases in photochemistry.

With the temperature held constant during measurement it is possible to estimate the apparent PSII electron transport rate (ETR) as the product of  $\phi\text{PSII}$  and actinic light intensity. The relationship between apparent PSII ETR and actinic light intensity is shown in figure 5.6b. From the data it can be seen that plants grown at lower irradiance have much lower saturating values of PSII ETR than those grown at higher irradiance. Furthermore the saturation point for lower light grown plants occurs at lower actinic light intensities. Interestingly both the point of saturation and the saturating value of PSII ETR for plants grown at  $400 \mu\text{mol m}^{-2} \text{s}^{-1}$  matches that of plants grown at  $600 \mu\text{mol m}^{-2} \text{s}^{-1}$  and not that of plants grown at  $200 \mu\text{mol m}^{-2} \text{s}^{-1}$ .

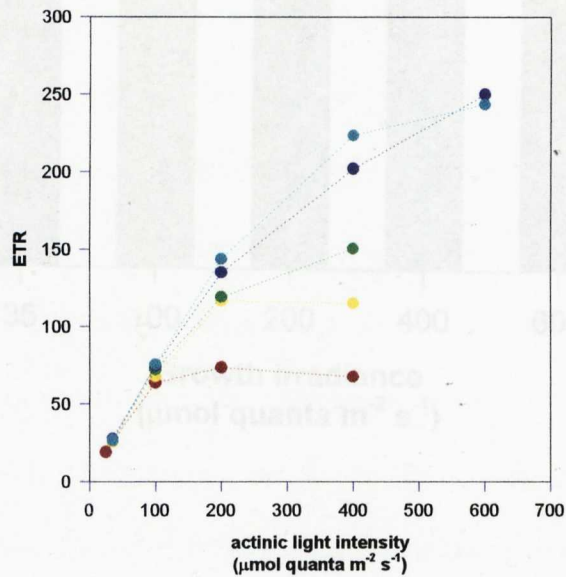
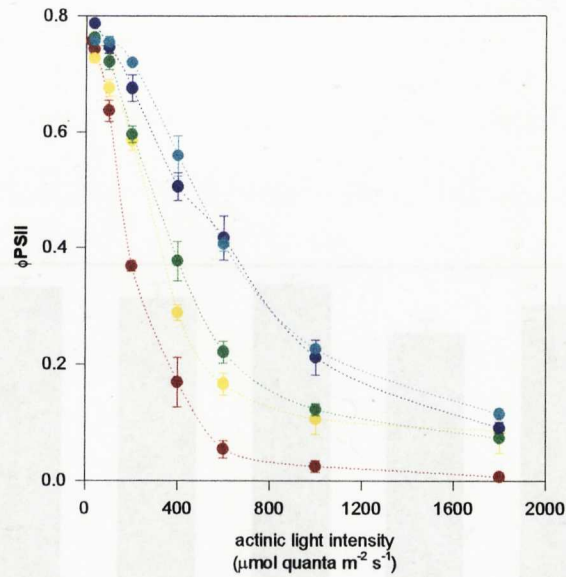
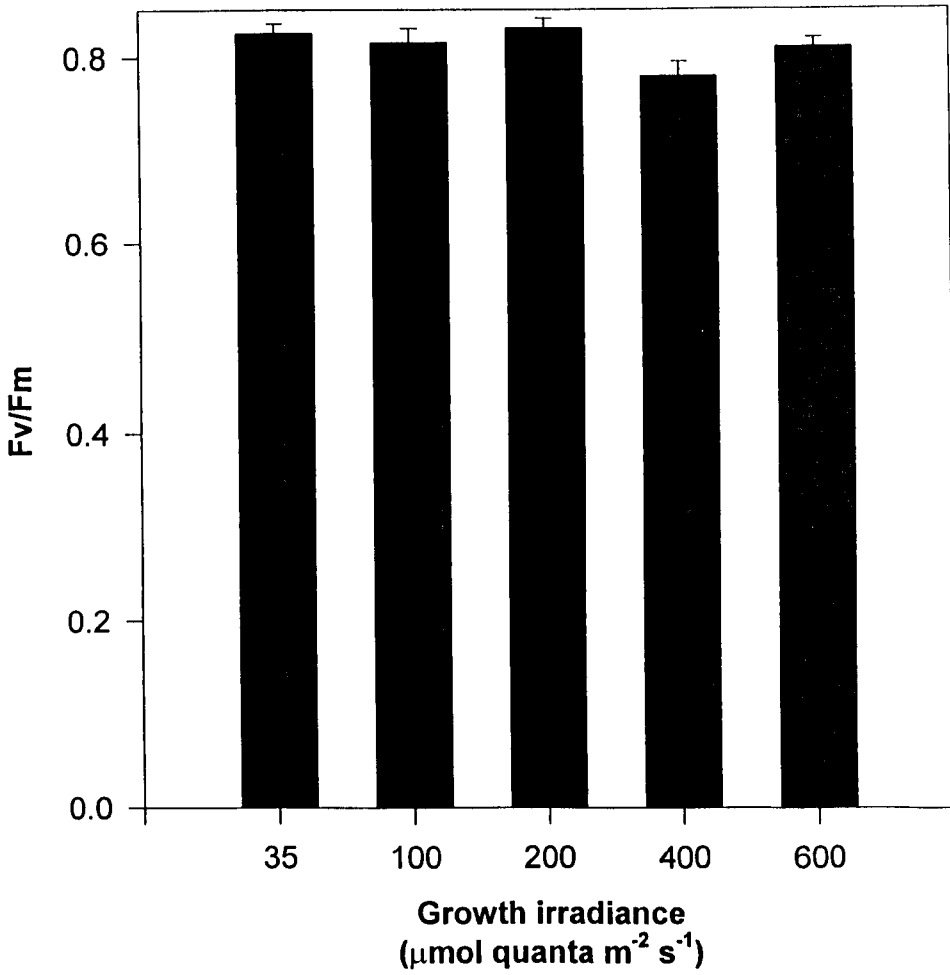


Figure 5.7 Relationship between dark adapted values of Fv/Fm and growth irradiance

**Figure 5.6** Relationship between **a.**  $\phi_{PSII}$  (top graph), **b.** electron transport rate (bottom graph) and actinic light intensity for *A.thaliana* grown over a range of irradiance. Growth lights: red  $35\mu\text{mol m}^{-2} \text{s}^{-1}$ , yellow  $100\mu\text{mol m}^{-2} \text{s}^{-1}$ , green  $200\mu\text{mol m}^{-2} \text{s}^{-1}$ , blue  $400\mu\text{mol m}^{-2} \text{s}^{-1}$ , cyan  $600\mu\text{mol m}^{-2} \text{s}^{-1}$  Means  $\pm$  se of at least 6 replicates from separate plants grown in 2 batches. qP, qN, qE, qI, PPSII and electron transport rate are all calculated from the same leaf sample.



**Figure 5.7** Relationship between dark adapted values of Fv/Fm and growth irradiance for *A.thaliana*. Means  $\pm$  se

## 5.5 Fv/Fm

Fv/Fm values for dark adapted leaves of *A.thaliana* grown over a range of irradiance are shown in figure 5.7. High values of between 0.8 and 0.82 are seen for plants grown at most irradiance however plants grown at  $400 \mu\text{mol m}^{-2} \text{s}^{-1}$  have slightly lower values of around 0.78. All plants were dark adapted under room light for 1 hour prior to measurement.

## 5.6 Carotenoid content.

It is well established that strong correlations exist between non-photochemical quenching of chlorophyll *a* fluorescence and the formation of zeaxanthin following the reversible deepoxidation of violaxanthin (reviewed in Demmig-Adams and Adams 1990). However the involvement of the xanthophyll cycle carotenoids in the formation of qE remains unclear with both direct and indirect roles having been suggested (Horton *et al* 1996). In order to establish whether the acclimation of the photosynthetic apparatus to irradiance is accompanied by changes in carotenoid composition, and in particular xanthophyll cycle carotenoids, a detailed analysis of the carotenoid content of *A. thaliana* leaves has been undertaken for plants grown at the five defined irradiances. The carotenoid content of *A.thaliana* leaves frozen straight from the growth chamber are shown in table 5.1. It can be seen from table 5 that lutein is the most abundant carotenoid in Arabidopsis leaves with a percentage composition of up to 50%. As expected from its role in the structure of LHCII there is a slight decrease in the content of lutein with increasing growth irradiance.  $\beta$ -carotene, the second most abundant carotenoid in Arabidopsis leaves appears to be subject to some variation between plants

Grow light $\mu\text{mol quanta m}^{-2} \text{ s}^{-1}$	lutein	anthera- xanthin	zeaxanthin	neoxanthin	violaxanthin	$\beta$ -carotene	Carotenoid: chlorophyll	Xanthophyll cycle pool size
35	50.36 $\pm 2.77$	0.505 $\pm 0.073$	ND	12.34 $\pm 0.47$	9.98 $\pm 1.13$	26.81 $\pm 2.1$	0.27 $\pm 0.04$	10.49 $\pm 1.14$
100	47.49 $\pm 2.66$	0.152 $\pm 0.074$	1.33 $\pm 0.17$	12.32 $\pm 0.95$	12.75 $\pm 0.95$	29.20 $\pm 1.72$	0.24 $\pm 0.01$	14.17 $\pm 0.87$
200	44.98 $\pm 2.48$	0.200 $\pm 0.04$	1.41 $\pm 0.3$	12.41 $\pm 0.4$	13.28 $\pm 1.3$	28.40 $\pm 2.2$	0.26 $\pm 0.04$	14.89 $\pm 1.11$
400	44.52 $\pm 3.11$	0.150 $\pm 0.054$	2.95 $\pm 0.48$	12.05 $\pm 0.25$	11.94 $\pm 2.16$	28.39 $\pm 1.7$	0.21 $\pm 0.01$	15.04 $\pm 1.86$
600	40.08 $\pm 0.22$	0.98 $\pm 0.38$	3.39 $\pm 1.12$	11.73 $\pm 1.16$	15.78 $\pm 0.5$	28.03 $\pm 2.38$	0.23 $\pm 0.03$	20.15 $\pm 1.04$

**Table 5.1** Percentage carotenoid composition for Leaves of *A. thaliana* grown over a range of irradiance. Means  $\pm$  se of at least 6 replicates from separate plants grown in 2 batches.

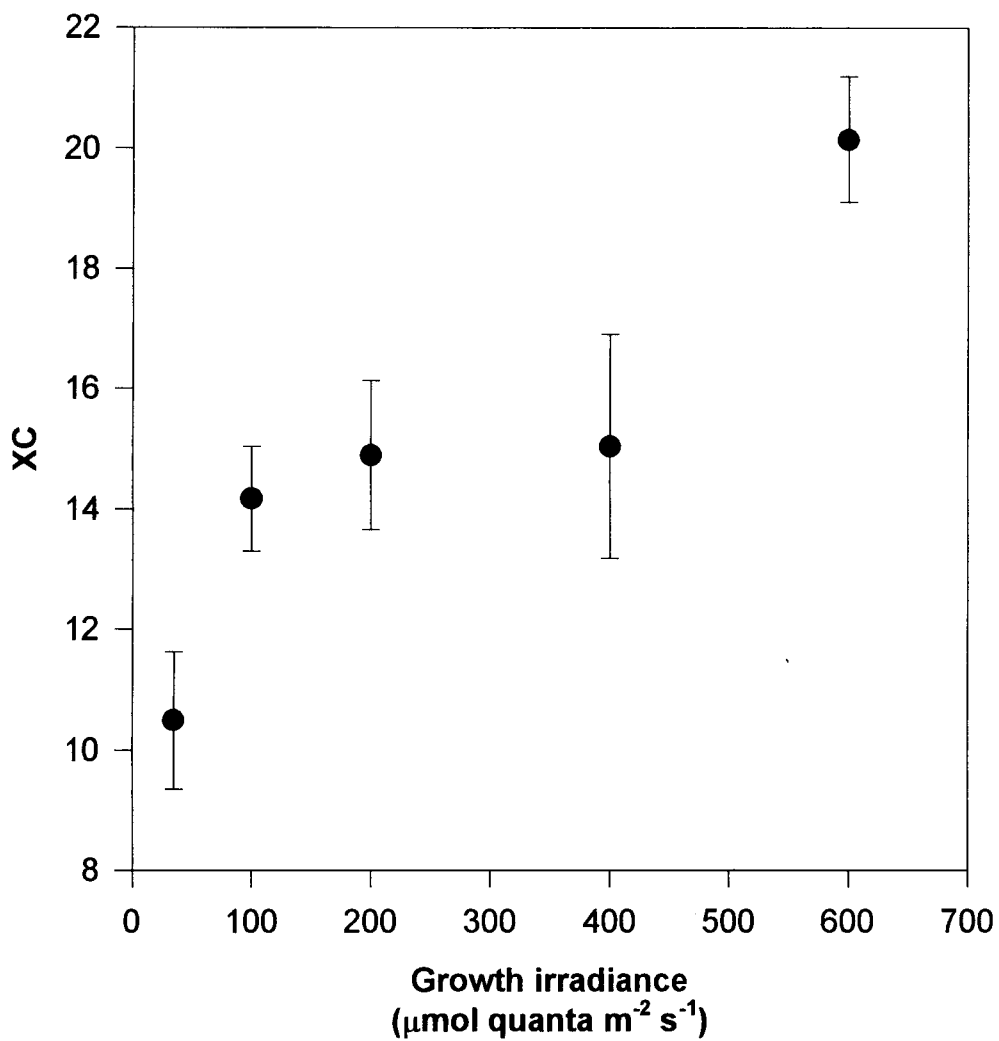


**Figure 5.8** Relationship between xanthophyll cycle pool size (XC) and growth irradiance for *A. thaliana*. Means  $\pm$  se of at least 6 replicates from separate plants grown in 2 batches.

**PAGE  
MISSING  
IN  
ORIGINAL**

A minor component of non-photochemical quenching can arise at low actinic irradiance as a result of the state transition. As discussed in section 1.5.3 the state transition involves the migration of phosphorylated LHCII away from PSII and toward PSI in the non-appressed region of the thylakoid membrane. The state transition responds to imbalances in intersystem electron transfer which is sensed by the redox poise of the cytochrome *b<sub>6</sub>f* complex. Using low levels of red and far red light to preferentially excite PSI and PSII it is possible to induce the state transition which can then be monitored by Chlorophyll *a* fluorescence. In order to assess whether the changes in the composition of the photosynthetic apparatus during photosynthetic acclimation had any effect upon the capacity for state transition the process was measured for *Arabidopsis thaliana* grown at a range of irradiance. Figure 5.11 Shows state transition levels for plants grown at the five defined growth light intensities. Values range from 0 to 1 with 1 being a large state transition and 0 being no state transition. It can be seen that growth at all irradiance results in a high capacity for state transition with high values of above 0.9 across the range. A very slight decrease is observed at the highest growth irradiance ( $600 \mu\text{mol m}^{-2} \text{s}^{-1}$ ) however the value is still high indicating efficient state transition even with very low levels of LHCII.

## 5.8 Discussion

Using the non-invasive technique of room temperature chlorophyll fluorometry this chapter has assessed the physiological performance of *Arabidopsis thaliana* grown at the five previously defined irradiance. It is clear from a number of the parameters measured in this chapter that plants acclimated to different growth irradiance have

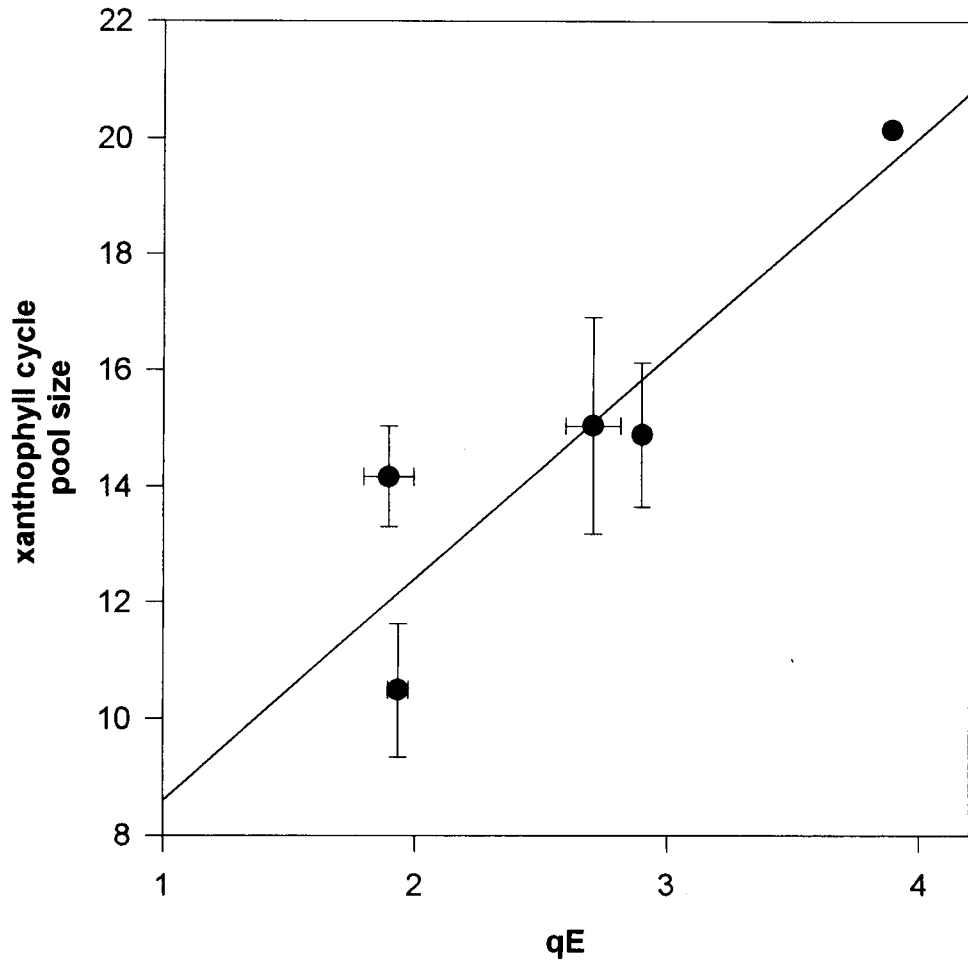


**Figure 5.10** Relationship between xanthophyll cycle pool size and  $qE$  for *A.thaliana* grown over a range of irradiance. Means  $\pm$  se of at least 6 replicates from separate plants grown in 2 batches for both  $qE$  and  $XC$ .  $qP$ ,  $qN$ ,  $qE$ ,  $qI$ ,  $PPSII$  and electron transport rate are all calculated from the same leaf sample, while  $XC$  was calculated from different leaf samples.

Growth irradiance $\mu\text{mol quanta m}^{-2} \text{ s}^{-1}$	De-epoxidation state		
	Frozen from growth cabinet	Dark treated	Light treated
35	2.44 $\pm$ 0.42	2.49 $\pm$ 0.08	48.47 $\pm$ 2.3
100	9.5 $\pm$ 2.18	10.96 $\pm$ 2.7	64.14 $\pm$ 3.7
200	9.6 $\pm$ 2.1	11.16 $\pm$ 3.2	50.89 $\pm$ 4.8
400	20.89 $\pm$ 5.5	20.53 $\pm$ 5.5	45.41 $\pm$ 2.36
600	18.89 $\pm$ 5.5	15.33 $\pm$ 3.6	58.01 $\pm$ 3.15

**Table 5.2** De-epoxidation state of leaves from *A. thaliana* grown over a range of irradiance and following light and dark sample treatment. Means  $\pm$  se of at least 6 replicates from separate plants grown in 2 batches.

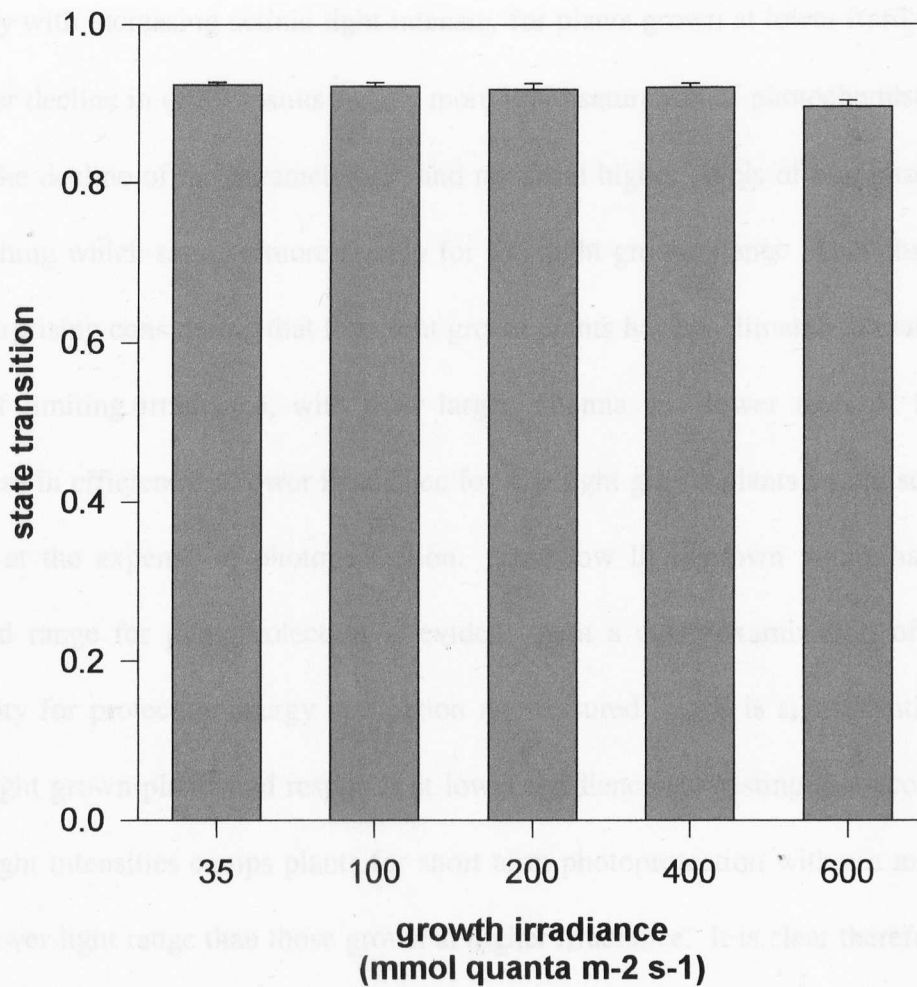


**Figure 5.13** Relationship between the capacity for state transition and growth irradiance for *A.thaliana*. Means  $\pm$  se of at least 6 replicates from separate plants grown in 2 batches.

distinct fluorescence profiles when exposed to a range of actinic light intensities. For example  $\phi\text{PSII}$ , which measures the quantum efficiency of photosystem II, declines more rapidly with increasing actinic light intensity for plants grown at lower irradiance. This sharper decline in  $\phi\text{PSII}$  results from a more rapid saturation of photochemistry, as seen with the decline of the parameter  $qP$ , and not from higher levels of non photochemical quenching which saturate more readily for low light grown plants. This observation is not surprising considering that low light grown plants have acclimated to make efficient use of limiting irradiance, with their larger antenna and lower rates of  $P_{\text{max}}$ . The increase in efficiency at lower irradiance for low light grown plants would seem to take place at the expense of photoprotection. That low light grown plants have a more limited range for photoprotection is evident upon a close examination of  $qN$ . The capacity for protective energy dissipation as measured by  $qE$  is significantly lower in low light grown plants and responds at lower irradiance suggesting that acclimation to low light intensities equips plants for short term photoprotection within a more limited and lower light range than those grown at higher irradiance. It is clear therefore that the acclimation response includes a change in the capacity for short term energy dissipation, although it is not known whether this is merely a consequence of the changes in the photosynthetic apparatus, described in chapter 4, or whether other changes occur during acclimation to allow for efficient energy dissipation. It has been demonstrated here that the changes in the maximum capacity for  $qE$  with growth irradiance are related to the general changes in acclimation profile of *Arabidopsis*, including Chlorophyll *a/b*. This may suggest that either decreases in LHClI levels or increases in PSII content are responsible for determining the capacity of  $qE$ . It may also suggest however that the capacity for  $qE$  is regulated by some other factor which responds to the same signals as  $P_{\text{max}}$  and Chl *a/b*. One such contributing factor must surely be the increase in the

xanthophyll cycle carotenoid pool size with increasing growth irradiance, which mirrors the acclimation profile of qE, chlorophyll *alb* and Pmax suggesting co-regulation.

Although the capacity for qE is lower in plants grown at lower irradiance the second component of non-photochemical quenching resolved in this chapter, qI, is actually higher. At the higher actinic light intensities the increased qI is unlikely to be related to a  $\Delta$ pH dependant , nigericin sensitive qE like component (Gilmore and Bjorkman 1995) and more likely to result from photoinhibition. Whether photoinhibition, as measured by sustained forms of non-photochemical quenching, reflects photodamage or some other light stress response remains unclear (Chow 1994). Either way, the higher levels of qI observed for plants grown at lower irradiance are a further indication that low light acclimation yields plants that show effective photoprotection over a more limited range of irradiance.

For *Arabidopsis* plants grown at most light intensities the differences observed in PSII efficiency, electron transport rate and qP are of the same magnitude as, and therefore probably reflect, the changes in photosynthetic capacity as measured by the maximum rate of oxygen evolution (Pmax) (see chapter 3). However plants grown at  $400 \mu\text{mol m}^{-2} \text{s}^{-1}$  have similar profiles for  $\phi\text{PSII}$ , PSII-ETR and qP as those grown at  $600 \mu\text{mol m}^{-2} \text{s}^{-1}$  despite having a Pmax that is almost as low as that of plants grown at  $200 \mu\text{mol m}^{-2} \text{s}^{-1}$ . Such a discrepancy would suggest that an alternative electron sink, other than  $\text{CO}_2$  fixation, is in operation at  $400 \mu\text{mol m}^{-2} \text{s}^{-1}$ . Furthermore this alternative sink would have to involve molecular oxygen as an electron acceptor. Two well documented electron sinks that use  $\text{O}_2$  as an electron acceptor are photorespiration and the Mehler reaction (Polle 1995). Photorespiration however is not active at saturating levels of  $\text{CO}_2$  and since all fluorescence measurements described in this chapter were measured under saturating  $\text{CO}_2$  conditions it seems unlikely that photorespiration could provide an

alternative electron sink in these experiments. The discrepancies between electron transport rate and oxygen evolution seen at a growth irradiance of  $400 \mu\text{mol m}^{-2} \text{s}^{-1}$  are likely to be explained by enhanced Mehler reaction activity. In addition it is possible that the Mehler reaction is coupled to the high activity of superoxide dismutases and ascorbate peroxidases which function to scavenge the potentially toxic intermediates of oxygen metabolism. This form of the Mehler reaction is known as the Mehler-peroxidase reaction (Schreiber and Neubauer 1990). Evidence in favour of the Mehler-peroxidase reaction operating with high activity for plants grown at  $400 \mu\text{mol m}^{-2} \text{s}^{-1}$  is seen with the measurement of qE and the levels of xanthophyll cycle carotenoids. For plants grown at  $400 \mu\text{mol m}^{-2} \text{s}^{-1}$  the measured levels of qE are lower than for plants grown  $600 \mu\text{mol m}^{-2} \text{s}^{-1}$  despite the apparent similarity in electron transport rate. In fact at higher actinic irradiance, qE levels for  $400 \mu\text{mol m}^{-2} \text{s}^{-1}$  plants are significantly lower than those of plants grown at  $200 \mu\text{mol m}^{-2} \text{s}^{-1}$ . This unexpected lowering of qE is probably the result of a persistent component of qE in dark adapted leaves. It can be seen from the de-epoxidation state of the xanthophyll cycle carotenoids (DES) that a higher residual amount of zeaxanthin remains in dark adapted leaves of plants grown at  $400 \mu\text{mol m}^{-2} \text{s}^{-1}$  when compared to plants grown at other light intensities. This remaining zeaxanthin would probably result in the formation of some qE, even in the dark. Consequently the true dark adapted Fm level would be underestimated which would result in an apparently lower level of non-photochemical quenching. A lower dark adapted level of Fv/Fm is observed for  $400 \mu\text{mol m}^{-2} \text{s}^{-1}$  grown plants. Previous studies have shown that the dimutase activity of the Mehler-peroxidase reaction contributes to non-photochemical quenching by the uptake of protons at the stromal side of the thylakoid membrane (Schreiber and Neubauer 1990). It is suggested that under the dark adaptation conditions described for experiments in this chapter the action of

superoxide dismutation may still be present at the time of Fm measurement. If the activity of the Mehler-peroxidase reaction is enhanced at a growth irradiance of  $400 \mu\text{mol m}^{-2} \text{s}^{-1}$  this may explain why the levels of non-photochemical quenching are lower than expected for these plants.

The activity of alternative reactions such as the Mehler-peroxidase reaction for plants grown at different light intensities has implications for the prediction of photosynthetic acclimation by the 'excitation pressure' hypothesis (see section 1.4.3.2). It has been suggested that photosynthetic acclimation responds to the redox state of PSII as measured by the fluorescence parameter qP ('excitation pressure' has previously been represented as  $1-qP$ ). According to the excitation pressure hypothesis, by measuring qP at a higher light intensity than the growth irradiance of a photosynthetic organism it should be possible to predict, from the lowering in qP and hence the increase in PSII 'excitation pressure', the state of acclimation for the same organism grown at the higher light intensity used for determining qP. However the values of qP for *Arabidopsis thaliana* grown at  $35 \mu\text{mol m}^{-2} \text{s}^{-1}$ , when measured at the growth irradiance of plants from the four other defined conditions, show a more linear decrease than expected. This is clearly not in agreement with the excitation pressure hypothesis since the acclimation profile for *Arabidopsis thaliana* grown over this irradiance range is non-linear. One explanation why the acclimation profile of *Arabidopsis thaliana* does not match that predicted from the redox state of PSII may be the enhanced Mehler-peroxidase activity at  $400 \mu\text{mol m}^{-2} \text{s}^{-1}$ . With this electron sink acting as a valve the actual PSII redox state of  $400 \mu\text{mol m}^{-2} \text{s}^{-1}$  grown plants would be lower than that predicted from the redox state of  $35 \mu\text{mol m}^{-2} \text{s}^{-1}$  grown plants, which do not have the enhanced Mehler-peroxidase activity, when measured at  $400 \mu\text{mol m}^{-2} \text{s}^{-1}$ . This does not suggest that the 'excitation pressure' hypothesis is incorrect, the alternative electron sink present at a

growth irradiance of  $400 \mu\text{mol m}^{-2} \text{s}^{-1}$  effectively ensures that plants grown at this irradiance have much lower excitation pressures than predicted and so they acclimate as if they were seeing a lower irradiance, in this case  $200 \mu\text{mol m}^{-2} \text{s}^{-1}$ .

The state transition is a well characterised process which allows plants to respond to imbalances in reaction centre turnover with the migration of the PSII peripheral antenna LHCII. However the capacity for state transition in plants acclimated to a range of growth irradiance has not previously been determined. Fluorescence data used in this chapter to show the extent of the state transition, reveal that plants grown at all five irradiance are able to achieve state transitions despite differences in the composition of their light harvesting antenna. The extent of the state transition for plants grown at  $600 \mu\text{mol m}^{-2} \text{s}^{-1}$ , which is almost equivalent of that for  $35 \mu\text{mol m}^{-2} \text{s}^{-1}$  grown plants, is slightly surprising given that they have a vastly decreased LHCII. This finding suggests that efficient state transition requires the migration of only small numbers of LHCII away from PSII.

## **Chapter Six**

### **Acclimation to a Change in Irradiance**

## 6.1 Introduction

It has so far been shown that photosynthetic acclimation takes place when *Arabidopsis thaliana* is grown over a wide range of irradiance. However it is known that for many plant species photosynthetic acclimation is a dynamic process which responds reversibly to changes in the levels of irradiance during growth (for review see Anderson 1995). For *Arabidopsis thaliana* the ability to respond to changes in irradiance has been previously demonstrated following a transfer of plants from moderately high ( $400 \mu\text{mol m}^{-2} \text{s}^{-1}$ ) to low light intensity ( $100 \mu\text{mol m}^{-2} \text{s}^{-1}$ ) (Walters and Horton 1994). Transferred plants acclimated to the lower growth irradiance by decreasing both Chl *a/b* and Pmax. In this chapter the dynamic response of *Arabidopsis* to changes in irradiance has been extended to include the transfer of plants from low to high light. Furthermore the involvement of the redox state of PSII, or the PSII 'excitation pressure' (see section 1.4.3.2) has been assessed by monitoring the fluorescence parameter qP following transfer. Non-photochemical fluorescence quenching parameters have also been monitored in order to determine the interplay between short and long term responses during both low to high and high to low transitions. Using the acclimation profile of *Arabidopsis* to growth at a range of irradiance as a guide (chapter 3), the maximum ( $600 \mu\text{mol m}^{-2} \text{s}^{-1}$ ) and minimum ( $35 \mu\text{mol m}^{-2} \text{s}^{-1}$ ) light intensities were selected to provide both significant stress and the largest signals during transfer. Pmax and chlorophyll *a/b* ratio have been measured as an index of acclimation while the fluorescence parameters qP, qN, qE, and qI provide an indication of the short term physiological response to both the initial stress and the subsequent acclimation. In addition chlorophyll content has also been monitored.

## 6.2 Transfer from low to high irradiance

*Arabidopsis* plants were grown to maturity (approximately 10 weeks from sowing) at a low irradiance of  $35 \mu\text{mol m}^{-2} \text{s}^{-1}$ . Plants were then transferred to a higher growth irradiance of  $600 \mu\text{mol m}^{-2} \text{s}^{-1}$ . All other parameters, including temperature and spectral quality, were maintained constant at both light intensities. Transfer took place at 12.00 noon (4 hours into an 8 hour photoperiod) and to avoid the complications imposed by circadian phenomena measurements of both control and transferred plants were sampled as close to noon as possible on subsequent days.

### 6.2.1 Plant morphology

A number of striking changes in plant morphology were observed following the transfer of low light grown plants to a higher light environment. First of all leaves which were fully expanded and slightly upturned during growth at  $35 \mu\text{mol m}^{-2} \text{s}^{-1}$  began to turn down and curl under at the edges. This effect, which is not believed to be water stress, was so dramatic that within 24 to 48 hours of transfer most of the leaves had assumed this new position. Almost as dramatic was the appearance of red pigment arising from the synthesis of anthocyanin, in the leaves of transferred plants. The onset of the red pigmentation was seen after 24 to 48 hours with the outer edges of leaves becoming red. The pigmentation then began to show up throughout the whole leaf at about day four where it quickly spread to give almost the entire leaf a deep red colour. Finally, perhaps the most significant morphological change in the high light transferred plants was the onset of flowering. Transferred plants began to bolt at around day 7 and by day 12 many plants showed extensive flowering.

## 6.2.2 Chlorophyll content

Leaf disks of both control plants ( $35 \mu\text{mol m}^{-2} \text{s}^{-1}$ ) and transferred plants ( $35$  to  $600 \mu\text{mol m}^{-2} \text{s}^{-1}$ ) were assayed for their chlorophyll content immediately following transfer (day 0) and then again every 24 hours. To avoid the possibility of artifacts arising from the removal of leaves (e.g ethylene induced changes and the transcription of stress genes) leaf disks were only taken from any single plant once. These plants were then disposed of. Changes in chlorophyll content per leaf area following a transfer from low to high irradiance are shown in figure 6.1a. It can be seen that there is no discernable difference between control plants (closed circles) and transferred plants for the 12 days following the shift.

Figure 6.1b shows the change in the ratio Chl *a/b* following a change from low to high irradiance. Control levels remain relatively constant over the 12 days following transfer, although there is a slight decrease in Chl *a/b* ratio for control plants after day 6. In contrast Chl *a/b* ratios for transferred plants show a significant increase which peaks at day 4 before apparently decreasing again. Most of the observed increase takes place between the second day of transfer and the fourth. The initial lag prior to this increase has been previously described for spinach (Lindahl *et al* 1995) and would appear to be characteristic of the chlorophyll response to high light transfer. There is a decrease in Chl *a/b* after day 4.

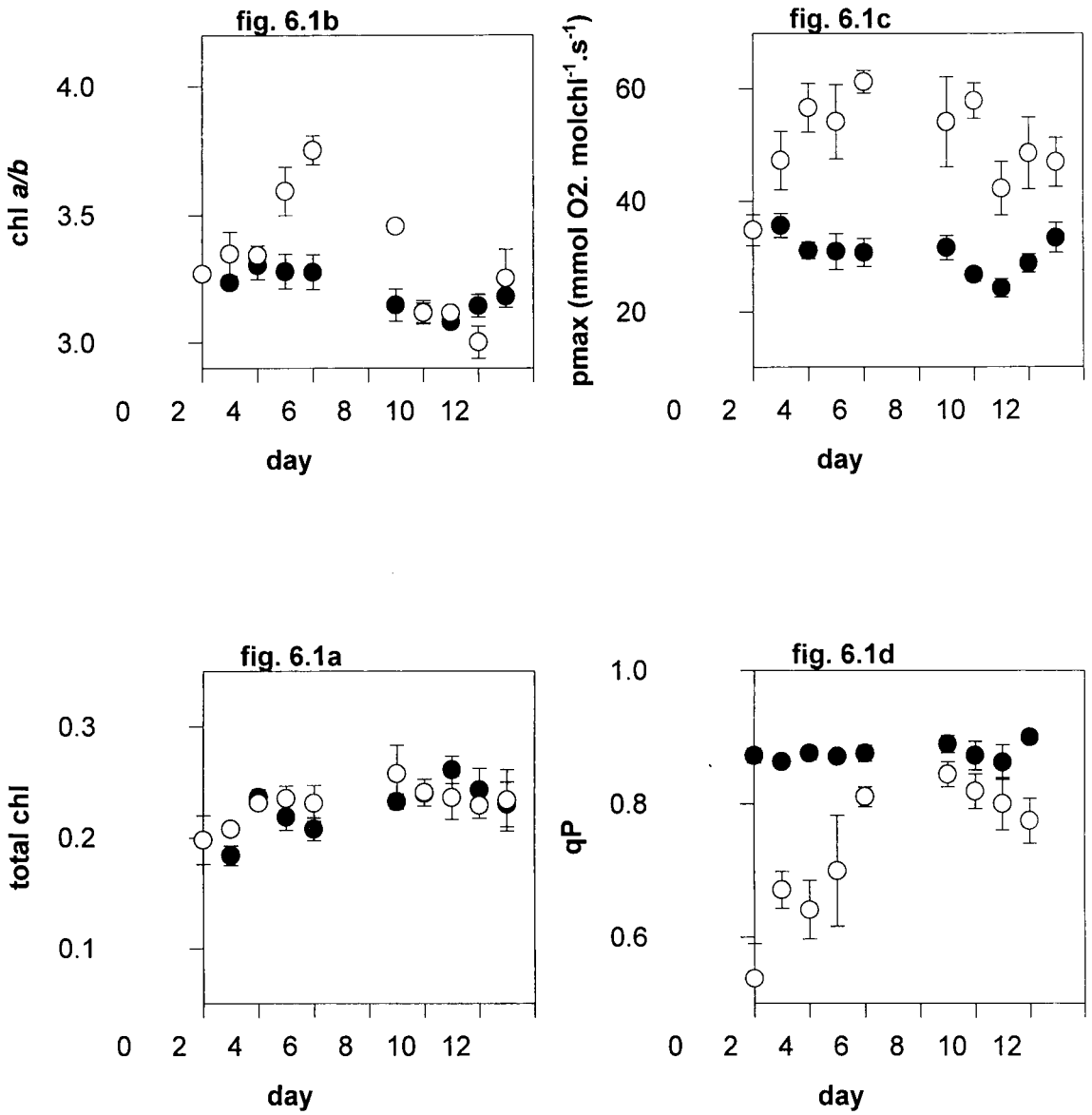


**Figure 6.1** Changes in chlorophyll content (fig. 6.1a), Chl *a/b* (fig. 6.1b), Pmax (fig. 6.1c) and *in situ* qP (fig. 6.1d) for *A.thaliana* following a transfer from low ( $35 \mu\text{mol m}^{-2} \text{s}^{-1}$ ) to high ( $600 \mu\text{mol m}^{-2} \text{s}^{-1}$ ) irradiance. For all graphs closed circles represent control plants and open circles represent transferred plants. Means  $\pm$  se of at least 6 replicates from separate plants grown in 2 batches. Chlorophyll content, chlorophyll *a/b* ratio and pmax taken from same leaf samples, qP measured in the same batch of plants.

### 6.2.3 P<sub>max</sub>

The maximum photosynthetic rate of both control plants and those transferred to higher irradiance was assayed by the oxygen evolution of leaves under saturating, but not photoinhibitory light (figure 6.1c). Since there is no change in the overall chlorophyll content per unit area the same trends are observed for P<sub>max</sub> whether expressed on a leaf area basis or per unit chlorophyll. It can be seen that, as with Chl *a/b*, there is an increase in P<sub>max</sub> for transferred plants relative to the control plants which remain largely unaltered throughout. Also like Chl *a/b* the increase in P<sub>max</sub> peaks at around day 4. Unlike Chl *a/b* however there is no 2 day lag for the response of P<sub>max</sub>. There is a small but significant drop in P<sub>max</sub> for the transferred plants from day 8. This may be related in some way to the onset of flowering which also commences at this time.

### 6.2.4 Room temperature chlorophyll fluorescence

Room temperature chlorophyll fluorescence was measured under conditions of saturating CO<sub>2</sub> at 20 °C. The actinic light intensity used was equivalent to the growth irradiance so for transferred plants this was 600 μmol m<sup>-2</sup> s<sup>-1</sup> while for control plants it was 35 μmol m<sup>-2</sup> s<sup>-1</sup>. Leaf disks were treated with actinic light for at least 45 minutes before φPSII, qP and qN were measured. qN was then further resolved into the components qE and qI following the relaxation of non-photochemical quenching in the dark. In addition qP was measured *in situ* at ambient CO<sub>2</sub> levels.

### 6.2.4.1 qP

The fluorescence parameter qP, which reflects the redox state of PSII, has been used previously as a measure of PSII 'excitation pressure' (see section 1.4.3.2). In order to determine the role of 'excitation pressure' during photosynthetic acclimation in *Arabidopsis*, qP has been measured both in the growth cabinet and in a leaf disk chamber for plants which have been transferred from low ( $35 \mu\text{mol m}^{-2} \text{s}^{-1}$ ) to high ( $600 \mu\text{mol m}^{-2} \text{s}^{-1}$ ) growth irradiance. Figure 6.1d shows qP for both control and transferred plants when measured *in situ*. While control plants show high values for qP throughout the experiment, indicating that PSII is kept highly oxidized, there is a large decrease in qP immediately following transfer to high light (day 0). The value for qP immediately following the shift is sufficiently low to indicate that the transferred plants are suffering from significant light stress with PSII being largely reduced. However when measured on subsequent days it can be seen that qP recovers gradually until day 4 where values remain just below those of the control plants, indicating that the initial light stress has been alleviated. When qP is measured under saturating levels of CO<sub>2</sub> (figure 6.2), at the same actinic light intensity and temperature, the same trend is observed. Control plants maintain a high value for qP while there is a significant initial decrease for plants transferred to high light. qP is then restored to just below control levels over the first four to five days following transfer. It is interesting to note however that when compared to a value of around 0.54 for the *in situ* measurements, a lower value for qP (0.3) is seen under conditions of saturating CO<sub>2</sub> immediately following transfer. This phenomenon may relate to the spectral quality of the actinic lights used in each experiment with a higher far red light content of the growth lights in the cabinet favouring more PSI turnover.

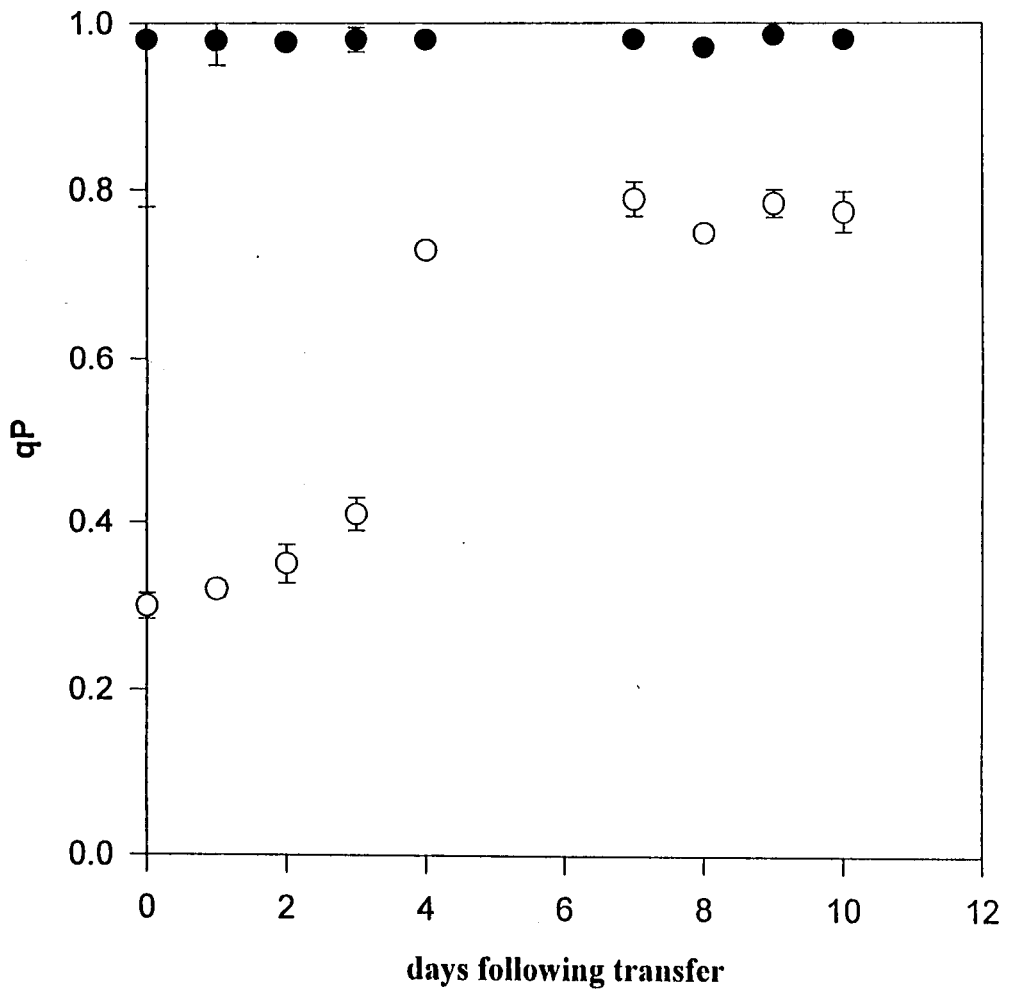


**Figure 6.2** Changes in qP for *A.thaliana* following a transfer from low ( $35 \mu\text{mol m}^{-2} \text{s}^{-1}$ ) to high ( $600 \mu\text{mol m}^{-2} \text{s}^{-1}$ ) irradiance. For all graphs closed circles represent control plants and open circles represent transferred plants. Means  $\pm$  se of at least 6 replicates from separate plants grown in 2 batches.

### 6.2.4.2 qN

Total qN was measured for *Arabidopsis thaliana* following a transfer from low to higher irradiance. As shown in Figure 6.3 there is an immediate increase in the value of qN relative to the control plants with levels of the latter being effectively zero throughout. Values of qN then show a tendency to rise significantly until day 3, although there is a decrease between days 1 and 2. At its peak the level of qN is actually higher than when plants grown at  $35 \mu\text{mol m}^{-2} \text{s}^{-1}$  were treated with three times the levels of actinic irradiance (see chapter 5). This increase in qN suggests that either the capacity for qE is increasing in the days following transfer or that the component qI is accumulating. Following the rise in qN upto day 3, values fall sharply to just below those measured immediately following transfer (day 0). The lower levels observed after day 4 are however still significantly higher than control values.

### 6.2.4.3 qE

Deconvolution of the curve for qN relaxation with time allowed the energy dependant component of non-photochemical quenching (qE) to be resolved for *Arabidopsis* plants following a transfer from low to higher irradiance. As shown in figure 6.4 the response of qE to an increase in growth irradiance mirrors that of qN. Immediately following transfer the levels of qE rise and then carry on increasing until day 3, although as with qN there is a slight decrease on day 2. Interestingly the value of qE on day 3 is more than 50% higher than the saturating value of qE for plants grown at  $35 \mu\text{mol m}^{-2} \text{s}^{-1}$  suggesting that the capacity for qE is itself acclimating to the new higher growth irradiance. Indeed the value of qE on day 3 is equivalent to the saturating levels for plants grown at 200 and  $400 \mu\text{mol m}^{-2} \text{s}^{-1}$ . As with total qN the value of qE decreases

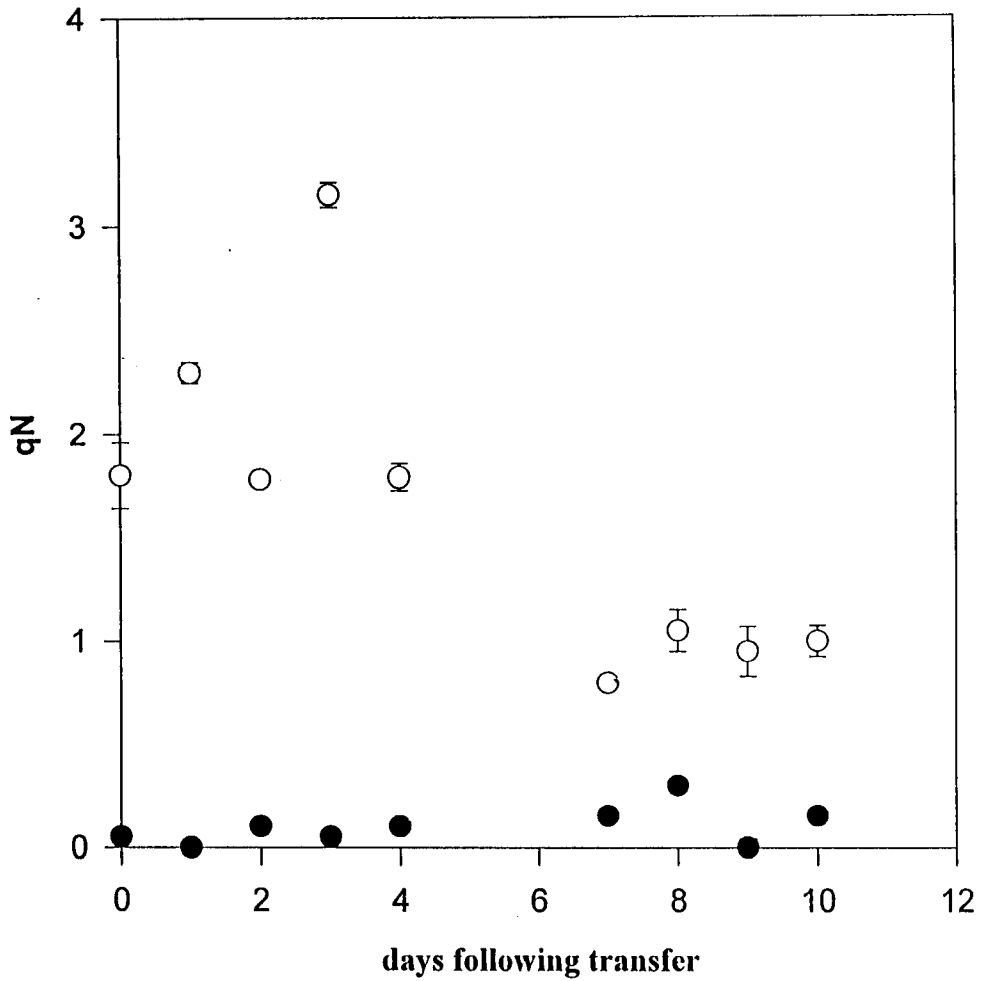


**Figure 6.3** Changes in  $qN$  for *A.thaliana* following a transfer from low ( $35 \mu\text{mol m}^{-2} \text{s}^{-1}$ ) to high ( $600 \mu\text{mol m}^{-2} \text{s}^{-1}$ ) irradiance. For all graphs closed circles represent control plants and open circles represent transferred plants. Means  $\pm$  se of at least 6 replicates from separate plants grown in 2 batches.

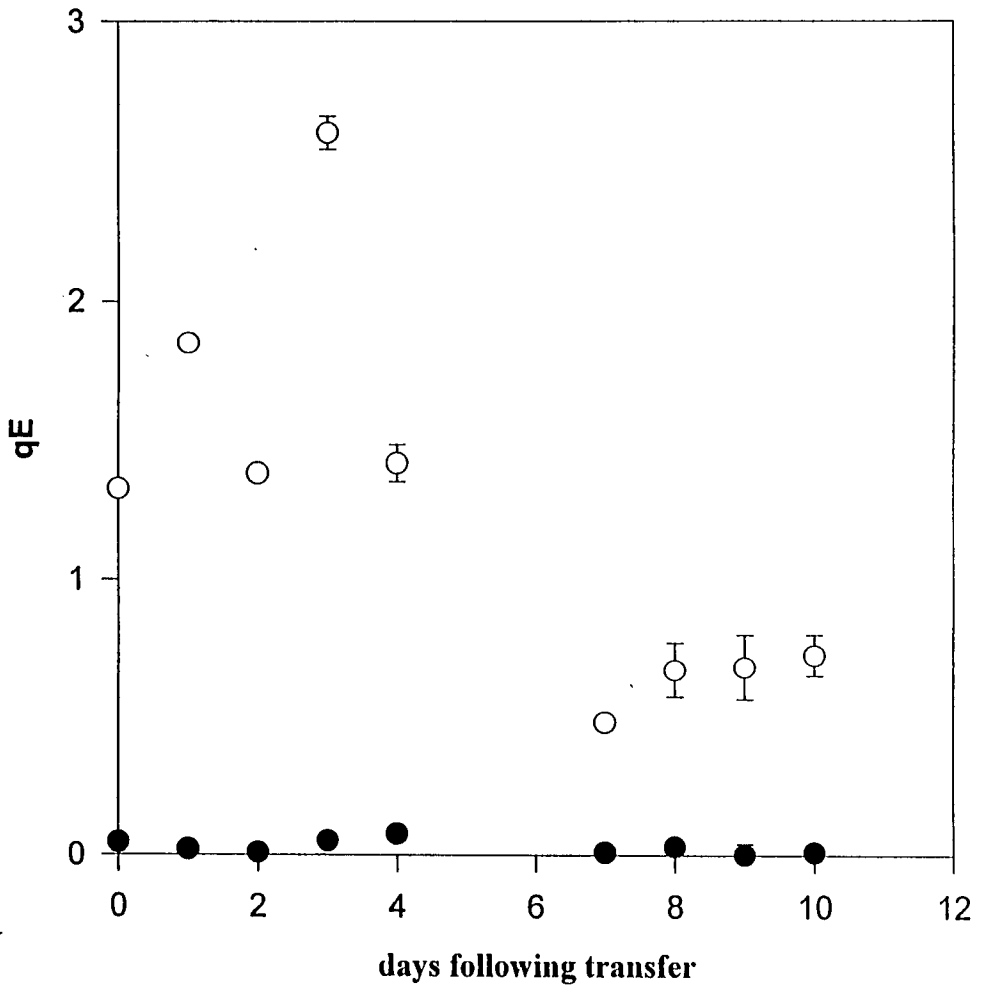


**Figure 6.4** Changes in  $qE$  for *A.thaliana* following a transfer from low ( $35 \mu\text{mol m}^{-2} \text{s}^{-1}$ ) to high ( $600 \mu\text{mol m}^{-2} \text{s}^{-1}$ ) irradiance. For all graphs closed circles represent control plants and open circles represent transferred plants. Means  $\pm$  se of at least 6 replicates from separate plants grown in 2 batches.

rapidly after day 3 until it reaches lower levels that are still significantly higher than that of control plants.

#### 6.2.4.4 qI

qI represents a sustained form of non-photochemical quenching that persists beyond 15 minutes and unlike qE is generally not believed to be energy dependant. Figure 6.5 Shows the values of qI for *Arabidopsis* plants following a transfer from low to higher irradiance. Relative to control plants (closed circles) there is an increase in qI immediately following transfer to the higher growth irradiance (day 0). This value of qI is identical to the previous value for plants grown at  $35 \mu\text{mol m}^{-2} \text{s}^{-1}$  when exposed to an actinic irradiance of  $600 \mu\text{mol m}^{-2} \text{s}^{-1}$ . Following this initial rise there is a steady decrease in the level of qI on all subsequent days. This steady decrease in qI further suggests that the increase in qN observed up to day 3 following transfer is due to the increased capacity for qE. The final level of qI on day 10 is still significantly higher than control plants.

#### 6.2.4.5 $\phi\text{PSII}$

The efficiency of Photosystem II, or  $\phi\text{PSII}$ , was measured for *Arabidopsis* plants following a transfer from low to higher irradiance (figure 6.6). While control levels remain high throughout there is a dramatic decrease in  $\phi\text{PSII}$  immediately following transfer to high light. Despite some increase in qP in the first three days  $\phi\text{PSII}$  remains depressed at very low levels until day 4 when it begins to increase. The maintenance of low levels of  $\phi\text{PSII}$  upto day 3 is probably the result of an increase in qE. Following the

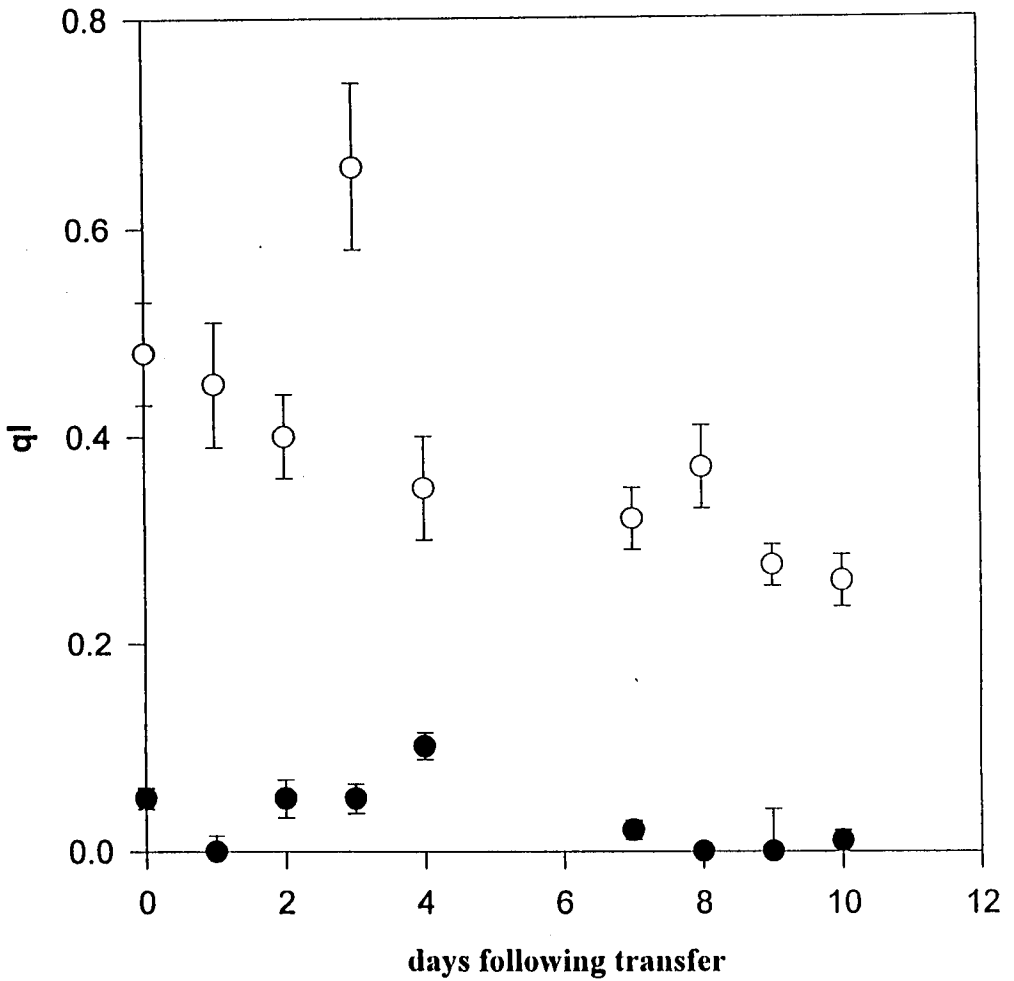


**Figure 6.5** Changes in  $qI$  for *A.thaliana* following a transfer from low ( $35 \mu\text{mol m}^{-2} \text{s}^{-1}$ ) to high ( $600 \mu\text{mol m}^{-2} \text{s}^{-1}$ ) irradiance. For all graphs closed circles represent control plants and open circles represent transferred plants. Means  $\pm$  se of at least 6 replicates from separate plants grown in 2 batches.

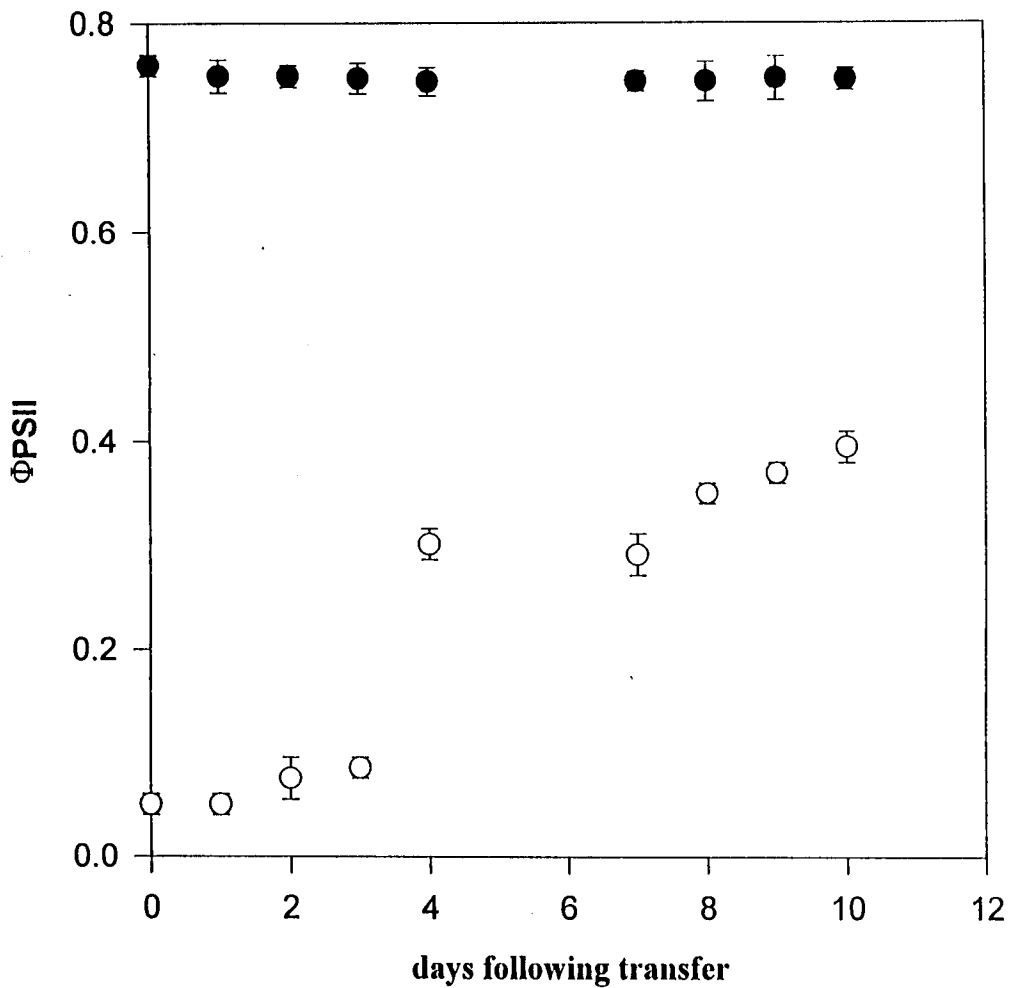


**Figure 6.6** Changes in  $\Phi_{PSII}$  for *A.thaliana* following a transfer from low ( $35 \mu\text{mol m}^{-2} \text{s}^{-1}$ ) to high ( $600 \mu\text{mol m}^{-2} \text{s}^{-1}$ ) irradiance. For all graphs closed circles represent control plants and open circles represent transferred plants. Means  $\pm$  se of at least 6 replicates from separate plants grown in 2 batches.

significant rise at day 4,  $\Phi$ PSII levels continue to rise more slowly reaching just half the level of control plants by day 10. The failure of  $\Phi$ PSII to return to either control levels or those of plants grown continually at  $600 \mu\text{mol m}^{-2} \text{s}^{-1}$  suggests that transfer plants are not fully acclimated to their new growth irradiance. PSII is not becoming as highly oxidized as for plants grown from seed at  $600 \mu\text{mol m}^{-2} \text{s}^{-1}$  and qE is being maintained for extra energy dissipation.

### 6.3 Transfer from high to low irradiance

*Arabidopsis thaliana* were grown to maturity for approximately 5 weeks at an irradiance of  $600 \mu\text{mol m}^{-2} \text{s}^{-1}$ . At 12.00 noon plants were transferred to a new environment which differed only in its irradiance which was lower ( $35 \mu\text{mol m}^{-2} \text{s}^{-1}$ ). As with the high to low transfer experiments, measurements of chlorophyll content, Pmax and room temperature chlorophyll fluorescence were taken on subsequent days as close to noon as possible to avoid any changes associated with circadian cycling.

#### 6.3.1 Plant Morphology

Some clear changes in plant morphology were observed following the transfer of plants from high to low irradiance. The most striking of these was the expansion and raising of leaves. While plants grown at  $600 \mu\text{mol m}^{-2} \text{s}^{-1}$  had turned down leaves which were curled under at the edges the transferred plants began expanding their leaves at the edges and the leaves were no longer turned down but faced upward in a similar manner to those of plants grown from seed at the lower irradiance. These changes, which were

maintained throughout the experiment, were observed just 24 hours after transfer. The second most notable change in morphology was evident in both control and transfer plants. By day 7 there was some evidence of bolting and by day 9 it was clear that most plants, whether transferred or not, had begun to flower. Early flowering is characteristic of plants grown from seed at an irradiance of  $600 \mu\text{mol m}^{-2} \text{s}^{-1}$  with the bolting usually occurring 1 or 2 weeks after plants become mature, at around week 6/7.

### 6.3.2 chlorophyll content

Figure 6.7a shows the chlorophyll content per unit leaf area for both control (closed circles) and transfer plants following a change from high to low irradiance. After 24 hours it is apparent that the total chlorophyll content per unit leaf area has increased significantly for transfer plants relative to the control. This higher level of chlorophyll is maintained throughout although control levels also increase on day 4 and remain equivalent to transfer levels through to day 9. While the increase in chlorophyll content for the transferred plants can be explained in terms of an increase in chlorophyll *b* (see below) it is not known why there are fluctuations in the control levels of chlorophyll.

A dramatic decrease in the ratio Chl *a/b* can be seen for *Arabidopsis* plants transferred from high to low irradiance when compared to control plants (fig. 6.7b). This decrease takes place mostly in the first 24 hours following transfer and occurs without any apparent lag. This large decrease in Chl *a/b* may explain the increase in total chlorophyll content observed for transferred plants after 24 hours. A second decrease in the Chl *a/b* of transferred plants takes place from day 7 and continues to decline until day 9. However this decline is far less dramatic than that observed after 24 hours and it is also mirrored by a decline in the Chl *a/b* for control plants.

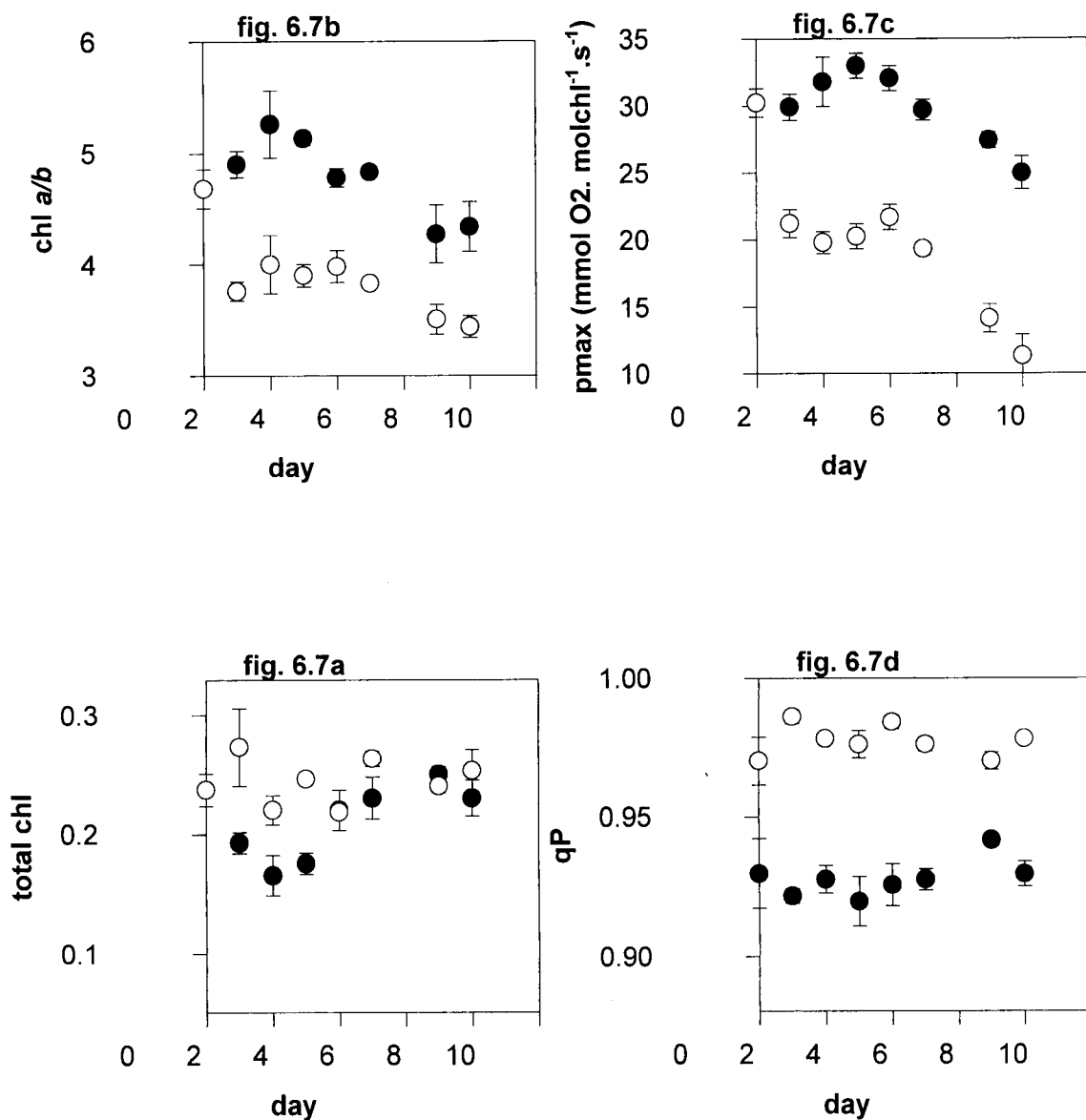


**Figure 6.7** Changes in chlorophyll content (fig. 6.7a), Chl *a/b* (fig. 6.7b), Pmax (fig. 6.7c) and *in situ* qP (fig. 6.7d) for *A.thaliana* following a transfer from high ( $600 \mu\text{mol m}^{-2} \text{s}^{-1}$ ) to low ( $35 \mu\text{mol m}^{-2} \text{s}^{-1}$ ) irradiance. For all graphs closed circles represent control plants and open circles represent transferred plants. Means  $\pm$  se of at least 6 replicates from separate plants grown in 2 batches. Chlorophyll content, chlorophyll *a/b* ratio and pmax taken from same leaf samples, qP measured in the same batch of plants.

### 6.3.3 P<sub>max</sub>

The saturating rate of oxygen evolution was measured for *Arabidopsis* plants following transfer from high to low irradiance ( figure 6.7c). As with Chl *a/b*, transferred plants show a large decrease in P<sub>max</sub>, relative to control levels. This decrease takes place almost entirely within the first 24 hours and lower levels are maintained until day 4. On day 7 the levels of P<sub>max</sub> for both transfer and control plants begin to decrease at approximately the same rate. Changes in P<sub>max</sub> and chlorophyll *a/b* for both control and transfer plants have also been observed in the later days of a previous transfer experiment in which *Arabidopsis thaliana* was transferred from 400 to 100  $\mu\text{mol m}^{-2} \text{s}^{-1}$  (Walters and Horton 1994). This decrease may be related to the onset of flowering which occurs at around day 7 for control and transfer plants. This decline does not effect the overall difference between transfer and control levels of either P<sub>max</sub> or Chl *a/b* which are about the same as those observed after the first 24 hours.

### 6.3.4 Room temperature chlorophyll fluorescence.

Room temperature chlorophyll fluorescence was measured for control and transferred plants under conditions of saturating CO<sub>2</sub> at 20 °C. The actinic light intensity used for control plants was equivalent to the growth irradiance i.e. 600  $\mu\text{mol m}^{-2} \text{s}^{-1}$ . In order to make the measurement meaningful, the actinic light intensity for transferred plants was also 600  $\mu\text{mol m}^{-2} \text{s}^{-1}$ . Leaf disks were treated with actinic light for at least 45 minutes before  $\phi\text{PSII}$ , qP and qN were measured. qN was then further resolved into the components qE and qI following the relaxation of non-photochemical quenching in the dark. In addition qP was resolved *in situ* at ambient CO<sub>2</sub> using growth lights as actinic.

### 6.3.4.1 qP

qP has been measured both at ambient CO<sub>2</sub> and under saturating CO<sub>2</sub> for *Arabidopsis* plants following a transfer from high to low irradiance. In addition to the levels of CO<sub>2</sub>, in situ measurements differ in the use of actinic irradiance. While the qP measurements under saturating CO<sub>2</sub> are made at 600 μmol m<sup>-2</sup> s<sup>-1</sup> the *in situ* measurements use the low growth light which provides 35 μmol m<sup>-2</sup> s<sup>-1</sup> actinic irradiance. Figure 6.8 shows qP for both control and transfer plants measured under saturating CO<sub>2</sub> at an actinic irradiance of 600 μmol m<sup>-2</sup> s<sup>-1</sup>. Control levels remain constant from day 0 through to day 4 and are followed by a slight decline from day 7 to day 9. qP values decrease in two phases for transferred plants. There is a slight decrease after the first 24 hours following transfer. This lower value is then maintained through to day 4. By day 7 qP has started to decrease again and continues to do so through to day 9. When qP is measured *in situ* at an actinic irradiance of 35 μmol m<sup>-2</sup> s<sup>-1</sup> a completely different pattern is observed (figure 6.7d). Transferred plants exhibit an instant increase in qP relative to the already high values seen for control plants. This higher level of qP is then maintained at around 0.98 throughout.

### 6.3.4.2 qN

Total qN was measured for *Arabidopsis* plants following a transfer from high to low irradiance at an actinic irradiance of 600 μmol m<sup>-2</sup> s<sup>-1</sup> (figure 6.9). There is an initial increase in qN after the first 24 hours. This then declines slightly from day 1 through to day 4 but still remains significantly higher than when measured on day 0. A second increase in qN is then observed by day 7 and then again from day 7 to day 8. Control levels of qN remain constant from day 0 through to day 9

**PAGE  
MISSING  
IN  
ORIGINAL**

### 6.3.4.3 qE

The energy dependant component of non-photochemical quenching (qE ) was resolved for *Arabidopsis* plants following a transfer from low to higher irradiance. As shown in figure 6.10 the response of qE to a decrease in growth irradiance mirrors that of qN. There is an initial rise after 24 hours which then decreases slightly through to day 4. qN then increases substantially on days 7 and 8 as do the control levels which were unchanged upto day 4.

### 6.3.4.4 qI

qI represents a second, more stable component of non-photochemical quenching that can be resolved by the deconvolution of the curve for qN relaxation with time. qI for *Arabidopsis* plants transferred from high to low irradiance is shown in figure 6.11. Surprisingly, there is almost no change in qI for both control and transferred plants between days 0 and 4, both of which have similar values of around 0.2. This suggests that all changes in total qN up to day 4 are entirely the result of energy dependant quenching qE. There is however an increase in the levels of qI for transfer plants on days 7 and 8 although this is almost matched by a similar increase in the control levels.

### 6.3.4.5 $\phi$ PSII

$\phi$ PSII, which monitors the efficiency of Photosystem II was measured for *Arabidopsis* plants following a transfer from low to higher irradiance (figure 6.12). Control levels remain constant from day 0 through to day 4 but then show a decline on days 7 and 8.

**PAGES  
MISSING  
IN  
ORIGINAL**

Meanwhile transferred plants show a significant decrease in  $\phi\text{PSII}$  24 hours after the transition from high to low irradiance. Although  $q\text{P}$  also decreases during this period, the changes relative to control levels are only small. It seems likely therefore that the decreases in  $\phi\text{PSII}$  24 hours after transfer are due to a change in the  $F_v'/F_m'$  and therefore most likely reflect an increase in  $q\text{E}$ , which does show significant changes, and not decreases in photochemistry. Following the initial decrease,  $\phi\text{PSII}$  levels for transferred plants remains constant through to day 4. As with control plants there is a significant decrease in  $\phi\text{PSII}$  on days 7 and 8. Both an increase in  $q\text{E}$  and a decrease in  $q\text{P}$  however accompany this decrease.

## 6.4 Discussion

While previous chapters have characterised photosynthetic acclimation for *Arabidopsis thaliana* grown from seed at different irradiance this chapter has demonstrated the dynamic nature of acclimation following transitions of mature plants between high and low irradiance.

Following the transitions, changes in the photosynthetic apparatus have been monitored using  $\text{Chl } a/b$  and  $\text{P}_{\text{max}}$  as a simple index. In addition room temperature chlorophyll fluorescence has been used to further assess the physiological characteristics of photosynthesis, including the capacity for short term regulation in the form of non-radiative energy dissipation. Of particular interest was the parameter  $q\text{P}$  which has been used previously as a measure of PSII 'excitation pressure' (see section 1.4.3.2).

For the low to high light transition the most extreme irradiance levels, 35 and 600  $\mu\text{mol m}^{-2} \text{s}^{-1}$ , were chosen from the acclimation profile of *Arabidopsis* when grown over a range of light intensities (see chapter 3). These irradiance levels were selected mainly

to allow for the largest changes to be measured. Following the transition there was a clear acclimation response with increases in the both Pmax and Chl *a/b*. For Pmax this was instant with large changes after 24 hours which were complete after approximately 48 hours. The response for Chl *a/b* ratio however showed the characteristic 48 to 72 hour lag (Lindhahl *et al* 1995) before increasing over the next two days. The measurement of Chl *a/b* may become complicated by the dramatic increase in anthocyanin after day 4. Kannangara and Hanson (1998) have demonstrated that chlorophyll accumulation is arrested with the onset of anthocyanin formation in *Euphorbia pulcherima*. It should be noted however that in a previous study using 3 different plant species whose anthocyanin levels change with leaf age it was concluded that chlorophyll determination is unaffected by this pigment (Manetas *et al* 1998).

There is a clear difference in the response to a high light shift between Pmax and Chl *a/b*. This may suggest that the two changes may respond to different signals. A more likely explanation however is that the response is carried out by different processes, for example protease enzymes and gene transcription. It has been shown for spinach that changes in Chl *a/b* following a similar transition to high light is caused by a decrease in LHCII. Furthermore the protease responsible for this decrease has been identified and the lag period in the increase in Chl *a/b* following an increase in irradiance has been attributed to either the expression or activation of this protease (Yang *et al* 1998). Changes in Pmax following an increase in irradiance presumably requires, amongst other things, the increased synthesis of the CO<sub>2</sub> fixing enzyme Rubisco, the expression of which may proceed without the lag associated with the LHCII protease. In addition the activation state of Rubisco may be altered instantly in response to the increase in irradiance (Seeman *et al* 1989), presumably through the action of Rubisco activase (Eckardt *et al* 1997). Indeed an increase in the activation state of Rubisco may in itself account for the rapid increase in Pmax without the need for Rubisco synthesis.

Although the increases in chlorophyll *a/b* and Pmax following a transition to high light are significant they fall short of a full acclimation response which would see levels rise to those for plants grown from seed at  $600 \mu\text{mol m}^{-2} \text{s}^{-1}$ . In fact the response would appear to give plants a Chl *a/b* ratio and Pmax that is equivalent to plants grown from seed at  $400 \mu\text{mol m}^{-2} \text{s}^{-1}$ . This inability of mature plants to acclimate fully to the higher growth light is also reflected in the fluorescence parameter qP. Whether measured *in situ* or at saturating CO<sub>2</sub> qP levels drop dramatically immediately following the transition to high irradiance. The levels are then restored over the next 4 days as the plant acclimates to the new irradiance. However since the plants never fully acclimate to the higher irradiance qP is not fully restored to that of control levels. One explanation for plants not acclimating fully to the higher growth irradiance may be the onset of flowering which is evident after day 4. It is possible that the transition from 35 to  $600 \mu\text{mol m}^{-2} \text{s}^{-1}$  imposes sufficient stress upon the plant that its major response is that of flowering and acclimation does not have to be fully attained as long as the plant survives long enough to achieve this end. An inability to acclimate fully following a transition to higher irradiance has also been demonstrated for eastern Hemlock tree seedlings (Mohammed and Parker 1999). This species show even less ability to return qP to control levels however when traced over 3 to 4 weeks it becomes apparent that new foliage is able to cope well with the new higher light intensity.

The fluorescence parameter qP has previously been used as a measure of the PSII 'excitation pressure' that is imposed when plants are exposed to either high irradiance or low temperatures (see section 1.4.3.2). PSII 'excitation pressure' is proposed to regulate the acclimation response in a feedback manner since the process of photosynthetic acclimation restores the redox state of qP. In the case of *Arabidopsis* it would appear that qP does in fact correlate well with the process of acclimation during a transition to higher irradiance. Both the increases in Chl *a/b* and Pmax between day 0

and day 4 serve to restore  $qP$ . However there is also an increase in  $qE$  following the transition which continues to increase as part of the process of acclimation up to day 3. The activity of  $qE$  should also contribute to restoring  $qP$ . The correlation between PSII redox poise and photosynthetic acclimation is therefore complicated by the involvement of other factors. Even without the involvement of  $qE$ , PSII 'excitation pressure' remains nothing more than a correlation and can in no way be implicated from this data as a signal for acclimation. The observed changes in  $qP$  would be expected merely as a consequence of acclimation.

Using the same two growth light intensities as the low to high light transition the ability of *Arabidopsis thaliana* to respond to a decrease in irradiance was also assessed. As with the high light transition there is a significant response in both Chl  $a/b$  and  $P_{max}$  following a shift to lower irradiance but in the opposite direction. Unlike the low to high light transition however the response shows no lag period for Chl  $a/b$ . Both  $P_{max}$  and Chl  $a/b$  have reached an acclimation plateau in just 24 hours which remains until day 7 when there is a further decrease. The second decrease however must reflect something more general than acclimation since the control plants show the same response. The most likely explanation would be leaf age and possibly even preparation for flowering. Interestingly if the second decrease at day 7 is ignored it can be seen that, like with the low to high light transition, acclimation to lower irradiance is incomplete. Both Chl  $a/b$  and  $P_{max}$  fail to reach the levels of plants grown at  $35 \mu\text{mol m}^{-2} \text{s}^{-1}$ . Again the plants have index parameters that are equivalent to those of *Arabidopsis* grown from seed at around  $400 \mu\text{mol m}^{-2} \text{s}^{-1}$ . This may be due to the onset of flowering however it is possible therefore that both high light grown and low light grown plants have a developmentally imposed limit to their acclimation capacity that is below that seen for plants grown from seed over a range irradiance.

The fluorescence parameter  $qP$  was again measured to test the PSII 'excitation pressure hypothesis'. For the high to low light transition it was necessary to measure  $qP$  both at the lower and the higher growth light. By measuring  $qP$  using the higher growth light level as actinic, it is possible to see how the changes brought about by acclimation have affected the plants ability to perform under its previous conditions. Surprisingly there was only a small decrease in  $qP$  in the first 24 hours when most of the acclimation took place. This can be explained in terms of an increase in  $qE$  which ensures that  $qP$  is maintained relatively high despite the changes in photosynthetic composition. Using the lower growth light as actinic the response of  $qP$  is to increase immediately to even higher levels despite the control levels already being very high. Upon transition to lower irradiance it is clear that there is no 'excitation pressure' imposed upon PSII. Furthermore  $qP$  remains at the new higher level during photosynthetic acclimation. There is no transient change in PSII redox state. It therefore seems unlikely that redox poise plays any role in a regulatory feedback mechanism for photosynthetic acclimation following a high to low light transition.

## **Chapter Seven**

### **Discussion**

## 7 Discussion

The main aim of this thesis was to characterise photosynthetic acclimation to irradiance in *A. thaliana*. This detailed characterisation would then form the basis for the long term aim of elucidating the regulatory mechanisms which underlie the process. Despite the fact that photosynthetic acclimation has previously been demonstrated for numerous plant species there still remains a need for the detailed characterisation of acclimation in *A. thaliana*. Previous studies have illustrated the potential for acclimation in *A. thaliana* (Walters and Horton 1994) however, as with most studies, only two growth light environments were chosen to reflect high and low irradiance.

In Chapter 3 it has been demonstrated that the capacity for photosynthetic acclimation in *Arabidopsis thaliana* extends over a wide range of irradiance including very high and very low light intensities. In general higher levels of growth irradiance were accommodated by increases in both Pmax and Chl *a/b* ratio. The extent of the change in both parameters is large with Chl *a/b* ranging from 3.17 to 4.75 and Pmax per unit chlorophyll ranging from 26 to 113 mmolO<sub>2</sub> molChl s<sup>-1</sup>. The only other study to measure Chl *a/b* ratio over an extensive range of growth irradiance was conducted with pea (Leong and Anderson 1984) and reported smaller changes of between 2.2 and 3.2. Murchie and Horton (1997) however report changes in Chl *a/b* ratio for *Chamerion angustifolium* of between 3 and 4.21 when grown under two different light regimes. While these changes approach the overall differences seen for *A.thaliana* the high values of Chl *a/b* reported here for growth at the highest light intensity are beyond those previously reported. Similarly the extent

of the change in  $P_{max}$  is greater than previously reported for most other plant species (Chow and Anderson 1987, Murchie and Horton 1997).

The observed changes in Chl  $a/b$  ratio and  $P_{max}$  for *A.thaliana* clearly indicate that a strategy of chloroplast level acclimation is employed during growth at different irradiance. However Murchie and Horton (1997) suggest that chloroplast level acclimation should be associated with a decrease in chlorophyll content per unit leaf area to account for the loss of LHCII at higher growth irradiance. No such decrease is evident for *A.thaliana*. This can be explained by the existence of a second, leaf level, strategy for acclimation. The changes at the leaf level observed with growth at higher irradiance, in particular increased leaf thickness, would tend to elevate the chlorophyll content per unit leaf area.

In addition to the interplay between leaf level and chloroplast level acclimation it is clear from the discontinuous nature of the acclimation profile for  $P_{max}$  and Chl  $a/b$  that *A.thaliana* adopts different strategies for high and low light acclimation. The complexity of the response at the chloroplast level, of Chl  $a/b$  in particular, to different levels of growth irradiance only becomes apparent following a detailed analysis of the composition and function of the photosynthetic apparatus. Until now it has been assumed that since chlorophyll  $b$  is bound predominantly by LHCII, and in particular peripheral or bulk LHCII, that changes in Chl  $a/b$  reflect differences in the levels of the PSII light harvesting antenna relative to core components. Evidence in favour of the relationship between Chl  $a/b$  and PSII antenna size was first provided by Leong and Anderson (1984) using non- denaturing or green gel analysis. It was observed that the amount of chlorophyll associated with LHCII increased relative to the amount associated with PSII for peas grown at low irradiance where the Chl  $a/b$  ratio was also low. Similar results were reported for a number of other plant species

(Chow and Anderson 1987, De la Torre and Burkey 1990). Furthermore most studies indicated that changes in reaction centre levels with irradiance, when observed, were not significant enough to greatly influence Chl *a/b* ratio and with evidence suggesting that PSI antenna size remained constant (Anderson 1986) the relationship between Chl *a/b* and PSII antenna size became the accepted dogma. While it is true that for many plant species decreases in bulk LHCII take place during high light growth, and these changes clearly contribute strongly to increases in Chl *a/b*, a detailed analysis of the response of all chlorophyll *a/b* binding light harvesting components to growth at different irradiance has so far been lacking. In Chapter 4 a full analysis of the composition of the chlorophyll binding components of the thylakoid membrane was provided for *A.thaliana* grown over a wide range of irradiance. From these data it is clear that at most growth irradiance changes in Lhcb1 and 2, which make up peripheral LHCII, are significant enough to account for most of the observed changes in Chl *a/b*. However there are also large changes in the minor light harvesting components of PSII as well as changes in LHCI content and composition and although these may have less effect on Chl *a/b* their significance can not be overlooked. Also there is no significant change in the level of Lhcb1 and 2 at the highest growth irradiance and yet Chl *a/b* increases significantly. In this case a large increase in the level of PSII, the extent of which is unprecedented, is sufficient to account for this. In addition increases in the PSI reaction centre content, which have never previously been reported for any plant species, are observed at very low growth irradiance. The magnitude of this change in PSI is also sufficiently large to contribute to the overall Chl *a/b*.

The detailed analysis of the composition of the thylakoid membrane highlights the point that Chl *a/b* ratio should not be assumed to relate to changes in LHCII alone.

In addition this analysis also served to confirm that *A.thaliana* employs different strategies for growth at low and high irradiance as indicated by the discontinuous nature of the acclimation profile for Pmax and Chl *a/b*. At very low irradiance there are fewer PSII units with more peripheral LHCII. As the growth light increases there is an increase in the number of PSII units with a decrease in the level of bulk LHCII, a phenomenon previously described by Anderson and Andersson (1988). The increase in PSII is particularly marked at very high irradiance. While it is obvious that low light plants need to increase their PSII absorption cross section in order to make use of limiting light it would appear that high light plants also increase their total absorption cross section by significantly increasing the number PSII reaction centres.

At low growth irradiance there are obvious advantages to employing a strategy of increased antenna size to maximise light capture. In terms of protein economy it is more energetically favourable since it is possible to increase the light harvesting pigment to protein ratio significantly using light harvesting polypeptides instead of just reaction centres. It also seems likely however that this strategy is adopted to ensure constant turnover of P680, in order to maintain the s-state cycle, under conditions of limiting light.

There are also clear advantages of employing a strategy of increasing PSII content while decreasing antenna size at higher irradiance. Increased photosynthetic rates may be supported while minimising the amount of absorbed light associated with each reaction centre. This strategy therefore serves to provide photoprotection. The need for enhanced photoprotection at higher growth irradiance may also be met in a less obvious manner by the changes in thylakoid composition. Data presented in Chapter 5 suggest that the capacity for non-photochemical quenching is itself subject

to acclimation with maximum values of qE rising at higher growth irradiance. The higher capacity for qE during high light growth correlates well with the overall Chl *a/b*. For plants grown at very high irradiance the changes in Chl *a/b* represent a combination of increasing levels of PSII along with decreasing levels of Lhcb1 and 2. One or both changes may therefore play a role in the increased capacity for qE. Recent analysis of the structure of PSII by single particle analysis (Boekema *et al* 1999) may help to explain how such a phenomenon might be possible. From single particle images it has been observed that peripheral LHCII can exist as an independent complex made up of a number subunits. These subunits may separate adjacent PSII core complexes thereby impairing their interaction. In the molecular mechanism for qE described by Horton *et al* (1996) it is suggested that qE formation involves chl-chl interaction brought about by LHCII aggregation. The nature of the LHCII units involved in aggregation is however unspecified. It is possible therefore that only LHCII associated with PSII reaction centres is responsible for such an interaction. If this is the case then it is also possible that removal of the peripheral LHCII associated with the independent complexes would allow for increased interaction between PSII associated LHCII and therefore increase the capacity for qE. Furthermore the introduction of more PSII units, assuming that they carry the LHCII component involved in quenching, would further increase the capacity for qE. In addition there are strong correlations between increasing capacity for qE and the xanthophyll cycle pool size with increasing irradiance suggesting a role for the levels of these carotenoid in high light acclimation.

A second part of the strategy for very low light acclimation involves a significant increase in the level of PSI, which almost doubles at  $35 \mu\text{mol m}^{-2} \text{s}^{-1}$ . One obvious explanation for this arrangement involves cyclic electron flow. It is suggested that

the extra PSI centres are involved in the cyclic flow of electrons in order to generate extra ATP essential for house keeping functions at low light intensities. It is interesting to note however that all PSI light harvesting polypeptides are significantly reduced on a reaction centre basis during low light growth suggesting that all or some PSI units may be deficient in their light harvesting capacity. The minor LHCII components Lhcb5 and Lhcb6 on the other hand both show a 2-fold increase at very low irradiance despite only small decreases in the levels of PSII. It is possible therefore that Lhcb5 and Lhcb6 associate with and provide a light harvesting function to the extra PSI subunits. Although there is no data to support this suggestion both polypeptides share sufficient homology with PSI light harvesting polypeptides to make such an interaction possible (Jansson 1994). The significance of utilising PSII light harvesting polypeptides in place of PSI light harvesting polypeptides is however unclear.

P<sub>max</sub> has also been widely employed as an indicator of the state of acclimation in numerous studies. As with the response of Chl *a/b* the non-linear nature of the P<sub>max</sub> acclimation profile for *A.thaliana* grown over a range of irradiance suggests different strategies for acclimation may be employed. Initially the close correlation between the Chl *a/b* and P<sub>max</sub> profiles suggests that the underlying molecular processes are co-regulated. However the complexity in the changes of those components which contribute to P<sub>max</sub> and in particular Chl *a/b* would tend to invalidate such a proposal.

The non-linear profile of P<sub>max</sub> arises from alternative fates for photosynthetically derived electrons at different growth irradiance. Fluorescence quenching analysis in chapter 5 revealed that for the majority of growth light environments used in this

study the apparent capacity for electron transport rate reflects the photosynthetic capacity as measured by oxygen evolution. However the electron transport rate of plants grown at  $400 \mu\text{mol m}^{-2} \text{s}^{-1}$  matches that of plants grown at  $600 \mu\text{mol m}^{-2} \text{s}^{-1}$  while  $P_{\text{max}}$  is equivalent to plants grown  $200 \mu\text{mol m}^{-2} \text{s}^{-1}$ . This clearly suggests an alternative fate for electrons, other than  $\text{CO}_2$  fixation, for plants grown at  $400 \mu\text{mol m}^{-2} \text{s}^{-1}$ . It is suggested that this alternative sink must be the Mehler reaction due to the involvement of  $\text{O}_2$  as an electron acceptor and given the assumed lack of photorespiration under the measuring conditions. It is unclear why an alternative electron sink may be in effect at a growth irradiance of  $400 \mu\text{mol m}^{-2} \text{s}^{-1}$ . However the presence of such a sink, in allowing high rates of electron transport, may negate the need for changes in the composition of the photosynthetic apparatus through photosynthetic acclimation. It is possible therefore that this phenomenon may be explained in terms of a hierarchy of responses similar to that previously described by Backausen *et al* (1994) but which also includes photosynthetic acclimation. When *Arabidopsis* plants are grown at intermediate rather than very low irradiance the differences observed involve photosynthetic acclimation because cyclic electron flow is less important and therefore PSI content is decreased. In addition there is no longer any need for a large PSII antenna to ensure constant turnover. However at intermediate irradiance (i.e.  $200 \mu\text{mol m}^{-2} \text{s}^{-1}$  to  $400 \mu\text{mol m}^{-2} \text{s}^{-1}$ ) no such acclimation takes place. Instead a hierarchy of alternative electron sinks including the malate valves and Mehler reaction can operate to ensure that electron transport rates are sufficiently high with increasing growth light intensity that no acclimation is necessary. However the alternative electron sinks each become saturated in turn at higher growth irradiance. When the Mehler reaction finally becomes saturated it is necessary for photosynthetic acclimation once more. This takes place beyond a

growth irradiance of  $400 \mu\text{mol m}^{-2} \text{s}^{-1}$  for *A. thaliana*. The photosynthetic acclimation seen at very high irradiance not only allows for increased electron transport, supported by elevated Rubisco levels, but may also provide for extra photoprotection as described above.

Given the complexity of the response of *A.thaliana* to growth at a range of irradiance it seems clear that equally complex processes might accommodate changes in irradiance during growth. An indication of this is provided by the response to a shift from very low to very high irradiance. Initially *A.thaliana* relies heavily on non-photochemical quenching mechanisms and shows the potential for stress as indicated by the low values of qP. However within 24-48 hours there is an increase in the Chl *a/b* ratio and Pmax with qP being restored to close to its original value. The composition of the thylakoid membrane and increased photosynthetic capacity never match that seen for plants grown from seed at  $600 \mu\text{mol m}^{-2} \text{s}^{-1}$  and values for  $\Phi\text{PSII}$  are never restored to a high value following the transfer. This suggests that both photosynthetic acclimation and non-photochemical quenching combine to provide protection just long enough for the plants to flower which takes place within 3-4 days.

In conclusion photosynthetic acclimation to growth irradiance appears to involve a number of different strategies which include changes in all light harvesting components as well as reaction centres, alternative electron sinks and changing capacity for short term regulation. Despite the complexity *A.thaliana* is able to maintain perfect quantum efficiency, as indicated by the high values for  $\Phi\text{PSII}$  and qP

when measured *in situ*, over the full range of growth irradiance employed in this study.

## 7.1 Future work

The work provided in this thesis provides a strong basis for the utilisation of *A.thaliana* in future work relating to photosynthetic acclimation to irradiance. This future work should focus on the elucidation of the regulatory mechanisms that underlie the responses presented here. It is clear from this study that the various aspects of photosynthetic acclimation respond to similar signals by a number of different regulatory pathways. A genetic approach to isolate mutants defective in these pathways is already underway. This should be accompanied by a detailed analysis of the level at which the various responses is exerted i.e. transcriptional, translational or post translational control. In addition the role and significance of alternative electron sinks during growth at different irradiance should be investigated further.

## **References**

**Allen JF** (1992) Protein Phosphorylation in Regulation of Photosynthesis. *Biochim. Biophys. Acta* **1098**: 275-335

**Allen JF** (1995) Thylakoid Protein Phosphorylation, State 1-State 2 Transitions and Photosystem Stoichiometry Adjustment: Redox Control at Multiple Levels of Gene Expression. *Physiol. Plant* **93**: 196-205

**Anderson JM, Andersson B** (1988) The Dynamic Photosynthetic Membrane and Regulation of Solar-energy Conversion. *Trends in Biochemical Sciences* **13**: 351-355.

**Anderson JM, Osmond CB** (1987) Shade-Sun Responses: Comprises Between Acclimation and Photoinhibition. In 'Photoinhibition' (DJ Kyle, CB Osmond and CJ Arntzen eds.) pp1-36. Elsevier Science Publishers B.V.

**Anderson JM, Chow WS, Goodchild DJ** (1988) Thylakoid Membrane Organisation in Sun/Shade Acclimation. *Aust. J. Plant Physiol.* **15**: 11-26

**Anderson JM** (1989) The Grana Margins of Plant Thylakoid Membranes. *Physiol. Plant* **76**: 243-248

**Anderson J M, Chow W S, Youn-II Park** (1995) The Grand Design of Photosynthesis: Acclimation of the Photosynthetic Apparatus to Environmental Cues *Phot. Res.* **46**: 129-139

**Arnon DI, Tang GM-S** (1988) Cytochrome *b*-559 and Proton Conductance in Oxygenic Photosynthesis. Proc. Natl. Acad. Sci. USA. **85**: 9524-9528

**Backausen JE, Kitzmann C, Scheibe R** (1994) Competition Between Electron Acceptors in Photosynthesis – Regulation of the Malate Valve During CO<sub>2</sub> Fixation and Nitrite Reduction. Photo. Res. **42**: 75-86.

**Bassi R, Rigoni F, Giacometti GM** (1990) Chlorophyll Binding Proteins with Antenna Function in Higher Plants and Green Algae. Photochemistry and Photobiology. **52**: 1187-1206

**Bassi R, Pineau B, Dainese P, Marquardt J** (1993) Carotenoid Binding Proteins of Photosystem II. Eur. J. Biochem. **212**: 297-303

**Bassi R, Guiffra E, Croce R, Dainese P, Bergantino E** (1996) Biochemistry and Molecular Biology of Pigment Binding Proteins. In: Light as an Energy Source and Information Carrier in Plant Physiology. (Jennings *et al.* Eds.) Plenum Press, New York. pp41-63

**Bendall DS, Manasse RS** (1995) Cyclic Photophosphorylation and Electron Transport. Biochim. Biophys. Acta **1229**: 23-38

**Berry S, Rumberg B** (1996) H<sup>+</sup>/ATP Coupling Ratio at the Unmodulated CF<sub>0</sub>CF<sub>1</sub>-ATP Synthase Determined by Proton Flux Measurements. Biochim. Biophys. Acta **1276**: 51-56

**Bjorkman O** (1981) Responses to Different Quantum Flux Densities. In: Encyclopedia of Plant Physiology (Lange *et al*, Eds.) pp 57-107 Springer Verlag, Berlin.

**Blankenship RE, Prince RC** (1985) Excited-State Redox Potentials and the Z Scheme of Photosynthesis. Trends in Biochemical Science **10**: 382-383

**Boekema EJ, van Roon H, Calkoen F, Bassi R, Dekker JP** (1999) Multiple Types of Association of Photosystem II and its Light-harvesting Antenna in Partially Solubilized Photosystem II Membranes. Biochem. **38**: 2233-2239.

**Boekema EJ, Wynn RM, Malkin R** (1991) The Structure of Spinach Photosystem I Studied by Electron Microscopy. Biochim. Biophys. Acta **1017**: 49-56

**Bohme H, Cramer WA** (1972) High Potential Cytochrome b-559 as a Secondary Quencher of Chloroplast Fluorescence in the presence of DCMU. Biochim. Biophys. Acta. **283**: 302-315

**Briantais JM, Verrotte C, Picaud M, Krause GH** (1979) A Quantitative Study of the Slow Decline of Chlorophyll *a* Fluorescence in Isolated Chloroplasts. Biochim. Biophys. Acta **548**: 128-138

**Bricker TM, Frankel LK** (1998) The Structure and Function of the 33 kDa Extrinsic Protein of Photosystem II: A Critical Assessment. Phot. Res. **56**: 157-173

**Brugnoli E, Scartazza A, Detullio MC, Monteverdi MC, Lauteri M, Augusti A**

(1998) Zeaxanthin and Non Photochemical Quenching in Sun and Shade Leaves of C3 and C4 Plants. *Physiologia Plantarum* **104**: 727-734

**Chitnis PR, Qiang X, Chitnis VP, Nechustai R** (1995) Function and Organisation of Photosystem I Polypeptides. *Phot. Res.* **44**: 23-40

**Chow WS, Anderson JM** (1987) Photosynthetic Responses of *Pisum sativum* to an Increase in Irradiance During Growth: Thylakoid Membrane Components. *Aust. J. Plant Physiol.* **14**: 9-19

**Chow WS, Hope AB** (1987) The Stoichiometries of Supramolecular Complexes in Thylakoid Membranes from Spinach Chloroplasts. *Aust. J. Plant Phys.* **14**: 21-28

**Chow WS, Hope AB, Anderson JM** (1989) Oxygen per Flash From Leaf Disks Quantifies Photosystem II. *Biochim. Biophys. Acta* **973**: 105-108

**Chow WS, Adamson HY, Anderson JM** (1991) Photosynthetic Acclimation of *Tradescantia albiflora* to Growth Irradiance : Lack of Adjustment of Light Harvesting Components and its Consequences. *Physiol. Plant.* **81**: 175-182

**Chow WS** (1994) Photoprotection and Photoinhibitory Damage. *Adv. Mol. Cell. Biol.* **10**: 151-196

**Cleland RE, Melis A, Neale PJ** (1986) Mechanism of Photoinhibition: Photochemical-Reaction Centre Inactivation in System-II of Chloroplasts. *Phot. Res.* **9**: 79-88

**Cleland RE, Bendall DS** (1992) PSI Cyclic Electron Transport: Measurement of Ferridoxin-Plastoquinone Reductase Activity. *Phot. Res.* **34**: 409-418

**Danielus RV, Satoh K, van Kan PJM, Plijter JJ, Nuijs AM, van Gorkom HJ** (1987) The Primary Reaction of Photosystem II in the D1-D2-cyt *b559* Complex. *FEBS Lett.* **213**: 241-244

**Dalwiche CF, Palmer JD** (1997) The Origin of Plastids and Their Spread Via Secondary Symbiosis. *Plant Systematics and Evolution* **511**: 53-86

**Dekker JP, van Roon H, Boekema EJ** (1999) Heptameric Association of Light Harvesting Complex II Trimers in Partially Solubilised Photosystem II Membranes (in press)

**De La Torre WR, Burkey KO** (1990) Acclimation of Barley to Changes in Light Intensity: Chlorophyll Organisation. *Phot. Res.* **24**: 117-125.

**Demmig-Adams B, Adams WW III** (1990). Photoprotection and Other Responses of Plants to High Light Stress *Ann. Rev. Plant Physiol. Plant Mol. Biol.* **43**: 599-629

**Diner B. A, Petrouleas V, Wendoloski JJ** (1991) The Iron-quinone Electron-acceptor Complex of Photosystem II. *Physiol. Plant* **81**: 423-436

**Durrant JR, Klug DR, Kwa SLS, van Grondell R, Porter G, Dekker JP** (1995) A Multimer Model for P680, the Primary Electron Donor of PSII. Proc. Natl Acad. Sci. USA. **92**: 4798-4802

**Eckhardt HC, vanRooyen N, Bredenkamp GJ** (1997) Plant Communities and species Richness of the *Agrostis Lachnanta eragrostis Plana* Wetlands of Northern KwaZulu-Natal. South African journal of Botany **62**: 306-315

**Enami I, Miyaoka T, Mochizuki y, Shen J-R, Satoh K, Katoh S** (1997). Nearest Neighbour Relationships Among Constituent Proteins of Oxygen Evolving Photosystem II membranes: Binding and Function of the Extrinsic 33 KDa Protein. Biochim. Biophys. Acta **973**: 35-40

**Escoubas JM, Lomas M, LaRoche J, Falkowski PG** (1995). Light Intensity Regulation of *cab* Gene Transcription is Signalled by the Redox State of the Plastoquinone Pool. Proc. Natl. Acad. Sci. USA. **92**: 10237-10241

**Evans JR** (1987) The Relationship Between Electron Transport Components and Photosynthetic Capacity in Pea Leaves Grown at Different Irradiances. Aust. J. Plant Physiol. **14**. 157-170.

**Falkowski PG, Fujita Y, Ley A, Mauzerall D** (1986) Evidence for Cyclic Electron Flow Around Photosystem II in *Chlorella pyrenoidosa*. Plant Physiol. **81**: 310-312

**Frank HA, Chua A, Chynwat V, Young A, Gosztola D, Wasielewski MR** (1994).

Photophysics of the Carotenoid Associated with the Xanthophyll Cycle in

Photosynthesis. *Phot. Res.* **41**: 389-395.

**Gilmore AM, Bjorkman O** (1995) Temperature Sensitive Coupling and Uncoupling of

ATPase Mediated NonRadiative Energy Dissipation: Similarities Between Chloroplasts

and Leaves. *Planta* **197**: 646-654

**Goldbeck JH** (1992) Structure and Function of Photosystem I. *Annu. Rev. Plant*

*Physiol. Plant Mol. Biol.* **43**: 293-324

**Graan T, Ort DR** (1986) Detection of Oxygen-Evolving Photosystem II Centers

Inactive in Plastoquinone Reduction. *Biochim. Biophys. Acta* **852**: 320-330

**Green BR, Pichersky E, Kloppstech K** (1991) Chlorophyll *a/b* Binding Proteins: an

Extended Family. *Trends in Biochemical Science* **16**: 181-186.

**Gray GR, Savitch LV, Ivanov AG, Huner NPA** (1996) Photosystem II Excitation

Pressure and Development of Resistance to Photoinhibition. *Plant Physiol.* **110**: 61-71

**Gray GR, Chauvin LP, Surhan F, Huner NPA** (1997). Cold Acclimation and

Freezing Tolerance. *Plant Physiol.* **114**: 467-474

**Guenther JE, Melis A** (1990) The Physiological Significance of Photosystem II

Heterogeneity in Chloroplasts. *Phot. Res.* **23**: 105-109

**Hall DO, Rao KK.** Photosynthesis, Fifth Ed. 1994. Cambridge University Press. pp 34

**Hankamer B, Barber J, Boekema EJ** (1997) Structure and Membrane Organization of Photosystem in Green Plants. *Ann. Rev. Plant Physiol. Plant Mol. Biol.* **48**: 641-671.

**Harbinson J, Genty B, Baker NR** (1989) Relationship Between the Quantum Efficiencies of PSI and PSII in Pea Leaves. *Plant Physiol.* **90**: 1029-1034

**Hastings G, Kleinherenbrink FAM, Lin S, Blankenship RE** (1994) Time Resolved Fluorescence and Absorption Spectroscopy of Photosystem-I. *Biochemistry.* **33**: 3185-3192

**Havaux M, Niyogi KK** (1999) The Violaxanthin Cycle Protects Plants from Photoprotective Damage by More Than One Mechanism. *PNAS* **96**: 8762-8767

**Havaux M, Tardy F,** (1999) Loss of Chlorophyll with Limited Reduction of Photosynthesis as an Adaptive Response of Syrian Barley Landacres to High Light and Heat Stress. *Aust. J. Plant Phys.* **26**: 569-578

**Heber U, Walker DA** (1992) Concerning a Dual Function of Coupled Cyclic Electron Transport in Leaves. *Plant. Physiol.* **100**: 1621-1626

**Hill R** (1960) The Z-Scheme of Oxygenic Photosynthetic Electron Transport. *Nature* **186**: 136-139

**Hoganson CW, Lydakis-Simantiris N, Tang XS, Tommos C, Warncke K, et al** (1995) A Hydrogen-atom Abstraction Model for the Function of  $Y_z$  in Photosynthetic Oxygen Evolution. *Phot. Res.* **46**: 177-184

**Horton P, Bowyer JR** (1990) Chlorophyll Fluorescence Transients. *Methods in Plant Biochemistry* **4**: 259-296.

**Horton P, Ruban AV, Walters RG** (1996) Regulation of Light Harvesting in Green Plants. *Annu. Rev. Plant Physiol.* **47**: 655-684

**Huang D, Everly RM, Cheng RH, Heymann JB, Schagger H et al** (1994) Characterisation of the chloroplast cytochrome *b<sub>6</sub>f* as a structural and functional dimer. *Biochemistry* **33**: 4401-4409

**Ikeuchi M, Hirano A, Inoue Y** (1991) Correspondence of Apoprotein of Light Harvesting Chlorophyll *a/b* Complexes Associated with Photosystem I to *CAB* Genes – Evidence for a Novel Type IV Apoprotein. *Plant and Cell Phys.* **32**: 103-112.

**Itzhaki H, Naveh L, Lindahl M, Cook M, Adam Z** (1998) Identification and Characterisation of DegP, a Serine Protease Associated with the Luminal Side of the Thylakoid Membrane. *J. Biol. Chem.* **273**: 7094-7098

**Jansson S, Pichersky E, Bassi R, Green BR, Ikeuchi M, Melis A, Simpson DJ, Spangfort M, Staehelin LA, Thornber JP** (1992) A Nomenclature for the Genes Encoding the Chlorophyll *a/b* Binding Proteins of Higher Plants. *Plant Mol. Biol. Reporter* **10**: 242-253

**Jansson S** (1994) The Light Harvesting Chlorophyll *a/b* Binding Proteins. *Biochim. Biophys. Acta* **1184**: 1-19

**Jansson S, Andersen B, Scheller HV** (1996) Nearest-Neighbor Analysis of Higher Plant Photosystem I Holocomplex. *Plant Physiol.* **112**: 409-420

**Jansson S, Stefansson H, Nystrom U, Gustafsson P, Albertsson P-A** (1997) Antenna Protein Composition of PSI and PSII in Thylakoid Sub-domains. *Biochim. Biophys. Acta* **1320**: 297-309

**Johnson GN, Scholes JD, Horton P, Young AJ** (1993) Relationships Between Carotenoid Composition and Growth Habitat in British Plant Species. *Plant Cell Environ.* **16**: 681-686

**Junge W, Sabbert D, Engelbrecht S** (1997) Rotary Catalysis by F-ATPase: Real Time Recording of Intersubunit Rotation. *Chemical Physics* **100**: 2014-2019

**Kannangara CG, Hanson M** (1998) Arrest of Chlorophyll Accumulation Prior to Anthocyanin Formation in *Euphorbia pulcherrima*. *Plant Phys. Biochem.* **36**: 843-848

**Knoetzel J, Simpson D** (1991) Expression and Organisation of Antenna Proteins in the Light Sensitive and Temperature Sensitive Barley Mutant Chlorina-104. *Planta* **185**: 111-123

**Kok B, Forbush B, McGloin MP** (1970) Cooperation of Charges in Photosynthetic Oxygen Evolution: A linear Four Step Mechanism. *Photochem. Photobiol.* **11**: 457-475

**Krause GH, Somersalo S, Zumbusch E, Weyers B, Laasch H (1990)** On the Mechanism of Photoinhibition in Chloroplasts. *J. Plant Phys* **136**: 472-479

**Krauss N, Hinrichs W, Witt I, Fromme P, Pritzkow W, Dauter Z, Betzel C, Wilson KS, Witt HT, Saenger W (1993)** Three Dimensional Structure of Photosystem I at 6 Å Resolution. *Nature* **361**: 326-331

**Kuhlbrandt W, Wang DN, Fujiyoshi Y (1994)** Atomic Model of Plant Light-Harvesting Complex by Electron Crystallography. *Nature* **367**: 614-621

**Laemmli UK (1970)** Cleavage of Structural Proteins During the Assembly of the Head of Bacteriophage T4. *Nature* **227**: 680-685

**Lam E, Ortiz W, Malkin R (1984)** Chlorophyll *a/b* proteins of Photosystem I. *FEBS Lett.* **168**: 10-14

**Larsson UK, Anderson JM, Andersson B (1987)** Variations in the Relative Content of the Peripheral and Inner Light Harvesting Chlorophyll *a/b* Protein Complex (LHCII) Subpopulations During Thylakoid Light Adaption and Development. *Biochim. Biophys. Acta.* **894** : 69-75

**Leegood R (1990)** Enzymes of the Calvin Cycle. In: (P.J.Lea Ed.), *Enzymes of Primary Metabolism*. pp. 15-37. Academic Press, London

**Leong TY, Anderson JM** (1984) Changes in Composition and Function of Thylakoid Membranes as a Result of Photosynthetic Adaptation of Chloroplasts from Pea Plants Grown Under Different Light Conditions. *Biochim. Biophys. Acta* **723**: 391-399

**Lichtentahler HK, Welburn AR** (1983) Determinations of Total Carotenoids and Chlorophyll *a* and *b* of Leaf Extracts in Different solvents. *Biochem. Soc. Trans.* **11**: 591-592

**Lindahl M, Yang D-H, Andersson B** (1995) Regulatory Proteolysis of the Major Light-harvesting Chlorophyll *a/b* Protein of Photosystem II by a Light-Induced Membrane-Associated Enzymic System. *Eur. J. Biochem.* **231**: 503-509

**Lindahl M, Tabak S, Cseke L, Pichersky E, Andersson B, Adam Z** (1996) Identification, Characterisation and Molecular Cloning of a Homologue of the Bacterial FtsH Protease in Chloroplasts of Higher Plants. *J. Biol. Chem.* **271**: 29329-29334

**Liscum E, Hangarter RP.** (1991) *Arabidopsis* Mutants Lacking Blue Light-Dependant Inhibition of Hypocotyl Elongation. *Plant Cell.* **3**: 685-694

**Malkin R, Canaani O** (1994) The Use and Characteristics of the Photoacoustic Method in the Study of Photosynthesis. *Annu. Rev. Plant Physiol. Plant Mol. Biol.* **45**: 493-526

**Malkin R** (1996) Photosystem Electron Transfer Reactions-Components and Kinetics. In: *Oxygenic Photosynthesis: The Light Reactions.* (Ort DR., Yocum CF. Eds) Kluwer Academic Publishers, Netherlands. pp 313-332

**Manetas Y, Grammatikopoulos G, Kyparissis A (1998)** The Use of the Portable SPAD-502 (Minolta) Chlorophyll Meter With Leaves of Varying Trichome Density and Anthocyanin Content. *J. Plant Phys.* **153**: 513-516

**Maxwell DP, Falk S, Trick CG, Huner NPA (1994)** Growth at Low Temperature Mimics High-Light Acclimation in *Chlorella Vulgaris*. *Plant Physiol.* **105**: 535-543

**Maxwell DP, Falk S, Huner NPA. (1995a)** Photosystem II Excitation Pressure and Development of Resistance to Photoinhibition. *Plant Physiol.* **107**: 687-694

**Maxwell DP, Laudenbach DE, Huner NPA (1995b).** Redox Regulation of Light-Harvesting Complex II and *cab* mRNA Abundance in *Dunalella salina*. *Plant Physiol.* **109**: 787-795

**Maxwell K, Marrison JL, Leech RM, Griffiths H, Horton P (1999)** Chloroplast Acclimation in Leaves of *Guzmania monostachia* in Response to High Light. *Plant Physiology* **121**:89-95

**Melis A, Manodori A, Glick RE, Ghirardi ML, McCauley SW, Neale PJ (1985)** The Mechanism of Photosynthetic Membrane Adaptation to Environmental Stress Conditions: A Hypothesis on the Role of Electron-Transport Capacity and of ATP/NADPH Pool in the Regulation of Thylakoid Membrane Organization and Function. *Physiol. Veg.* **23**: 757-765

**Melis A (1991)** Dynamics of Photosynthetic Membrane Composition and Function. *Biochim. Biophys. Acta* **1058**: 87-106

**Miao JH, Irrgang KD, Salnikow J, Franke P, Vater J** (1998) Close Vicinity of Lhcb1 and Lhcb4 in Photosystem II Membrane Fragments as Verified by Chemical Cross Linking. *Eur. J. Biochem* **257**: 586-591

**Mitchell P** (1966) Chemiosmotic Coupling in Oxidative and Photosynthetic Phosphorylation. *Biol. Rev.* **41**: 445-502

**Mitchell P** (1976) Possible Molecular Mechanisms of the Proton motive Function of Cytochrome Systems. *J. Theo. Biol.* **62**:327-367

**Mohammed GH, Parker WC** (1999) Photosynthetic Acclimation in Eastern Hemlock (*Tsuga canadensis*) Seedlings Following Transfer of Shade Grown Seedlings to High Light. *Tree Structure and Function* **13**: 117-124

**Montane MH, Tardy F, Kloppstech K, Havaux M** (1998) Differential Control of Xanthophylls and Light Induced Stress Proteins as Opposed to Light Harvesting Chlorophyll *a/b* Proteins During Photosynthetic Acclimation of Barley Leaves to Light Irradiance. *Plant Phys.* **118**: 227-235

**Murchie EH, Horton P** (1997) Acclimation of Photosynthesis to Irradiance and Spectral Quality in British Plant Species: Chlorophyll Content, Photosynthetic Capacity and Habitat Preference. *Plant Cell and Environment* **20**: 438-448

**Murchie EH, Horton P** (1998) Contrasting Patterns of Photosynthetic Acclimation to the Light Environment are Dependant on the Differential Expression of the Responses to Altered irradiance and Spectral Quality. *Plant Cell and Environment* **21**: 139-148

**Namba O, Satoh K** (1987) Isolation of a PSII Reaction Centre Consisting of D1, D2 Polypeptides and Cyt b-559. *Proc. Natl. Acad. Sci. USA.* **84**: 109-112

**Nechushtai R, Eden A, Cohen Y, Klein J** (1996) Introduction to Photosystem I: Reaction Centre Function Composition and Structure. In: *Oxygenic Photosynthesis: The Light Reactions.* (Ort DR, Yocum CF. Eds) Kluwer Academic Publishers, Netherlands. pp 313-332

**Noctor G, Rees D, Young AJ, Horton P** (1991) The Relationship Between Zeaxanthin, Energy-Dependant Quenching of Chlorophyll Fluorescence and the Trans-Thylakoid pH Gradient in Isolated Chloroplasts. *Biochim. Biophys. Acta* **1057**: 320-330

**Oquist G, Chow WS, Anderson JM** (1992) Photoinhibition of Photosynthesis Represents a Mechanism for the Long Term Regulation of Photosystem II. *Planta* **186**: 450-460

**Ort D, Whitmarsh J** (1996) Photosynthetic Electron Transfer and Energy Transduction in Plants. In: *Light as an Energy Source and Information Carrier in Plant Physiology.* (Jennings *et al.* Eds) Plenum Press, New York. pp17-29

**Park YI, Chow WS, Anderson J** (1996) Differential Susceptibility of Photosystem II to Photoinhibition in Light Acclimated Pea Leaves Depends on the Capacity for

Photochemical and Non-radiative Dissipation of Excess Light. *Plant Science* **2**, 137-149.

**Pascal A, Gradinaru C, Wacker U, Peterman E, Calkoen F, Irrgang KD, Horton P, Renger G, van Grondelle R, Robert B, van Amerongen H** (1999) Spectroscopic Characterisation of the Spinach Lhcb4 Protein (CP29), a Minor Light Harvesting Complex of Photosystem II. *Eur. J. Biochem.* **262**: 817-823

**Peter GF, Thornber JP** (1991) Biochemical Composition and Organization of Higher Plant Photosystem II Light-harvesting Pigment-proteins. *J. Biol. Chem.* **266**: 16745-16754

**Pfannschmidt T, Nilsson A, Allen JF** Photosynthetic Control of Chloroplast Gene Expression. *Nature* **397**: 625-628

**Polle A** (1995) Mehler Reaction: Friend or Foe in Photosynthesis? *Botanica Acta* **109**: 84-89.

**Renger G** (1993) Water Cleavage by Solar Radiation-An Inspiring Challenge of Photosynthesis Research. *Phot. Res.* **38**: 229-247

**Rich PR** (1988) A Critical Examination of the Supposed Variable Proton Stoichiometry of the Chloroplast Cytochrome *b<sub>6</sub>f* complex. *Biochim. Biophys. Acta* **932**:33-42

**Robson PRH, Whitelam GC, Smith H** (1993) Selected Components of the Shade Avoidance Syndrome are Displayed in a Normal Manner in Mutants of *A. thaliana* and *Brassica napa* Deficient in phytochrome B. *Plant Physiol.* **102**: 1179-1184

**Ruban AV, Horton P, Young AJ** (1993a) Aggregation of Higher Plant Xanthophylls: Differences in Absorption Spectra and in the Dependency on Solvent Polarity. *J. Photobiol. Photochem.* **21**: 229-234

**Ruban AV, Young AJ, Horton P** (1993b) Induction of Non-Photochemical Energy Dissipation and absorbance Changes in Leaves: Evidence for Changes in the State of the Light Harvesting System of Photosystem II *in vivo*. *Plant Physiol.* **102**: 741-50

**Ruban AV, Horton P** (1995) An investigation of the Sustained Component of Non-Photochemical Quenching of Chlorophyll Fluorescence in Isolated Chloroplasts and Leaves of Spinach. *Plant Physiol.* **108**: 721-726

**Ruban AV, Horton P**, (1999) The Xanthophyll Cycle Modulates the Kinetics of Nonphotochemical Energy Dissipation in Isolated Light Harvesting Complexes, Intact Chloroplasts and Leaves of Spinach. *Plant Phys.* **119**: 531-542

**Ruban AV, Lee PJ, Wentworth M, Young AJ, Horton P**, (1999) Determination of the Stoichiometry and Strength of Binding of Xanthophylls to the Photosystem II Light Harvesting Complexes. *J. Biol. Chem.* **274**: 10458-10465

**Scheller HV, Svedson I, Moller BL** (1989) Subunit Composition of Photosystem I and Identification of Centre X as [4Fe-4S] Iron-Sulphur Cluster. *J. Biol. Chem.* **264**: 18402-18406

**Schreiber U, Neubauer C** (1990) O<sup>2</sup> Dependant Electron Flow, Membrane Energisation and the Mechanism of Non-Photochemical Quenching of Chlorophyll Fluorescence. *Phot. Res.* **25**: 279-293.

**Schubert WD, Klukas O, Kraus N, Saenger W, Fromme P, Witt HT** (1997) Photosystem I of *Synechocystis elongatus* at 4 Å Resolution: Comprehensive Structure Analysis. *J. Mol. Biol.* **272**: 741-769

**Seeman JR, Sharkey TD, Wang J Osmond CB** (1989) Environmental effects on Photosynthesis, Nitrogen Use Efficiency, and Metabolite Pools in Leaves of Sun and Shade plants. *Plant Physiol.* **84**: 796-803.

**Smith H** (1982) Light Quality, Photoreception and Plant Strategy. *Annu. Rev. Plant. Physiol.* **33**: 481-518

**Spangfort M, Andersson B** (1989) Subpopulations of the Main Chlorophyll *a/b* Light-harvesting Complex II-Isolation and Biochemical Characterisation. *Biochim. Biophys. Acta* . **977**: 163-170.

**Stitt M** (1986) Limitation of Photosynthesis by Carbon Metabolism I. Evidence for Excess Electron Transport Capacity in Leaves Carrying Out Photosynthesis in Saturating Light and CO<sub>2</sub>. *FEBS Lett.* **177**: 95-98.